DRUG TARGET IDENTIFICATION IN SPHINGOLIPID METABOLISM AGAINST *G. LAMBLIA*

by

Fatma Banu Yavuztürk

B. S. in ChE., Yeditepe University, 2006

Submitted to the Institute for Graduate Studies in
Science and Engineering in partial fulfillment of
the requirements for the degree of
Master of Science

Graduate Program in Chemical Engineering
Boğaziçi University
2009

ABSTRACT

DRUG TARGET IDENTIFICATION IN SPHINGOLIPID METABOLISM AGAINST *G. LAMBLIA*

Sphingolipids are essential cell compounds, mostly found in membranes and participated in cell events such as cell signaling, proliferation and apoptosis. Sphingolipid biosynthesis pathways have recently been highlighted as a promising target for therapeutic intervention against pathogens, including parasites. *Giardia lamblia* is a common cause of diarrhea in humans and other mammals throughout the world. Currently available anti-*G. lamblia* drugs cause serious in vivo side effects, often in the gastrointestinal tract, which frequently necessitate treatment interruption. Recently, it has been shown that the inhibition of the activity of glucosylceramide (GlcCer) synthase by PPMP (1-phenyl-2-palmitoylamino-3-morpholino-1-propanol) inhibitor prevented the proliferation and differentiation of *G. lamblia* in a dose dependent manner (Sonda *et al.*, 2008). This result indicated that as-yet-uncharacterized sphingolipid biosynthetic pathways are potential drug targets for the development of anti-*G.lamblia* agents. In the present study, a metabolic model for the *G.lamblia* sphingolipid metabolism was developed and by the application of flux balance analysis (FBA) *in silico* gene deletion simulations were performed to gain insight about the metabolic consequences of drug actions on candidate enzymes. An experimental study was also conducted with wild type and DPP1 deletion mutant of *S.cerevisiae* and the effects of gene deletions on the sphingolipid metabolism were investigated. It was observed that the production of D-Cer was increased in the DPP1 mutant strain and a distinct increase in dihydrosphingosine favoring the increase of ceramide production was also noted. Other complex sphingolipids, MIPC and $M(IP)_2C$, were similarly found to increase. When the *in silico* deletion mutants of *G. lamblia* simulating the anti-Giardia drug effects were investigated by FBA, the inhibitions of the enzymes encoded by the genes of Ugcg or DPP1 resulted in higher fluxes of ceramide synthesis. These increases are around 2 to 10 % of those of the wildtype strain. One can conclude that the results of the present simulation study agree well with the experimental findings reported in literature.

ÖZET

SİFİNGOLİPİT METABOLİZMASINDA G. LAMBLIA PARAZİTİNE KARŞI İLAÇ HEDEFLERİNİN SAPTANMASI

Sifingolipitler genellikle hücre duvarında bulunan ve çoğalma, apoptoz ve sinyal iletimi gibi birçok hücre olayında yer alan bileşiklerdir. Son yıllarda sifingolipit metabolizması birçok patojen, özellikle parazit tedavisi hedefi olarak mercek altına alınmaktadır. *Giardia lamblia* insanda ve birçok memelide diyareye neden olmaktadır. Günümüzde *G lamblia*'ya karşı kullanılan ilaçların, genellikle gastrointestinal sistemde olmak üzere, ciddi yan etkileri bulunmuştur ve bu yan etkiler tedavinin durdurulmasını gerektirmektedir. Son olarak yapılan bir çalışmada, glukozilseramid (GlcCer) sentaz aktivitesinin PPMP (1-fenil-2-palmitoylamino-3-morfolino-1-propanol) tarafından inhibe edilerek doza bağlı bir şekilde *G. lamblia*'nın çoğalmasını önlediği görülmüştür (Sonda, 2008). Bu sonuç *G lamblia*'da henüz tanımlanmamış olan sifingolipit metabolizmasının, bu organizmaya karşı geliştirilebilecek potansiyel ilaç hedeflerini içerdiğini ortaya koymaktadır. Bu çalışmada, *G. lamblia*'da yer alan sifingolipit metabolizmasının metabolik modellenmesi yapılarak ilaçların, ele alınan enzimler üzerindeki metabolik etkilerini gözlemlemek amacıyla akı denge analizi metodu (FBA) uygulanarak çeşitli gen delesyonu simulasyonları yapılmıştır. Deneysel bir çalışma ile de DPP1 mutantı ve yabanıl tip *S. cerevisiae* kullanılarak gen delesyonları sonuçları sifingolipit metabolizması için incelenmiştir. DPP1 mutant suşunda, D-Cer maddesinin arttığı ve bu artışında seramid artışını sağladığı görülmüştür. MIPC ve M(IP)2C, gibi diğer karmaşık yapıdaki sifingolipitlerin de arttığı gözlenmiştir. *G. lamblia*'ya karşı ilaç etkilerinin teorik gen delesyonları ve FBA yardımıyla yapılan simulasyonları ele alınan her iki enzim inhibisyonu (GlcCer ve DPP1) içinde seramid salgısının artmasıyla sonuçlanmıştır. Genel artma miktarı yabanıl tip baz alınırsa % 2 -10 arasında değişmektedir. Bu tez kapsamında elde edilen sonuçlar, simulasyon çalışmalarının literatürde yeralan deneysel çalışmalarla paralel olduğunu göstermektedir.

TABLE OF CONTENTS

LIST OF FIGURES

LIST OF TABLES

LIST OF SYMBOLS/ABBREVIATIONS

b	External metabolites
c	Objective Function
H	Hydrogen
S	S matrix
v	Enzymatic Reactions
x	Fluxes

3PSer	3P-Serine
bGLAC	b-galactose
C2-Cer	C2-Ceramide
C8-Cer	C8-Ceramide
C_{26}CoA	C26-Coenzyme
C1P	Ceramide-1-phosphate
CDPDAG	CDP-diacylglycerol
CDPE	Diacylglycerol ethanolamine
CER	Ceramide
CHO	Choline
CMP	Cytidine-5'-monophosphate
DAG	Diacylglycerol
DHCer	Dihydroceramide
DHS	Dihydrosphingosine
DP	Diphosphate
FA	Fattyacid
FBA	Flux Balance Analysis
GALCER	Galactosylceramide
GCER (GlcCer)	Glycosylceramide
Hexco	Hexacosanoate
hsa	Homo Sapiens
INO	Inositol

IPC	Inositol-phosphoceramide
KDHS	Dehydrosphinganine
LCER	Lactosylceramide
Mal-CoA	Malonyl-Coenzyme
man	Mannose
MAPK	Mitogen-activated protein kinase
MIPCDH	Mannose-inositol-phosphoceramide
$M(IP)_2CDH$	Mannose-(inositol phosphate) 2-ceramide
mmu	Mus Musculus
PalCoA	PalmitoilCoenzyme
PA	Palmitoyl
PC	Phosphatidylcholine
PCHO	Phosphatidyl choline
PE	Phosphatidylethanolamine
PHS	Pytosphingosine
PHCer (P-Cer)	Pytoceramide
PKC	Proteinkinase C
PI	Phosphadidate
PS	Phosphatidylserine
S1P	Sphingosine-1-phosphate
sce	Saccromyces cerevisiae
Ser	Serine
SM	Sphingomyelin
SPN	Sphingosine
UDPGAL	UDP-galactose

1. INTRODUCTION

Lipids are integral structural components of cell membranes, which through their ability to form a bilayer produce a permeability barrier between extracellular and intracellular compartments, a function essential for cell survival. In addition, lipids are essential for signal transduction in response to agonist stimulation as their hydrolysis produces bioactive molecules known to trigger many downstream signalling cascades. The first evidence for such a signalling role came in 1970s with the discovery of the phosphoinositide (PI) cycle. More recently, 3-phosphoinositides generated following growth factor and G protein-coupled receptor activation by the action of PI 3-kinases (PI3Ks) on inositol phospholipids have been recognised as important signalling lipids (Leevers *et al*., 1999). One target of these lipid messengers is PKB/Akt an important cell survival pathway. In addition to glycerolipids, a second class of lipids – sphingolipids – are now known to act as a reservoir of signalling molecules. Sphingolipids, of which there are over 300, are found in all eukaryotic cells and are enriched in plasma membranes, Golgi membranes and lysosomes. In 1986, the sphingolipid derivative sphingosine was shown to inhibit PKC (Hannun *et al*., 1986) indicating that this class of lipid was involved in cell signalling. Another sphingolipid-derived second messenger is ceramide, a product of sphingomyelin. We now know that many stress stimuli (e.g. cytokines, cytotoxic agents, environmental stress and injury or infection) increase cellular ceramide levels through hydrolysis of sphingomyelin and there is substantial evidence that ceramide is involved in apoptosis (Ohanian and Ohanian, 2001).

With the importance of sphingolipids especially ceramide, involving in apoptosis process, the potential drug target studies have focused on the sphingolipid metabolism. Employing the computational systems biology tools (metabolic control and metabolic pathway analyses) several drug target enzymes which are expected to induce apoptosis and thus can be employed in cancer therapy approaches have been identified (Kavun, 2007). In the present work, the effects of the two candidate enzymes (Ucgc and DPP1) on the sphingolipid metabolism was further investigated using the deletion mutants of *S. cerevisiae* experimentally and then using both wild type and *in silico* deletion mutants of *Giardia lamblia,* one of the most common parasites found in the intestinal tracts of vertebrates and humans, computationally. A stoichiometric model of SL metabolic pathways was reconstructed using literature information on reactions and the databases. Flux balance analysis was performed to get the flux distributions under normal (healthy) and perturbed (drug action) conditions.

The theoretical background section gives the basic information on the structure and function of sphingolipids in general, the biochemistry and metabolism of *G. lamblia* and the mutant strains considered in this study. The procedures followed in the experiments and Flux Balance Analysis (FBA) with pathway reconstruction information are explained in Materials and Methods section. The Results and Discussion part is comprised of the results obtained from experimental and computational studies applied to wild type and *in silico* mutants of *G. lamblia*. As a final part, the conclusions on enzyme inhibitions and the recommendations to improve the model system of G. lamblia’s sphingolipid metabolism are given.

2. THEORY

Sphingolipids are found in essentially all animals, plants, and fungi, as well as some prokaryotic organisms and viruses. They mostly are in membranes, but are also major constituents of lipoproteins.

2.1. Sphingolipids Structure

Sphingolipids were first described by Johann L.W. Thudichum in *A Treatise on the Chemical Construction of Brain* (1884). Among the described compounds were sphingomyelin, cerebroside, cerebrosulfade (Figure 2.1), which encompass categories of sphingolipids that are phosphosphingolipids, neutral and acidic glycosphingolipids. Sphingolipids contribute to the formation of regions of plasma membrane which are enriched in growing factor receptors, transporters and other proteins, especially proteins with glycosylphosphatidylinositol-lipid anchor (Vance, 2002).

The term sphingolipids covers hundreds of lipid compounds differing in their chemical structure and biological functions but united by a common feature, namely, the sphingoid base. The sphingoid bases (sphingoids) are amino alcohols with a long hydrocarbon chain. Sphingosine (sphinganine) is an aminodiol containing 18 atoms in its chain and an double bond in position 4. It is most abundant among the sphingoid constituents of sphingolipids from human and animal cells. According to contemporary biochemical nomenclature, a sphingoid containing a double bond in position 4 is called sphingenine, and its saturated analogue is called sphinganine. However, their old trivial names, sphingosine (instead of sphingenine) and dihydrosphingosine, respectively, are still used more often in scientific publications (Vance, 2002).

The molecule of sphingosine contains two chiral centers in positions 2 and 3 and, thus, it can exist in four stereomeric forms that differ in the spatial arrangement of functional groups. The natural sphingolipids contain only D-erythro-sphingosine, i.e., (2S,3R,4E)-2-amino-4-octadecen-l,3-diol. The modification of functional groups permits the transformation of the sphingosine molecule into complicated sphingolipids.

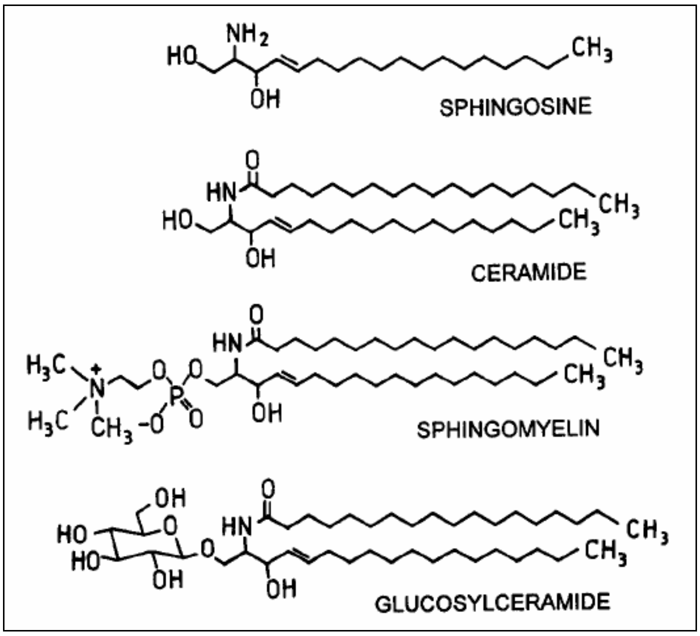

Figure 2.1. Structures of sphingosine, ceramide, sphingomyelin and a cerebroside

Sphingosine is the product of sphingolipid catabolism. Only sphinganine (dihydrosphingosine) is the product of biosynthesis. The next stage is its acylation with fatty acids, yielding dihydroceramide. The subsequent dehydration of the latter by dihydroceramide desaturase (Michael *et al*., 1997) gives a ceramide already containing sphingosine, which can be cleaved from ceramide by ceramidase (Rother *et al*., 1992).

Like all amphiphilic molecules, sphingolipids organize themselves in aqueous systems so as to maintain water contact with the hydrophilic portion but avoid it for the hydrophobic portion; therefore, aggregation as micelles or bilayer structures (vesicles) occurs (Tanford, 1989).

2.2. Sphingolipids in Yeast

Many roles for sphingolipids have been identified in mammals. Available data suggest that sphingolipids and their intermediates also have diverse roles in *Saccharomyces cerevisiae*. These roles include signal transduction during the heat stress response, regulation of calcium homeostasis or components in calcium-mediated signaling pathways, regulation of the cell cycle, and functions as components in trafficking of secretory vesicles from the endoplasmic reticulum to the Golgi apparatus and as the lipid moiety in many glycosylphosphatidylinositol-anchored proteins. *S. cerevisiae* is likely to be the first organism in which all genes involved in sphingolipid metabolism are identified. This information will provide an unprecedented opportunity to determine, for the first time in any organism, how sphingolipid synthesis is regulated. Through the use of both genetic and biochemical techniques, the identification of the complete array of processes regulated by sphingolipid signals is likely to be possible, as is the quantification of the physiological contribution of each (Dickson and Lester, 1999).

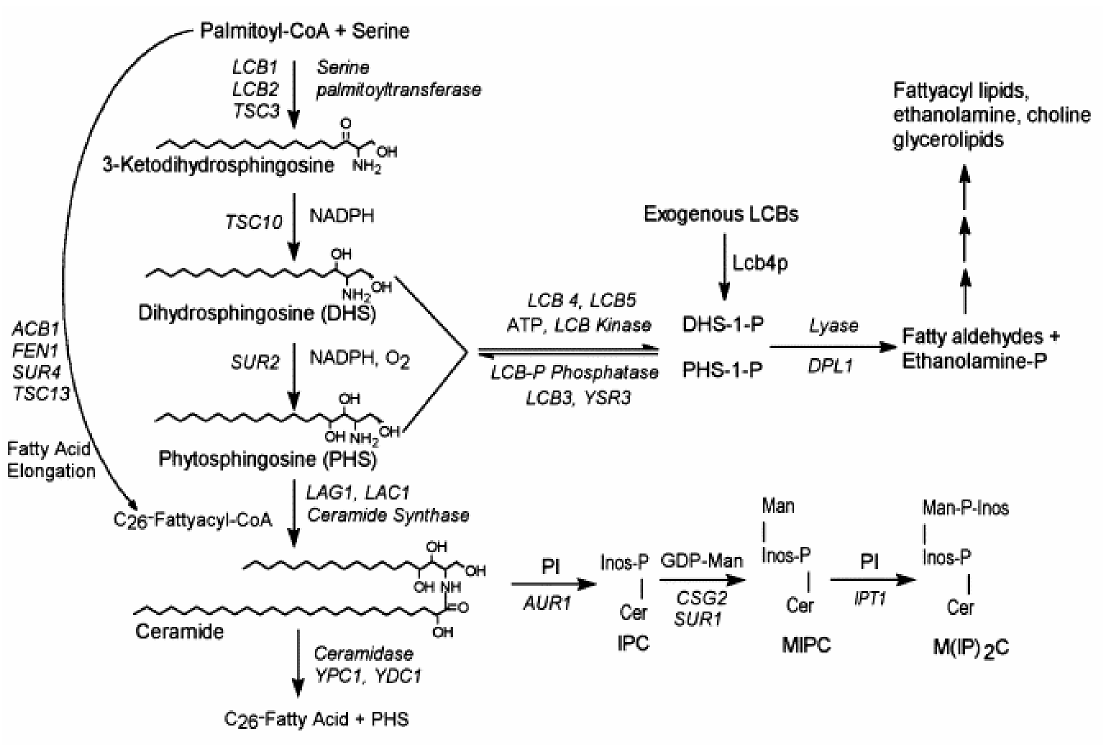

Figure 2.2. Metabolic Pathway of Sphingolipids *in Saccharomyces Cerevisiae*

Sphingolipids are essential components of the plasma membrane in all eukaryotic cells. *S. cerevisiae* cells make three complex sphingolipids (Figure 3.1): inositol-phosphoceramide (IPC), mannose-inositol-phosphoceramide (MIPC), and mannose-(inositol phosphate) 2-ceramide (M(IP)2C). In the yeast plasma membrane, sphingolipids concentrate with ergosterol to form lipid rafts, specialized membrane microdomains implicated in a variety of cellular processes, including sorting of membrane proteins and lipids, as well as organizing and regulating signaling cascades. Intermediates in sphingolipid biosynthesis have been shown to play important roles as signaling molecules and growth regulators. Sphingolipid long chain bases (LCBs), dihydrosphingosine (DHS) and phytosphingosine (PHS), have been implicated as secondary messengers in signaling pathways that regulate heat stress response. Other intermediates, phytoceramide and long-chain base phosphates (LCBPs), have been shown to be components of the tightly-controlled ceramide/LCBP rheostat, which regulates cell growth. Since phosphoinositol-containing sphingolipids are unique to fungi, the sphingolipid biosynthesis pathway is considered as a target for antifungal drugs (Dickson and Lester, 1999).

2.3. Sphingolipids in Mammalian

Sphingolipids are characterised by their sphingoid backbone. In mammalian cells, sphingosine is the most common sphingoid base, while in yeast and plant cells, phytosphingosine is more common. Sphingolipid biosynthesis represented in Figure 2.3, begins with the condensation of serine and palmitoylCoA forming 3-ketosphingosine which in turn undergoes reduction to dihydrosphingosine. A fatty acyl group is added by an amide linkage to form dihydroceramide, which is converted directly to ceramide, the precursor of all sphingolipids, by the introduction of a trans double bond between carbons 4 and 5 of the sphingoid base (Vance, 2002). Different headgroups may then be added to ceramide to form more complex sphingolipids, the simplest of which is ceramide-1-phosphate formed by ceramide kinase. More complex headgroups include linked glucose- or galactose-cerebrosides, the addition of a sulphate group to galactosylceramide yields sulphatides and di-, tri- and tetra-glycosylceramides are known as glycosphingolipids. Gangliosides are a subclass of glycosphingolipids identified by the presence of sialic acid in the carbohydrate headgroup (Huwiler *et al.*, 2000). The addition of phosphorylcholine to ceramide forms sphingomyelin (Vance, 2002). Lyso-sphingolipids, N-deacylated derivatives such as 1-galactosylsphingosine, glucosylsphingosine, sphingosine-1-phosphate and lysosphingomyelin are also found in mammals. These sphingolipids are present at very low concentrations but may have important signalling effects either as second messengers, e.g. sphingosine-1-phosphate, or through their lytic and membrane-destabilising effects (Hakamori and Igırashi, 1993).

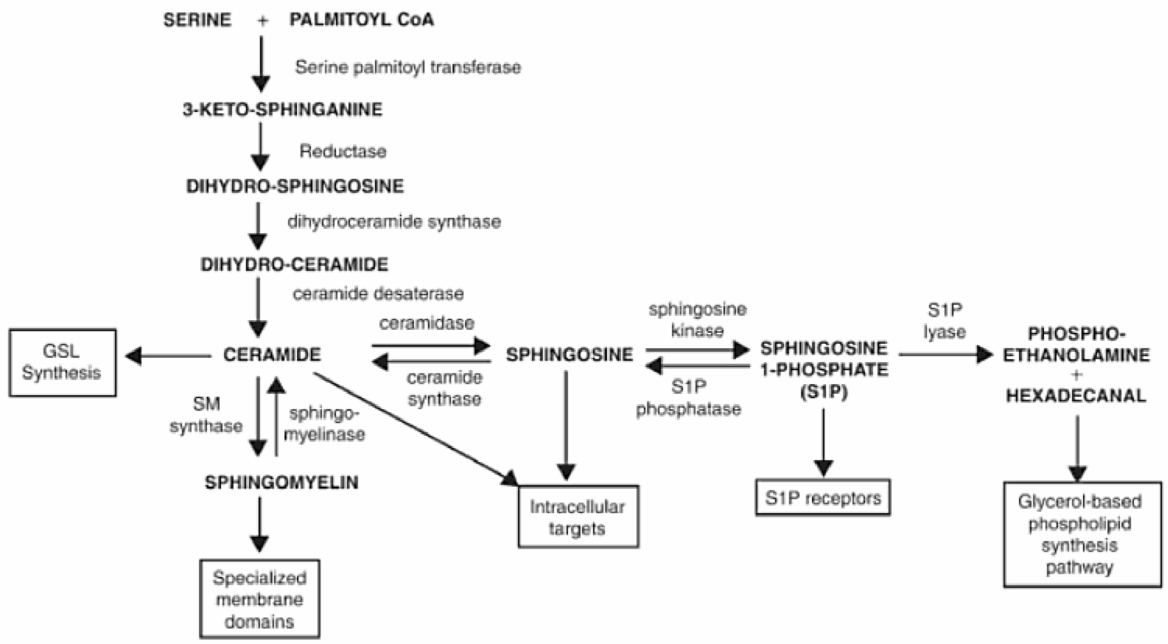

Figure 2.3. Sphingolipid Metabolism in Mammals

2.3.1. Sphingomyelin

Sphingomyelin is made up of a long-chain sphingoid base, predominantly D-erythro-sphingosine in mammalian cells, an amide-linked acyl chain which may be of long or intermediate length (Slotte, 1999) and a phosphorylcholine headgroup. The acyl chain composition varies between tissues; for example in the brain, white matter sphingomyelin contains predominantly nervonic acid (O'Brein and Sampson, 1965). In contrast, a mixed population of sphingomyelins appears to be present in non-neuronal cells (Slotte, 1999). Differences in the fatty acid composition of the amide-linked acyl side chain in sphingomyelins may have effects on membrane properties. For example, a predominance of saturated acyl chains contributes to the high phase transition temperature characteristics of sphingolipids (Koynova and Caffrey, 1995).

Sphingomyelin is present in most eukaryotic cell membranes. Subcellular fractionation studies indicate that greater than 50% of cellular sphingomyelin is located in the plasma membrane (Koval and Pagano, 1991). There is also evidence that in response to apoptotic stimuli or elevated intracellular calcium, phospholipid scrambling occurs such that sphingomyelin moves from the outer to the inner plasma membrane leaflet (Tepper *et al.*, 2000).

2.3.2. Ceramide

Activation of sphingomyelinases occurs in response to a variety of stimuli, including cytokines, antibody receptors, receptors, steroids, G protein-coupled receptors and cellular stress and ceramide has been implicated in apoptosis, cellular senescence, growth arrest and differentiation. The ceramide formed during cell stimulation can be further processed to sphingosine and sphingosine 1-phosphate (S1P), both of which are signalling molecules in their own right (Ohanian and Ohanian, 2001).

Ceramide levels may be reduced by the action of glucosylceramide and lactosylceramide synthases (Huwiler *et al*., 2000). Whilst considerable research into sphingomyelinases and the production of ceramide has been undertaken, fewer studies have investigated the regulation of the enzymes involved in its clearance.

De novo synthesis of ceramide is emerging as an important pathway for increasing ceramide levels in response to TNF and chemotherapeutic agents. Ceramide produced by this pathway is delayed, and ceramide synthase appears to be the regulated enzyme. De novo production of ceramide is implicated in cell cycle arrest and apoptosis. Other signalling events in which ceramide has been implicated include activation of MAPKs, inhibition of PI3K activation, regulation of smooth muscle tone, oxidative stress responses and nitric oxide signalling. The evidence that ceramide is an important second messenger in many cellular functions in response to diverse stimuli has been reviewed extensively (Ohanian and Ohanian, 2001).

2.3.3. Sphingosine and Sphingosine-1-Phosphate

Cell signalling functions have been ascribed to both sphingosine and S1P. Sphingosine has been shown to inhibit PKC and to stimulate cell growth and differentiation. S1P is implicated in migration, differentiation, mitogenesis and apoptosis (Spiegel and Merrill, 1996). Sphingosine is formed by deacylation of ceramide catalysed by ceramidases and because there is no evidence for de novo synthesis of sphingosine in mammalian cells, ceramidases may be important regulators of ceramide and sphingosine levels during agonist stimulation. Three main forms of ceramidase activity have been identified: acid, neutral and alkaline. Acidic and neutral ceramidases can be activated by cytokines, whereas alkaline ceramidase is stimulated by growth factors but not cytokines (Ohanian and Ohanian, 2001).

2.4. Functions of Sphingolipids

The functions of sphingolipids are still being discovered but the main three are, structure, recognition and signal transduction. Relatively simple sphingolipid metabolites, such as ceramide and sphingosine-1-phosphate, have been shown to be important mediators in the signaling cascades involved in apoptosis, proliferation, and stress responses (Hannun and Obeid, 2002). Sphingolipids are specific signalling molecules for cell-to-cell communication (mediator function) as well as for intracellular signalling processes (second messenger function). In addition, glycosylated sphingolipids are essential building blocks of rafts thereby participating in the initiation of receptor mediated signalling events. In immunology, processes such as T cell apoptosis, Th1 versus Th2, T cell differentiation, phagocytosis, and allergic excitability are either influenced or directly regulated by this class of lipids.

2.4.1. Sphingolipids in Cell Growth and Signalling

The suggestion that sphingolipids might be directly implicated in intracellular signaling pathways followed the discovery that sphingosine, a product of complex sphingolipid metabolism, inhibited protein kinase C (PKC) activity. In 1989 Hannun and coworkers first described the stimulus-regulated breakdown of sphingomyelin, named the "sphingomyelin cycle". According to this cycle the binding of a particular extracellular ligand to its receptor activated a plasma membrane-bound sphingomyelinase, giving origin to ceramide, the mediator of the intracellular effects of the ligand. This evidence stimulated several studies, and in recent years these have grown exponentially, revealing that different stimuli applied to cultured cells or animals elicit a series of metabolic events that result in the production of distinct sphingoid molecules which, in turn, participate in the intracellular signalling network. The relevance of sphingoid molecules as intracellular biomediators is highlighted by the observation that the activation of sphingolipid signaling can be mimicked in cell-free extracts, and that treatments leading to an increase in the intracellular concentration of specific sphingoid molecules can induce a biological response, mimicking the final biological effect of the stimulatory agent (Riboni *et al*., 1997).

Thus sphingolipid signalling is emerging as a sophisticated mechanism that is strictly integrated with other cellular signal pathways. The present picture of sphingolipid signalling is very complex and is characterized by (a) a plurality of activators, (b) the involvement of different metabolic pathways (even activated by the same stimulus) that produce the bioactive sphingoid molecule, (c) the production upon stimulation of different sphingoid biomediators (strictly connected in their metabolism) possessing biological, often diverse, activities, and (d) the existence of multiple interactions between the sphingolipid pathways and other cellular signalling systems, which include activation, cooperation, synergism and antagonism (Riboni *et al*., 1997).

2.4.2. Sphingolipids in Heat Stress

Sphingolipids are required for many cellular functions including response to heat shock. On heat stress, cells reduce the rate of synthesis of proteins that were expressed before the heat shock and change their transcription profile dramatically to produce mainly heat shock responsive proteins (Gasch *et al.,* 2000).

For example, heat stress in *S. cerevisiae* activates SPT and induces accumulation of sphingoid bases, their phosphates, and ceramides over a time frame of 10-120 min (Dickson and Leste, 1999). Evidence has been provided for a necessary role for this pathway in inducing the transient cell cycle arrest and the down-regulation of nutrient permeases seen in response to heat stress (Hannun and Obeid, 2002). Thus, strong parallels are emerging on the function of bioactive sphingolipids between mammals and yeast, and this promises significant insight generated from the combined use of genetics and biochemistry in probing the mechanisms of these pathways and their function (Hannun and Obeid, 2002).

2.4.3. Sphingolipids in Apoptosis

Ceramide (N-Acyl-Sphingosine) is the precuror of sphingophospholipids which are part of the cell membrane. Naturally occurring ceramides consist of a long-chain sphingoid base with an amid-linked fatty acid substituent (typically 16-24 carbon atoms long). There is evidence that the generation of ceramide by hydrolysis of sphingophospholipids (e.g. sphingomyelin) is associated with the induction of apoptotic cell death. Ceramide is generated in cells as a result of three distinct enzymes: neutral and acidic sphingomyelinase (N-SMase and A-SMase) and ceramide synthase (Hannun and Obeid, 2002).

Ligation of TNFR1 by TNF alpha or Fas receptor by FasL promotes activation of N SMase and A-SMase, leading to increased formation of ceramide. It is not clear if A-SMase or N-SMase is responsible for the generation of apoptosis-inducing ceramide. It was supposed that in TNF- or Fas-meditated apoptosis the apoptotic effect might be mediated by ceramide that was generated by A-SMase activity though it was also reported that Fas induces ceramide formation in the absence of functional A-Smase (Hannun and Obeid, 2002).

Other apoptotic stimuli, e.g. IFN-gamma, daunorubicin, radiation or serum withdrawal, also activate ceramide generation. Therefore, a conserved role for ceramide as a primary effector in apoptosis has been proposed. In support of this view, experimental manipulations that increase intracellular ceramide levels (e.g., overexpression of sphingomyelinase or treatment of cells with ceramide analogs like C2-ceramide = N-Acetyl-sphingosine) potently induce apoptosis in mammalian cells (Hannun and Obeid, 2002)

In some systems ceramide might mediate its apoptotic effect in combination with its metabolites, the sphingoid bases sphingosine and dihydrosphingosine (= sphinganine). In some systems (e.g. human neutrophils) only exogenous sphingosine, but not ceramide, induced apoptosis. Sphingosine and sphinganine inhibit the "conventional" and "novel" isoforms of PKC (cPKC/nPKC) and by this the MAPK cascade: by blocking this cytoprotective pathway, they might support the apoptotic effect of ceramide. In cooperation with N,N-dimethylsphingosine, sphingosine might also be involved in other events effecting apoptosis. Additionally, both ceramide and sphingosine promote dephosphorylation of the retinoblastoma gene product (RB) and by this Go/G1 cell cycle arrest. Sphingosine-1-phosphate (the initial intermediate product in the catabolism of sphingosine) was reported to prevent ceramide-mediated apoptosis (Igirashi, 1997)

2.5. Giardia Lamblia

Giardia lamblia is one of the most common parasites found in the intestinal tracts of vertebrates, including humans, and is the causative agent of giardiasis, an acute or chronic infection of the intestine. The binucleated parasite is found worldwide, but the incidence of giardiasis in humans is highest in developing countries, where the disease is a significant cause of morbidity, especially in children. In addition, giardiasis is regarded as one of the most common causes of traveler's diarrhea (Sonda *et al*., 2008).

Giardia lamblia can be distinguished from other *Giardia* species by light or electron microscopy. The two major genotypes of *G. lamblia* that infect humans are so different genetically and biologically that they may warrant separate species or subspecies designations. Trophozoites have nuclei and a well-developed cytoskeleton but lack mitochondria, peroxisomes, and the components of oxidative phosphorylation. They have an endomembrane system with at least some characteristics of the Golgi complex and endoplasmic reticulum, which becomes more extensive in encysting organisms. The primitive nature of the organelles and metabolism, as well as small-subunit rRNA phylogeny, has led to the proposal that *Giardia* spp. are among the most primitive eukaryotes. *G. lamblia* probably has a ploidy of 4 and a genome size of approximately 10 to 12 Mb divided among five chromosomes (Adam, 2001).

2.5.1. Classification of *G. Lamblia*

G. lamblia is a typical eukaryotic organism in that it has a distinct nucleus and nuclear membrane, cytoskeleton, and endomembrane system, but it lacks other organelles that are nearly universal in eukaryotes, such as nucleoli and peroxisomes. In addition, *G. lamblia* is anaerobic, lacking mitochondria or any of the components of oxidative phosphorylation. The hypothesis that eukaryotes arose through endosymbiotic events, resulting in the origin of plastids and mitochondria and the use of oxidative phosphorylation as the major source of energy production, has become widely accepted (Gray, 1989).

An appropriate classification for *Giardia* spp. is critical to an understanding of the pathogenesis and epidemiology of infection, as well as the biology of the organism. This process has been difficult for a number of reasons: (i) The (presumed) asexual nature of the organism does not allow mating experiments to allow species designation. For clonal organisms in the same clade, there are no well-defined criteria for species designation; these designations remain controversial. (ii) Many of the earlier descriptions of *Giardia* spp. assumed a different species for each host and consequently overestimated the number of species. Subsequent species descriptions based on morphologic differences detected by light microscopy have probably underestimated the differences among isolates, strains, or species. (iii) Cross-transmission experiments of *Giardia* from one host to another have yielded inconsistent results. (iv) The available tools for distinguishing *Giardia* isolates have been inadequate until the recent introduction of molecular and electron micrographic techniques for classifying *Giardia* spp. In view of these concerns, a review of the history of the description of *Giardia* and the designation of *Giardia* species is warranted (Adam, 2001).

Molecular classification tools have been of great value in understanding the pathogenesis and host range of *Giardia* isolates obtained from humans and a variety of other mammals. The first study of the molecular differences of *G. lamblia* isolates (Bertram *et al.*, 1983) was a zymodeme analysis of five axenized isolates, three from humans, one from a guinea pig, and one from a cat, using six metabolic enzymes. Zymodeme analysis consists of the typing of organisms based on the migration of a set of enzymes on a starch gel in the presence of an electric field. The migration depends on the size, structure, and isoelectric point of these enzymes. Since these properties are a function of the primary amino acid sequence, differences in the zymodemes should reflect differences in the sequences of the genes encoding these enzymes. Likewise, classification by surface antigens is limited by antigenic variation of the variant-specific proteins (VSPs).

These studies have been very useful, but the conclusions that can be drawn from these types of data are limited by the semiquantitative nature of the data (Adam, 2001)

2.5.2. Biochemistry and Metabolism of *Giardia lamblia*

2.5.2.1. Carbohydrate Metabolism. Most eukaryotic organisms depend primarily on aerobic metabolism for their energy production. However, certain eukaryotes, including *Trichomonas* spp., *Entamoeba* spp., and *Giardia* spp., are characterized by their lack of mitochondria and cytochrome-mediated oxidative phosphorylation. They rely on fermentative metabolism (even when oxygen is present) for energy conservation. Glycolysis and its brief extensions generate ATP, with generation dependent only on substrate level phosphorylation. Glucose is not completely oxidized to CO_2 and H_2O as in aerobic metabolism but is incompletely catabolized to acetate, ethanol, alanine, and CO_2. The balance of end product formation is sensitive to the O_2 tension and glucose concentration in the medium (Adam, 2001).

Acetyl-CoA can be converted directly to acetate by ADP-forming acetyl-CoA synthetase, resulting in the production of ATP from ADP as acetyl-CoA is converted to acetate. Alternatively, acetyl-CoA is converted to ethanol, using acetaldehyde as an intermediate, by the bifunctional enzyme alcohol dehydrogenase E (Dan and Wang, 2000). Alcohol dehydrogenase E has an acetaldehyde dehydrogenase activity in the amino terminus that catalyzes the conversion of acetyl-CoA to acetaldehyde and an alcohol dehydrogenase activity in the carboxy terminus that converts the acetaldehyde to ethanol (Adam, 2001).

2.5.2.2. Amino Acid Metabolism. Amino acids are becoming increasingly recognized as important components of the energy metabolism of *G. lamblia*. The uptake of aspartate, alanine, and arginine from the extracellular medium, as well as the documentation of glucose-independent metabolism, suggests the potential importance of amino acid metabolism for energy production in *Giardia* (Adam, 2001).

The arginine dihydrolase pathway is one potential source of energy (Edwards *et al*., 1992). This pathway is present in a number of prokaryotic organisms, but among the eukaryotes it has been documented only in *T. vaginalis* and *G. lamblia*. In the arginine dihydrolase pathway, arginine is converted to ornithine and ammonia with the generation of ATP from ADP by substrate-level phosphorylation. Ornithine is subsequently exported in exchange for extracellular arginine by a transporter mechanism (Adam, 2001).

Aspartate is another potential source of energy. It is converted to oxaloacetate by aspartate transaminase, entering the intermediary pathway, where it is converted to pyruvate via a malate intermediate. Alanine also appears to play an important role in allowing trophozoites to adapt to hypoosmotic challenge. This transporter acts as an antiport, exchanging intracellular alanine for these other amino acids from the extracellular environment (Adam *et al*., 2001).

2.5.2.3. Lipid Metabolism. The growth of trophozoites predominantly in the duodenum and jejunum initially suggested the possible importance of bile in the growth of *Giardia* trophozoites. Short-term axenic growth in the absence of serum can be supported by bile (Gillin *et al*., 1986). The biliary lipids cholesterol and phosphatidylcholine and the bile salts glycocholate and glycodeoxycholate will also support this growth (Gillin *et al*., 1986). Serum is required for longer-term axenic growth, but it has been shown that the Cohn IV-1 fraction of bovine serum (enriched in alpha globulins, lipoproteins, and growth factors) can substitute for whole serum. In fact, insulin-like growth factor II, which is present in fraction IV-1, stimulates trophozoite growth and cysteine uptake. The same fraction from a number of other mammals was also effective in supporting growth, although in some cases antibody depletion was required (Adam, 2001).

G. lamblia trophozoites do not have the capacity of de novo synthesis of fatty acids, with the possible exception of certain minor fatty acids (Ellis *et al*., 1996). However, free fatty acids are toxic to trophozoites. In fact, the toxicity of human milk for *G. lamblia* trophozoites appears to be mediated through products of milk lipolysis. The trophozoites appear to satisfy their lipid requirements by obtaining cholesterol and phosphatidylcholine from the external environment (Farthing *et al*., 1985). The cholesterol and phospholipids are supplied by lipoproteins, β-cyclodextrins, and bile salts, with transfer of lipids to the parasite surface being facilitated by bile salts. It has also been suggested that a low level of endocytosis of lipids occurs. Conjugated bile acids appear to be taken up by a carrier-mediated mechanism that includes different carriers for cholyltaurine and cholylglycine (Hoffman and Hagey, 2008).

The major fatty acids found in axenically grown trophozoites are palmitic acid, stearic acid, and oleic acid (Ellis *et al*.,1996). Fatty acid desaturase activity, including desaturation of oleate to linoleate and linolenate, has been documented (Ellis *et al*.,1996). Arachidonic acid is incorporated into neutral lipids, phospholipids, and a wide variety of cellular lipids, while palmitic acid, myristic acid, and oleic acid are transesterified primarily into phospholipids (Blair *et al*., 1987), including cellular phospholipids, (e.g., phosphatidylglycerol, phosphatidylcholine, phosphatidylethanolamine, and phosphatidylinositol). Interesterification also occurs with incorporation of conjugated fatty acids into phosphatidylglycerol (Gibbson *et al*., 1999). The toxicity of certain analogs of phosphatidylglycerol for trophozoites has been documented, although the mechanism of this toxicity has not been determined (Gibbson *et al*., 1999).

Isoprenoids are lipids derived from mevalonate that are commonly found in eukaryotic cells. The most notable end product is cholesterol, but isoprenoids are also incorporated into proteins such as the GTP-binding proteins by posttranslational modification. Isoprenylation of proteins has been demonstrated by the incorporation of radiolabeled mevalonate into trophozoite proteins. Incorporation of mevalonate and cell growth were inhibited in a reversible manner by competitive inhibitors of 3-hydroxy-3-methylglutoryl (HMG)-CoA reductase. Inhibitors of later steps of isoprenylation permanently inhibited cell growth (Adam, 1996).

Giardia has a very limited ability to synthesize sphingolipids de novo and depends on exogenous sources for energy production and other metabolic activities (Hernandez *et al*., 2008). Interestingly, however, it has been shown the inhibition of the activity of glucosylceramide (GlcCer) synthase by PPMP (1-phenyl-2-palmitoylamino-3-morpholino-1-propanol) inhibitor prevented the proliferation and differentiation of *G. lamblia* in a dose dependent manner (Sonda *et al.,* 2008). This result indicated that as-yet-uncharacterized sphingolipid biosynthetic pathways are potential drug targets for the development of anti-*G.lamblia* agents.

2.6. Mutant Strains

In our previous study, by using metabolic control analysis (MCA) and metabolic pathway analysis (MPA), we identified several drug target enzymes which are expected to induce apoptosis and thus can be employed in cancer therapy approaches. In the present work, the effects of these candidate enzymes on the sphingolipid metabolism was further investigated using deletion mutants (both experimental and in silico) of *S. cerevisiae*. The mutants used in this study was *Ugcg*Δ of *G. lamblia* and *Dpp1*Δ of *G. lamblia* and *S. cerevisiae.*

2.6.1. Diacylglycerol pyrophosphate phosphatase (DPP1) encoding gene and its function

As well as being present in plant cells, Diacylglycerol pyrophosphate (DGPP) phosphatase activity is also present in membrane fractions of Escherichia coli, Saccharomyces cerevisiae, and rat liver (Heim *et al.,*1987). Diacylglycerol pyrophosphate (DGPP) phosphatase is a novel membrane-associated enzyme that catalyzes the dephosphorylation of the β-phosphate of DGPP to yield phosphatidate and P (Wu *et al.*, 1996).

$$H_2O + \text{Phosphadidate} \text{ -> } \text{Diacyglycerol} + P \qquad (2.1)$$

DGPP phosphatase activity was associated with the 34-kDa protein. DGPP phosphatase had a broad pH optimum between 6.0 and 8.5 and was dependent on Triton X-100 for maximum activity. DGPP was the preferred substrate for the enzyme with a specificity constant 10-fold greater than that for phosphatidate. In addition, DGPP potently inhibited the dephosphorylation of phosphatidate by a competitive mechanism whereas phosphatidate did not inhibit the dephosphorylation of DGPP. DGPP was neither a substrate nor an inhibitor of pure phosphatidate phosphatase from *S. cerevisiae*. DGPP was synthesized from phosphatidate via the phosphatidate kinase reaction. (Wu *et al.*,1996).

Analyses of DGPP phosphatase mRNA and protein levels, and expression of β-galactosidase activity driven by a P_{DPP1}-*lacZ* reporter gene indicated that a transcriptional mechanism was responsible for this regulation. Phospholipid composition analysis of a *Dpp1*Δ mutant showed that DGPP phosphatase played a role in the regulation of phospholipid metabolism by inositol, as well as regulating the cellular levels of phosphatidylinositol (Toke *et al.*, 1998).

2.6.2. Glucosylceramide synthase encoding gene and its function

An important step in the sphingolipid biosynthesis pathways is the glucosylation of ceramide mediated by glucosylceramide (GlcCer) synthase. *Ugcg* catalyses the reaction of the synthesis of glucosylceramide from ceramide as follows:

UDP glucose + N Acylsphingosine(Ceramide) <=> UDP + Glucosylceramide (2.1)

GlcCer is the precursor of hundreds of different glycosphingolipids. This cerebroside is synthesized from uridine diphosphate-glucose and ceramide by a glucosyltransferase, GlcCer synthase. GlcCer-based sphingolipids have been identified as important mediators of a variety of cellular functions, including proliferation, differentiation, development, and cell-cell recognition (Hakamori and Igirashi, 1993).

Ugcg activities are stimulated by treatments which elevate the intracellular ceramide level such as the addition of bacterial sphingomyelinase, endoglycoceramidase, GlcT-1 inhibitors, or short chain ceramide. The gene spans approximately 32 kb and is composed of 9 exons and 8 introns. The promoter region was found to lack TATA and CAAT boxes but contains Sp1 binding sites, which are indicators of typical housekeeping genes. (Ichikawa *et al.*,1998).

3. MATERIALS AND METHODS

3.1. Materials

3.1.1. Microorganisms

BY4743 as parent strain Saccharomyces cerevisiae, and the homozygous deletion mutant of this strain *DPP1 Δ / DPP1Δ* were used in the experiments. The strains are provided by Prof. Stephen G. Oliver (Faculty of life Sciences, University of Manchester). The deletion mutant is generated by European *Saccharomyces cerevisiae* Archive for Functional Analysis (EUROSCARF).

3.1.2. Chemicals and Disposable Materials

3.1.2.1. Culture Media. In experiments, YPD complex medium in liquid form was used as the culture media. For YPD medium, Yeast Extract 1 per cent (Lab M), Bacteriological Peptone 2 per cent (Acumedia), D-Glucose 2 per cent (Merk), and for solid media Agar-Agar 1.8 percent (Merk) were mixed. Sterilized glucose is added separately to autoclaved YPD medium.

3.1.2.2. Glassware Required for the Analyses. Glass pipettes were used for pipetting purposes. Pasteur pipettes, micropipettes of volumes of 1-5, 10 and 20 µl, were purchased from Hirschmann Laborgerate. Pyrex centrifuge tubes of 100 ml were purchased from DuPont.

3.1.2.3. Buffers and Chemicals required for HPLC Applications. All sphingolipid standards were purchased from Sigma and Avanti Polar Lipids. HPLC grade chloroform, methanol, ethanol and n-hexane were obtained from Sigma.

Mobile phase which was required for HPLC analysis was as follows: HPLC grade chloroform ($CHCl_3$)/Ethanol (EtOH)/Triethylamine (TEA)/Formic Acid (FA) (90:10:1:1 v/v). The concentrations for TEA and FA were 70 and 220 mM, respectively.

3.1.3. Laboratory Equipment

Autoclave	ALP Model CL-40M (Japan)
Balance	Precisa 80A-200M (Switzerland)
Centrifuge	Avanti J-26 XPI Refrigerated Superspeed Centrifuge, Beckmann Coulter (USA)
Deep freezers	-80 ^{o}C, New Brunswick Scientific U410 (England) -20 ^{o}C, BOSCH (Germany)
Incubators	NUVE EN500 (Turkey)
Orbital Shakers	GFL3032, GFL (Germany) INNOVA 4340 Illuminated refrigerated Incubator Shaker, New Brunswick Scientific (USA) EXCELLA El Open air shaker, New Brunswick Scientific (USA)
HPLC System	1515 Binary IIPLC Pump, Waters (USA) 717 plus Autosampler, Waters (USA) 2420ELSD, Waters (USA)
Ovens	lncucell, MMM Group (Germany) VO 400 vacuum oven, Memmert (Germany)
Refrigerators	+4^{o}C Arçelik (Turkey)
Spectrophotometer	DU 640 Beckman (USA)
Water Purification Systems	Millipore, Milli Ro Plus (USA) Millipore, Milli-Q UF Plus (USA)

3.2. Methods

3.2.1. Experimental Methods

3.2.1.1. Sterilization. Sterilizatins were carried out to prevent contamination through the study. Generally, steam sterilization was preferred due to its short cycle time and good penetration properties. The sterilization was performed in the autoclave at 15 psig pressure and 121^{o}C. It is important to take into account the external contacts after sterilization, so some measures were also included in this step, such as sealing the necks of bottles.

The sterilization time is different for different materials. For example, for culture media and similar chemicals the duration of sterilization is 15 minutes. For glucose, on the other hand, taking into account the caramelization process that glucose undergoes at elevated temperatures, the sterilization time is 3 minutes. The glassware and plasticware used during the experiments are sterilized for 20 minutes.

3.2.1.2. Cultivation Conditions. All precultures were prepared in 150 ml of YPD medium. A single colony of cells from agar plates was used for inoculations which were done by flame sterilized inoculation needles. The precultures were incubated in orbital shakers at 30 ^{o}C and 180 rpm. The preculture was ready to be used at its late exponential phase for inoculation when the optical density was measured to be between 0 .9 and 1.1.

Batch cultivations were carried out in 500 ml Erlenmeyer flasks with a cultivation volume of 120 ml of YPD medium. The experiments were performed in orbital shakers at 30 ^{o}C and 180 rpm. l-2 ml of preculture was used to inoculate the culture. The pH was kept between 5.5 and 6.5. Samples were collected on an hour basis and checked whether steady state is reached, then steady state samples were collected at about 24th h of the experiment.

3.2.1.3. Lipid Extraction. In the extraction procedure which was kindly provided by Jens Nielsen's laboratory group, the cells were first harvested by centrifuging for 5 min at 3000 rpm and 4^{o}C and the supernatant was discarded. The pellet was resuspended in deionized water and the centrifugation was repeated and the sample was left to freeze at -20 ^{o}C overnight. Then 12 mL of $CHCl_3$: MeOH (1:2) was added to the frozen pellets and the samples were shaken for 3hr at 4^{o}C using Excella El benchtop open air shaker at medium speed. After three hours, 4mL $CHCI_3$ and 4mL 0.73% (w/v) NaCl were added. Samples were shaken again for about 15 minutes at medium speed. It was observed that two phases were formed and lower phase was taken with the aid of a Pasteur pipette and it was saved in another glass tube. 6ml of $CHCI_3$: MeOH (85:15) was added to the remaining cell extracts, samples were left overnight at 4 ^{o}C and the next day lower phase was collected. This step was repeated for two times. Finally, the solvent of the extracted lipids was evaporated at 40 ^{o}C under vacuum (~300 mb). Dried lipids were resuspended in 500 µL of $CHCI_3$: MeOH (2:1). All centrifugations were performed using Avanti J-26 XPI, Beckman-Coulter centrifuge with JA-14 rotor.

3.2.1.4. HPLC Analysis of the Extracted Lipids. HPLC analysis of lipids were performed using 3 µm C_{18} Silica column (4.6x150 mm) and a guard column of the same material (4.6x25mm) provided by Waters. The components of the HPLC system were described in part 3.1.4. and the parameters (McNabb *et al.*, 1999) used in the system are given in Table 3.1. ELSD detector was used with nitrogen gas at high pressure. Isocratic elution procedure was adopted in HPLC analysis.

Table 3.1. Parameters of the HPLC system

Flowrate (ml/min)	0.5
Column Temperature (^{o}C)	25
Drift Tube Temperature (^{o}C)	70
Gas Pressure (bar)	1.9

Various injection volumes were tried for sample analysis, and the optimum value for yeast lipid extracts was found to be 40 µl. Prior to injection, the column and guard column were washed with 20 column volumes of HPLC grade methanol, ~ 25 ml. While the column was being washed with methanol, the mobile phase, the composition of which was given in section 3.1.3.3, was prepared and degassed under helium sparging for about 20 min. The standards dissolved in HPLC grade chloroform and the extracted lipids to be analyzed were diluted so that the final analytes were chloroform/ethanol 9:1 (v/v).

The chromatography adopted in this study was a normal phase HPLC which was separating analytes based on polarity. The polar stationary phase was silica and the nonpolar mobile phase was $CHCl_3$/EtOH mixture. The polar analyte, i.e. lipid, was retained by the polar stationary phase. Adsorption strengths increase with analyte polarity, and the interaction between the polar analyte and the polar stationary phase (relative to the mobile phase) increases the elution time.

3.2.2. Computational Studies

<u>3.2.2.1. Pathway Construction.</u> In this study, for the construction of the sphingolipid pathway *S.cerevisiae* was first considered as a model organism. It is the first eukaryotic genome that was fully sequenced, annotated, and made publicly available and its sphingolipid pathway was studied previously (Sheikh *et al*., 2005).

Gene names and ORF names are determined by exploring the Kyoto Encyclopedia of Genes and Genomes database (Kanehisa *et al*., 2003). The nucleotide sequences/gene names are loaded to NCBI BLAST tool which gives the sequence similarities between *S. cerevisiae* and *G. lamblia* genes (Johnson *et al*., 2008). Different taxonomies such as *Giardia* (taxid:5740) (ATC catalog number 5740), *Giardia intestinalis* (ATC catalog number 5741), *Giardia Muris* (ATC catalog number 5742) and *Giardia lamblia* virus (ATC catalog number 29255) of *Giardia* species were examined for sequence similarity. The results are given in Appendix B. The highest similarity is observed in *G. lamblia* (ATCC catalog number 50803) and the treshold e-value is determined as 0.1 for both nucleotide and protein sequence similarities in selection of homologous proteins and resulting reactions.

In all organisms sphingolipid synthesis begins with condensing serine and palmitoyl-CoA to yield 3-ketodihydrosphingosine. This irreversible reaction is catalyzed by serine palmitoyltransferase (SPT, 3-ketodihydrosphingosine synthase; EC 2.3.1.50), a pyridoxal phosphate-containing enzyme that is the target of several potent natural inhibitors. For the activity of SPT, two genes, LCB1 and LCB2, are necessary and are thought to encode subunits of the enzyme (Nagiec *et al.,* 1994). The reduction of 3-ketodihydrosphingosine by an NADPH-requiring reaction yields the long-chain base dihydrosphingosine (sphinganine) (Dickson and Lester, 1999). The enzyme(s) and gene(s) necessary for catalyzing this step have not been identifed, and it remains one of the most poorly characterized reactions in the early part of the biosynthetic pathway.

Sphingosine is then amine-linked to yield dihydroceramide with a fatty acid with usually 26, sometimes 24 carbons long. The reaction is catalyzed by dihydrosphingosine (sphinganine) N-acyltransferase (ceramide synthase, LAG1). Hydroxylation of C_4 in the dihydrosphingosine component of dihydroceramide yields a ceramide (sometimes referred to as phytoceramide) containing the long-chain base phytosphingosine. Phytosphingosine is found in most fungal and plant ceramides (Dickson and Lester, 1999). It differs from the primary long-chain base, sphingosine, found in mammalian sphingolipids because it lacks a 4,5-double bond and has instead an hydroxyl on C4. Further phosphorylation of sphingosine leads to the production of sphingosine-1-phosphate or reincorporated into ceramide in mammalians, catalyzed by sphingosine kinase enzyme.

Since *G. Lamblia* is an eukaryotic organism and has been considered as “a more animal-like” of the unicellular eukaryotes as a member of protozoas, the reactions unique for *S. cerevisiae* and other fungi and plants are removed, but instead phosphocholine to form sphingomyelin and glucose or galactose conversion reactions were added (Futerman and Hannun, 2004). For an animal-like organism the crucial reactions in sphingolipid pathway are bioactive sphingolipids such as ceramide, glycosylceramide (GlcCer), sphingosine, and sphingosine-1-phosphate (S1P) which also act as bioeffector molecules, and play important roles in various aspects of cancer biology including apoptosis, cell proliferation, cell migration, senescence, and inflammation (Ogretmen and Hannun, 2004). In mammalians, ceramide was converted into either sphingomyelin (SM) catalysed by sphingomyelin synthase or cerebrosides such as glucosylceramide catalyzed by glucosylceramide synthase. Further phosphorylation of ceramide results in ceramide-1-phosphate catalysed by ceramide kinase enzyme. The considered reactions are added into the model by analysing other organisms such as *M. musculus* and *H. sapiens*. Similarity studies are also included for added reactions.

3.2.2.2. FBA. FBA has been shown to be a very useful technique for understanding cellular behavior. The reaction set in the model pathway were mathematically represented via a stoichiometric matrix, $\mathbf{S}_{m \times n}$, with rows presenting each metabolite (m metabolites) and columns presenting each reaction (n reactions). The entries in each column correspond to the stoichiometric coefficients of the metabolites (negative for reactants and positive for products) for each reaction. The i^{th} row of the matrix is the participation of a particular metabolite across all metabolic reactions, and the j^{th} column provides the stoichiometry of all metabolites in that reaction. Exchange fluxes were considered for metabolites that are typically exchanged with the environment (e.g., ATP, ADP, NAD[P], NAD[P]H etc.) and those that are not produced by the system, or those that are produced in the system for use in other metabolic pathways. Such metabolites, referred to as external metabolites, will have corresponding exchange fluxes in the pathway. The metabolites produced by the system are accounted as internal metabolites and they are consumed within the system itself. The external metabolites in the pathway model were identified manually.

FBA is based on a steady state approach for the system in question. The system can be governed by physicochemical constraints and optimized with respect to objective functions such as maximization of production of a choosen metabolite or minimization of consumption of nutrients (Edwards and Palsson, 2000). This flux distribution is then used to interpret the metabolic behavior of the system. Using the stoichiometric matrix which related the concentrations of metabolites $\mathbf{x}_{m \times 1}$ with enzymatic reactions, $\mathbf{v}_{n \times 1}$, the metabolic flux distribution is depicted as

$$\frac{dx}{dt} = S\,\mathrm{v} \qquad (3.1)$$

$$v = [v_1\, v_2 \, \dots \, v_n \;\; b_1 \;\; b_2 \dots \;\; b_{next}]^T \qquad (3.2)$$

For n number of metabolites, v_i representing the internal fluxes, b_i is symbolizing the exchange fluxes with external metabolites.

For steady state assumption, the system is solved for v, with null space S by designation of an optimization criterion for the under-determined system, and it becomes an LP problem.

$$\min_{\mathrm{v}} c^T \mathrm{v} \text{ s.t. } \mathrm{S}\ \mathrm{v} = 0 \tag{3.3}$$

where **c** represents the objective function, in terms of the fluxes. Further, we can constrain:

$$0 < v_i < \infty \tag{3.4}$$

$$-\infty < b_i < \infty \tag{3.5}$$

All the internal reactions are represented in positive direction and the external reactions are represented in both negative and positive directions. By thinking of cellular physiology a finite upper bound can be set. In our system, upper bound was set to hundered, which gave the relative fluxes effectively. The problem was solved by using MATLAB (http://www.mathworks.com/). The "linprog" routine from the Optimization Toolbox was employed which uses a large-scale interior point algorithm.

3.2.2.3. Perturbations. The perturbations onto the system are observed by the help of FBA analysis. The enzyme inhibition / gene deletion effects are analysed by constraining fixed values to the related fluxes. The upper and lower bounds are fixed as zero for the fluxes of responsible genes encoding the drug target enzymes.

4. RESULTS AND DISCUSSION

4.1. Experimental Results

To investigate the sphingolipid metabolism and solve its role on apoptosis, the wild type strain BY4743 and the homozygous deletion mutant DPP1Δ/ DPP1Δ were studied in batch experiments. The results stated here aim to gain further insight on sphingolipid mechanism and to quantify the sphingolipid species in *S. cerevisiae* with an ultimate goal of the determination of potential drug targets for the parasite *G. lamblia* by computational tools.

Table 4.1. Sphingolipid concentrations for BY4743 at steady-state (Börklü-Yücel, 2005)

Metabolite	Concentration (mol%)
DHS	0.0100
D-Cer	0.036
DHS-P	0.0010
PHS	0.0500
PHS-P	0.0050
P-Cer	0.0520
IPC	0.1020
MIPC	0.1400
$M(IP)_2C$	0.0085

The sphingolipid concentrations for wild type yeast strain in mole per cents, the concentrations of sphingoid bases or phosphatidate over the concentration of total phospholipids, were available in literature (Table 4.1) which enabled the lipid identification and annotation processes.

The strains were grown in YPD medium. The experiments were carried out batchwise in 500 ml erlenmeyer flasks with a working volume of 110 ml at 30 ^{o}C and 180 rpm.

For the quantification and qualification of yeast sphingolipids, standards of PHS, C18-DHS, C20-DHS, P-Cer, C2-Cer, C6-Cer and C8-Cer were used. Calibration curves were built before according to these standards. The peak chromatograms of these standards according to injection volumes and retention times were loaded to the HPLC software.

4.1.1. Sphingolipid Profile of the Wildtype Strain BY4743

Wild type strain was grown in YPD medium which is a rich medium in terms of amino acids such as serine, or other vital compounds, such as inositol, also present in the yeast extract in unknown amounts. Sphingolipid chromatogram of wild type strain grown in YPD medium is given in Figure 4.1. According to this chromatogram, some of the peaks which had retention time values matching with the standards tested were identified.

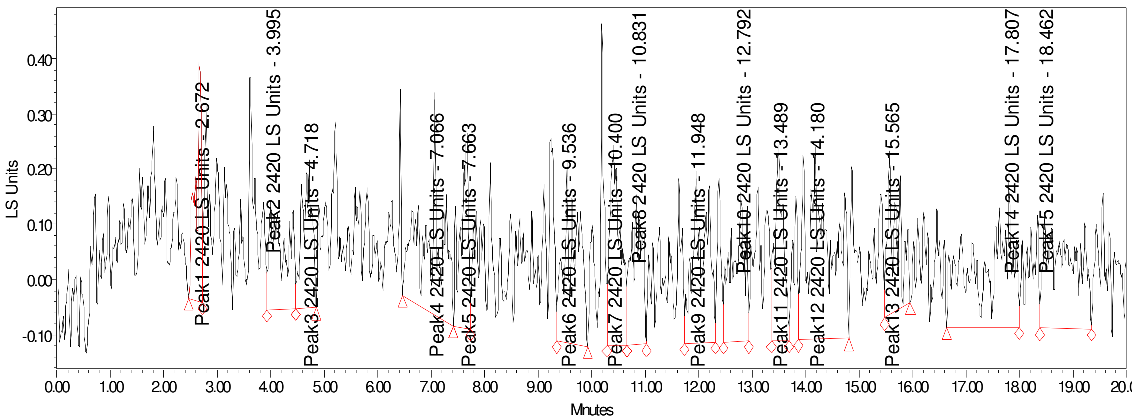

Figure 4.1. Chromatogram of BY743 grown in YPD

C8-Cer was attributed to IPC and C2-Cer was attributed to DHS-P in yeast because of the polarity similarities between these compounds. The groups required for the polarity of C8-Cer and IPC, -OH groups and =O bond, were quite in accordance with each other. When the polarity due to =O group in C2-Cer and DHS-P were compared, it was noticed that they were also similar. Beside the polarity, the molecular weights were also close to each other, which rendered the detection of DHS-P in yeast by the presence of C2-Cer peaks in its chromatogram.

Table 4.2. Summary of sphingolipid profiles of BY4743 grown in YPD

Peaks	Retention Time (min)	Area (μVxsec)	Standard matched	Experimental Concentration (mM)	Possible Compound
1	2.672	3264			
2	3.995	3932			
3	4.718	3296	C8-Cer	0.077427236	IPC
4	7.066	6826	PHS	0.007844787	PHS
5	7.663	3336	P-Cer	0.001932716	P-Cer
6	9.536	5388			
7	10.4	4873	C2-Cer	0.0000284841	DHS-P
8	10.831	3590			
9	11.948	5406			
10	12.792	4321			
11	13.489	3725			MIPC
12	14.18	10309	C18-DHS	0.000355616	DHS
13	15.565	3696			
14	17.807	8949			$M(IP)_2C$
15	18.462	7203			D-Cer

It can be observed from both Figure 4.1 and Table 4.2 the peaks matched with the standards meaning the existence of related sphingolipids in rich medium with glucose and other components at high concentrations.

4.1.2. Sphingolipid Profiles of DPP1 Deletion Mutant

Homozygous deletion mutant was also grown in YPD medium. The comparision of the two figures (Figure 4.2 and 4.1) and two tables (Table 4.2 and 4.3) with represented results showed that complex sphingolipids can be observed for both the mutant strain and the wild type strain. The amounts of MIPC, $M(IP)_2C$ and D-Cer in deletion mutants were calculated with respect to the values of wild type strain. An assumption was made that the concentrations of these compounds changed linearly with the peak areas. Then, from the calculated experimental values of MIPC, $M(IP)_2C$ and D-Cer in wild type strain grown in

YPD, the concentrations belonging to the mutant strain was calculated on the basis of the above assumption. So considering the areas there is an increase in the production of D-Cer and the concentrations also reflect a distinct increase in dihydrosphingosine favoring the increase of ceramide production. Other complex sphingolipids, MIPC and M(IP)$_2$C, similarly increase in concentrations considering the increase in the areas of the peaks for *DPP1Δ/ DPP1Δ* mutant.

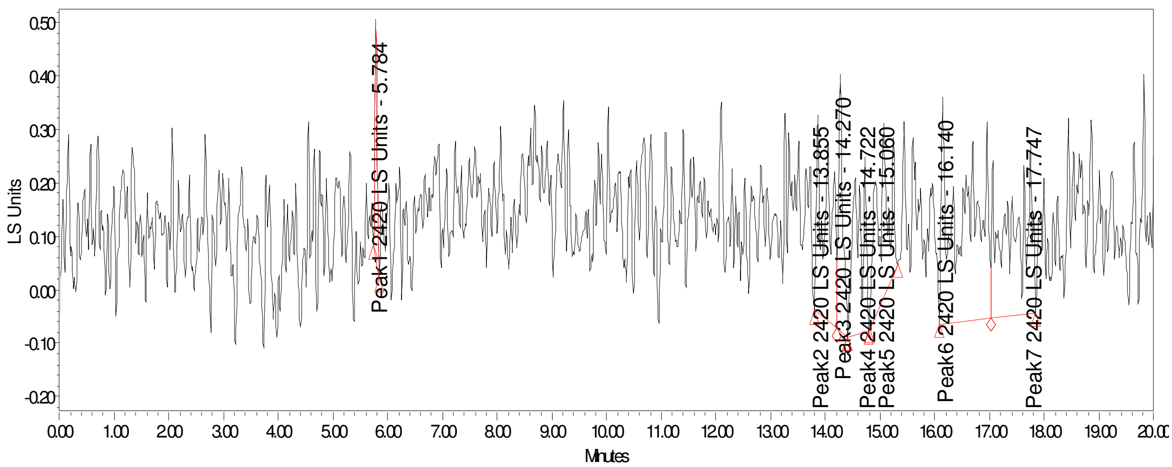

Figure 4.2. Chromatogram of DPP1Δ/DPP1Δ grown in YPD

Table 4.3. Sphingolipid profiles of DPP1Δ/DPP1Δ deletion mutant grown in YPD

Peaks	Retention Time (min)	Area (μVxsec)	Standard matched	Experimental Concentration (mM)	Possible Compound
1	5.784	1188	C8-Cer	0.027776	IPC
2	13.855	5031		0.002110	MIPC
3	14.27	2588			
4	14.722	3975			
5	15.06	4551	C18-DHS	0.001509	DHS
6	16.14	11068		0.001047	M(IP)$_2$C
7	17.747	7710		0.002372	D-Cer

4.2. Modelling Studies

4.2.1. Model Description

The pathways related to the biosynthesis of ceramide in *G. lamblia* were constructed using three organisms: *S. cerevisiae*. *H. sapiens* and *M. musculus.* The reference (no organism specific representation) pathway shows the reactions involved in sphingolipid metabolism considering all organisms. The pathway is investigated in three parts, (A) *de novo* (sphinganine related reactions), (B) Sphingosine related reactions, (C) Ceramide related reactions.

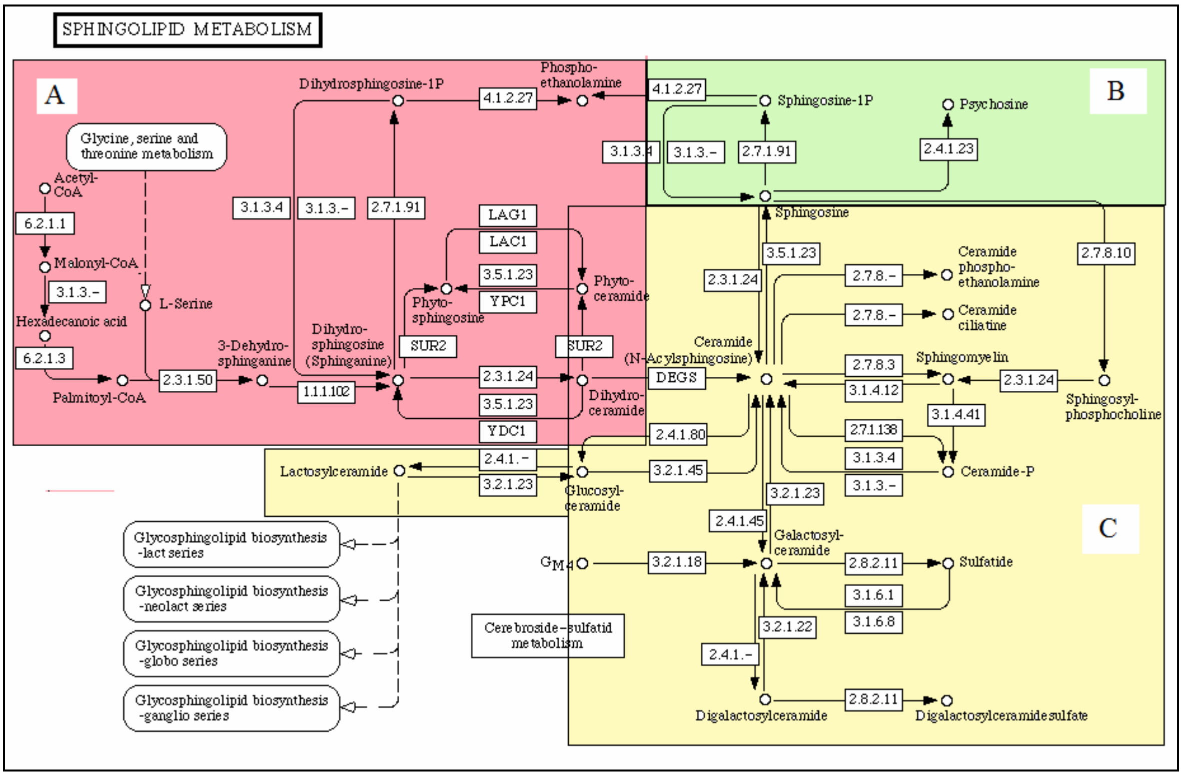

Figure 4.3. Reference pathway for Sphingolipid metabolism (KEGG)

Regarding only the first model organism, *S. cerevisiae,* the pathway is constructed until the dihydroceramide synthesis because the complex sphingolipids are different in higher organisms. The three *myo*-inositol-containing sphingolipids in *S. cerevisiae* (Figure 4.3) are inositol-phosphoceramide (IPC), mannose-inositol-phosphoceramide (MIPC) and mannose-(inositol-P)$_2$-ceramide (MIP$_2$C) (Dickson *et al.*,1999). They are fungi specific metabolites. So this part of the pathway is specific for *S. cerevisiae* and it also lacks the ceramide synthesis part of the pathway. Therefore, for an animal- like organism, *G. lamblia,* other organisms, *H. Sapiens* and *M. musculus*, are taken into account in order to construct the sphingosine and ceramide pathways of the sphingolipid metabolism.

<u>4.2.1.1. Sphinganine related reactions.</u> De novo biosynthesis of sphingoid bases begins with the condensation of palmitoyl-CoA with serine, to form 3-ketosphinganine with release of a CO_2 molecule. 3-Ketosphinganine is reduced to sphinganine by the action of a NADPH (H +)-dependent oxidoreductase which is a very potent enzyme responsible for the apparent undetectability of 3-ketosphinganines in vivo (Stoffel *et al.,* 1968).

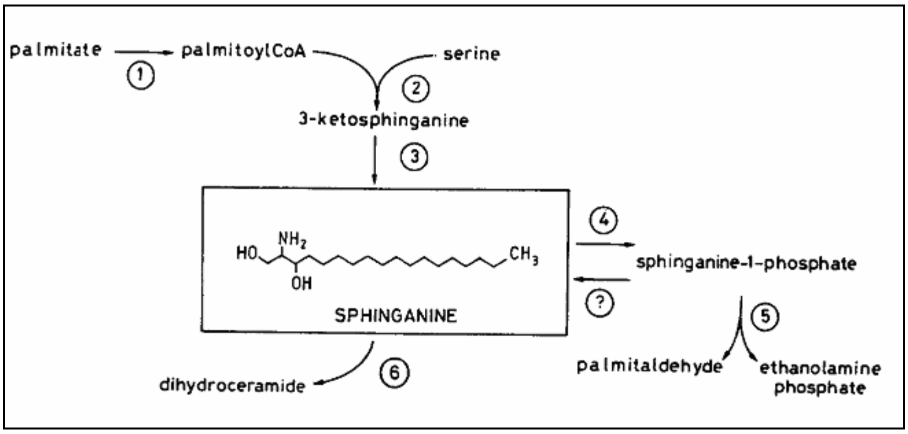

Figure 4.4. Sphinganine metabolism

Sphinganine is converted to dihydroceramide (N-acyl-sphinganine) by the acyl-CoA:sphingoid base N-acyltransferase (dihydroceramide synthase) that uses as the acyl donor, fatty acyl-CoAs and appears to be present in multiple forms, having different substrate specificity and tissue distribution (Ullman *et al.,* 1972).

The beginning of the pathway is assumed to be the same for *G. lamblia* by studying the similarities of nucleotide and protein sequences of the related enzymes catalyzing the above mentioned reactions.

Table 4.4. BLAST results for suggested reactions of de novo part of the pathway

Rxn No	Org.	Enzyme Name	EC Number	Protein-Protein Blast/ Nucleotide Blast (*G. lamblia*)		e value	EC Number
1	sce	palmitoyl-CoA synthase	6.2.1.3	pblast	Long chain fatty acid CoA ligase 5	1e-53	6.2.1.3
2	sce	serine C-palmitoyltransferase	2.3.1.50	pblast	Serine palmitoyltransferase 2	7e-28	2.3.1.50
3	sce	3-Dehydrosphinganine reductase	1.1.1.102	pblast	Hypothetical protein GL50803_13942	0.061	-
4	sce	sphingosine-1-phosphate phosphatase 1	3.1.3.-	pblast	Methionyl-tRNA synthetase	1.0	6.1.1.10
5	sce	Sphinganine-1-phosphate aldolase	4.1.2.27	pblast	Cysteine desulfurase	0.041	4.4.1.-
6	sce	Ceramide-1 synthase (26C)	2.3.1.24	pblast	Hypothetical protein GL50803_5939	0.00003	-

As we can see from Table 4.4, for the initial part of the sphingolipid pathway, the Blast results of the first two reactions are quite high and the EC numbers are the same for the enzymes in *G. lamblia*. As the threshold for the e value is considered to be 0.1, the hypothetical proteins were accepted despite their low similarities. For the fourth reaction, however, the enzyme obtained from BLAST analysis was not used in the reconstructed reaction system for *G. lamblia* due to its very low similarity score and the distinctions in EC numbers also indicated that the functions of the enzymes are different. For the fifth reaction in spite of the considerable similarity value, the enzyme cysteine desulfurase found by blast study has sulfur removal function catalyzing cysteine alanine synthesis and therefore can not be regarded as the part of the pathway in *G. lamblia*. So the existence of the above mentioned enzymes catalyzing the reactions numbered as 1,2,3 and 6 are assumed to be proved for *G. lamblia*. The first four reactions of the pathway are taken from the genome scale model of yeast (Forster *et al.,*2005).

<u>4.2.1.2. Sphingosine related reactions.</u> The dihydroceramide is unsaturated at the 4,5 position of the sphingoid base tail, by the action of a NAD-dependent oxidoreductase with the formation of ceramide. The sphingolipid delta-4 desaturase enzyme catalyses this reaction. By looking at Table 4.5, the blast analysis gives a hypothetical protein for that enzyme, however the e value is lower than 0.1, so the reaction can be a part of sphingosine metabolism in *G. lamblia*. The reactions considered and the numbers of related reactions are represented in Figure 4.5. For the reactions numbered as seven and eight, the blast

results are acceptable and these hypothetical proteins and the reactions are included in the pathway.

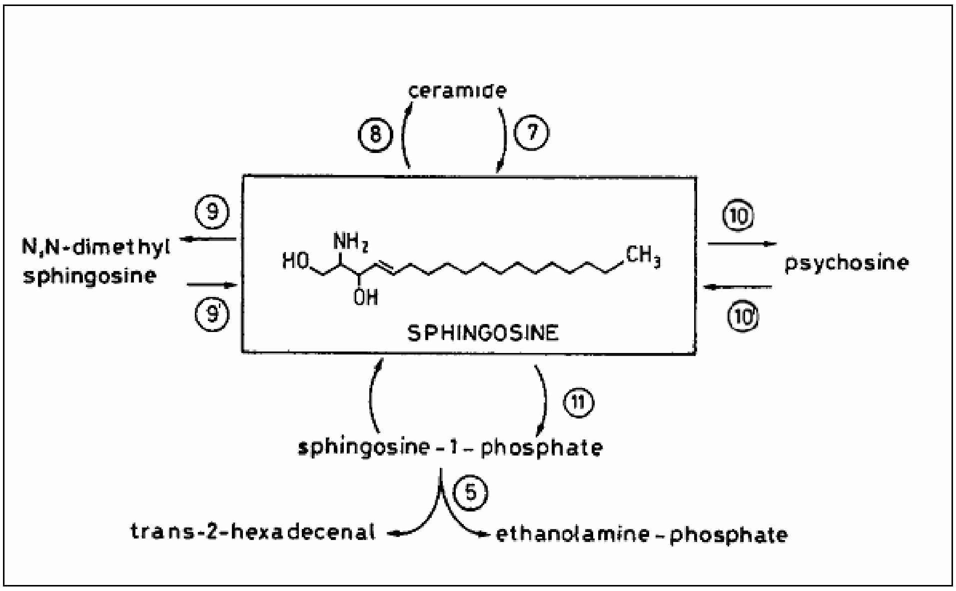

Figure 4.5. Sphingosine metabolism

Table 4.5. BLAST results for the suggested reactions of sphingosine

Rxn No	Org.	Enzyme Name	EC Number	Protein-Protein Blast/ Nucleotide Blast (*G. lamblia*)		e value	EC Number
	mmu	sphingolipid delta-4 desaturase	1.14.-.-	nblast	Hypothetical protein (GL50803_17174)	0.013	-
7	mmu	N-acylsphingosine amidohydrolase	3.5.1.23	nblast	Hypothetical protein (GL50803_14242)	0.038	-
8	hsa	ceramide synthase	-	pblast	Hypothetical protein (GL50803_5939)	1e-8	-
11	mmu	Sphingosine Kinase	2.7.1.91	pblast	Kinase	0.21	-
5	sce	Sphinganine-1-phosphate aldolase	4.1.2.27	pblast	Cysteine desulfurase	0.041	4.4.1.-

N,N dimethyl sphingosine synthesis reaction (r9) catalysed by sphingosine-N-methyltransferase and psychosine synthesis reaction (r10) catalysed by sphingosine galactosyltransferase are not found as the part of the sphingolipid pathway for both *M. musculus* and *H. sapiens* (in KEGG pathway). So enough information was not avaliable for the ninth and tenth reactions. The phosphorylation of sphingosine could have been considered to be taking place in *G. lamblia,* since the e-value obtained from the blast result was relatively low and indicated the same protein. However although the blast result pointed some resemblance, the aldolase have different activity than desulfurase, so the aldol reactions are not considered in the constructed pathway.

As a result, the sphingosine related pathway included the sphingosine synthesis from ceramide and further phophorylation of sphingosine.

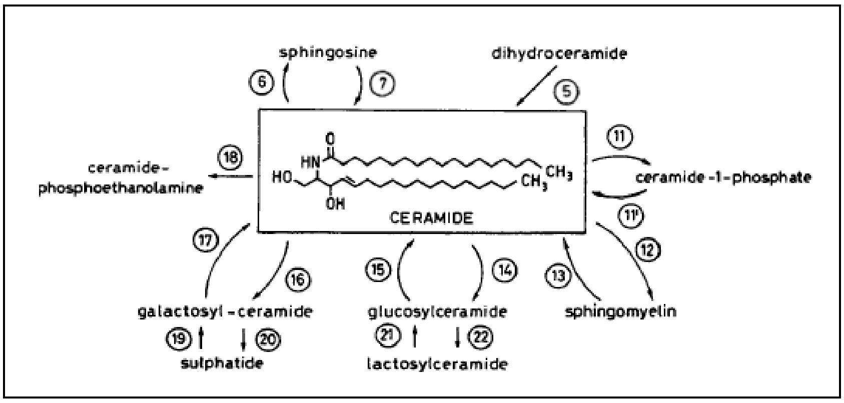

Figure 4.6. Ceramide related reactions

<u>4.2.1.3. Ceramide related reactions.</u> As a central metabolite, ceramide is converted to complex sphingolipids, by the addition of different head groups. The simplest of which is ceramide-1-phosphate formed by ceramide kinase. The Blast results for this enzymatic reaction give an e-value relatively close to treshold which is an acceptable result for this system. Current studies point to sphingomyelin as the major precursor for ceramide and to sphingomyelinase as the major enzyme responsible for ceramide generation. Sphingomyelin synthesis reaction is catalysed by ceramide choline phosphotransferase in *M. musculus*. By considering Blast result the homologous hypothetical protein is acceptable for *G. lamblia*. The reaction is reversible and the break down of phosphocholine is catalysed by phosphodiesterase enzyme in *G. lamblia*.

Table 4.6. BLAST results for the suggested reactions of ceramide

Rxn No	Org.	Enzyme Name	EC Number	Protein-Protein Blast/ Nucleotide Blast (*G. lamblia*)		e value	EC Number
11*	mmu	ceramide kinase	2.7.1.138	pblast	Multidrug resistance-associated protein 1	0.91	
11'	hsa	phosphatidate phosphatase	3.1.3.4	-	-	-	-
12	mmu	Ceramide choline phosphotransferase	2.7.8.3	pblast	Hypothetical protein GL50803_35341	0.12	-
13	mmu	Sphingomyelin phosphodiesterase	3.1.4.12	pblast	Acid sphingomyelinase-like phosphodiesterase 3b precursor	1e-16	3.1.4.-
14*[1]	hsa	UDP-glucose ceramide glucosyltransferase	2.4.1.80	nbast	Multidrug resistance assoc. protein Mrp2	0.67	-
				pblast	Ceramide glucosyltransferase	4.6	-
15	hsa	acid beta glucosidase	3.2.1.45	nblast	Protein 21.1	0.075	-
16	mmu-hsa	UDP-glycosyltransferase	2.4.1.45	nblast	Hypothetical protein (GL50803_20517)	0.076	-
17	mmu	Galactosidase	3.2.1.23	pblast	Hypothetical protein (GL50803_14242)	0.095	-
18	mmu	-	-	-	-	-	-
19	mmu	arylsulfatase A	3.1.6.8	nblast pblast	-	-	-
20	mmu	galactose-3-O-sulfotransferase	2.8.2.11	nblast pblast	-	-	-
21	mmu	fucosyltransferase 4	2.4.1.-	nblast	Hypothetical protein (GL50803_2167) partial mRNA	0.005	-
22	mmu	Galactosidase	3.2.1.23	pblast	Hypothetical protein (GL50803_14242)	0.095	-

*[1] Sonda et al., 2008

Another step in the sphingolipid biosynthesis is the glucosylation of ceramide mediated by glucosylceramide (GlcCer) synthase in both *H. sapiens* and *G. lamblia*. However, the sequence analysis result by BLAST gives a relatively high e-value. But the presence of this enzyme in *G. lamblia* is justified by indirect experimental evidence (Sonda *et al*., 2008). Higher glycosylation of glycosyl ceramide gives lactosyl ceramide. Based on the sequence annotations galactosylceramide synthesis also occurs in *G. lamblia*. The addition of a sulphate group to galactosylceramide yielding sulfatides is not considered for this organism.

The final form of the constructed pathways with the above explained reactions based on the sequence annotations and experimental results for sphingolipid metabolism in *G. Lamblia* is presented in Figure 4.5.

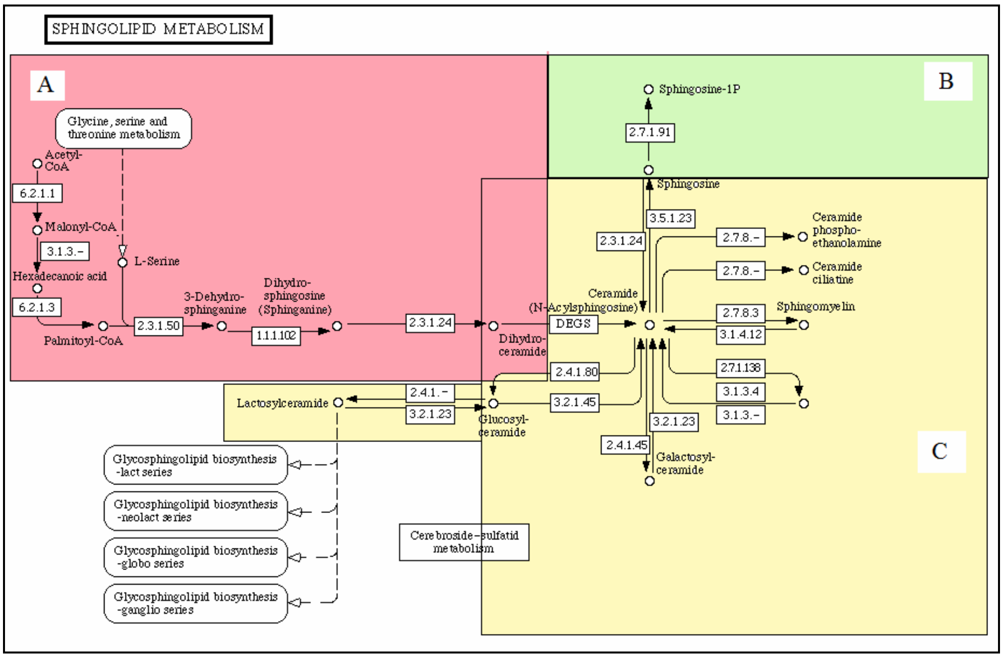

Figure 4.7. Pathway with 20 reactions for *G. Lamblia* without considering the reaction catalyzed by the enzyme encoded by DPP1 gene

<u>4.2.1.4. Additional reactions.</u> As a part of the sphingolipid metabolism, acyl transferation of acyl-CoA was also taken into account when the metabolite palmitoyl-CoA was considered for the synthesis of phosphatidate. DGPP phosphatase (DGPP phosphohydrolase) is a membrane-associated 34-kDa enzyme from *Saccharomyces cerevisiae* and it catalyzes the dephosphorylation of DGPP to yield phosphatidate (PA) and then catalyzes the dephosphorylation of PA to yield diacylglycerol (Toke *et. al.,* 1998).

In the experimental part of the study, the effect of DPP1 gene on ceramide synthesis was found to be important in *S. cerevisiae*. The enzymatic reaction was also considered in the genome scale model of the organism *M. musculus* (Sheikh *et al.*,2005). When DPP1 is functionally investigated it is a phosphatidate phosphatase. The homologous enzymes in *M. musculus* and *G. lamblia* were searched by BLAST analysis (Table 4.7) and the results show an acceptable value for *M. musculus* for the existence of the responsible enzyme of diacylglycerol synthesis when DPP1 gene in *S. cerevisiae* was taken as the query.

Nevertheless, due to the importance of the enzyme encoded by DPP1 gene, that particular reaction (r22) was included into the sphingolipid pathway constructed for *G. lamblia*.

Serine participates in *de novo* biosynthesis metabolism. It is further converted to choline by choline kinase and phophocholine by cytidyltransferase enzymes considering the addition of phosphocholine to ceramide for the synthesis of sphingomyelin.

Table 4.7. BLAST results for the additional reactions

Rxn No	Org.	Enzyme Name	EC Number	Protein-Protein Blast/ Nucleotide Blast(*G. lamblia*)		e value	EC Number
21	mmu	1-acylglycerol-3-phosphate O-acyltransferase	2.3.1.51	pblast	Lysophosphatidic acid acyltransferase	3e-53	-
22	mmu	Lipid phosphate phosphohydrolase 2	3.1.3.4	pblast	Kinase, CMGC SRPK	0.11	-
19	sce	Phosphoserine phosphatase	3.1.3.3	nblast	Kinase, CMGC DYRK	0.043	-
23	sce	phosphatidylserine synthase	2.7.8.8	pblast	Hypothetical protein GL50803_17427	3e-05	-
24	mmu	choline kinase	2.7.1.32	pblast	Ethanolamine kinase	3e-06	
25	hsa	phosphate Cytidyltransferase 1, Choline, alpha isoform	2.7.7.15	nblast	Hypothetical protein (GL50803_137754)	0.054	-

Finally, the model pathway constructed consists of 25 reactions and 45 metabolites through 24 proteins as demonstrated in Figure 4.6. Data related to 24 genes encoding the enzymes catalyzing the pathway reactions are shown in Table 4.8. The list of reactions has also been given in Table 4.9.

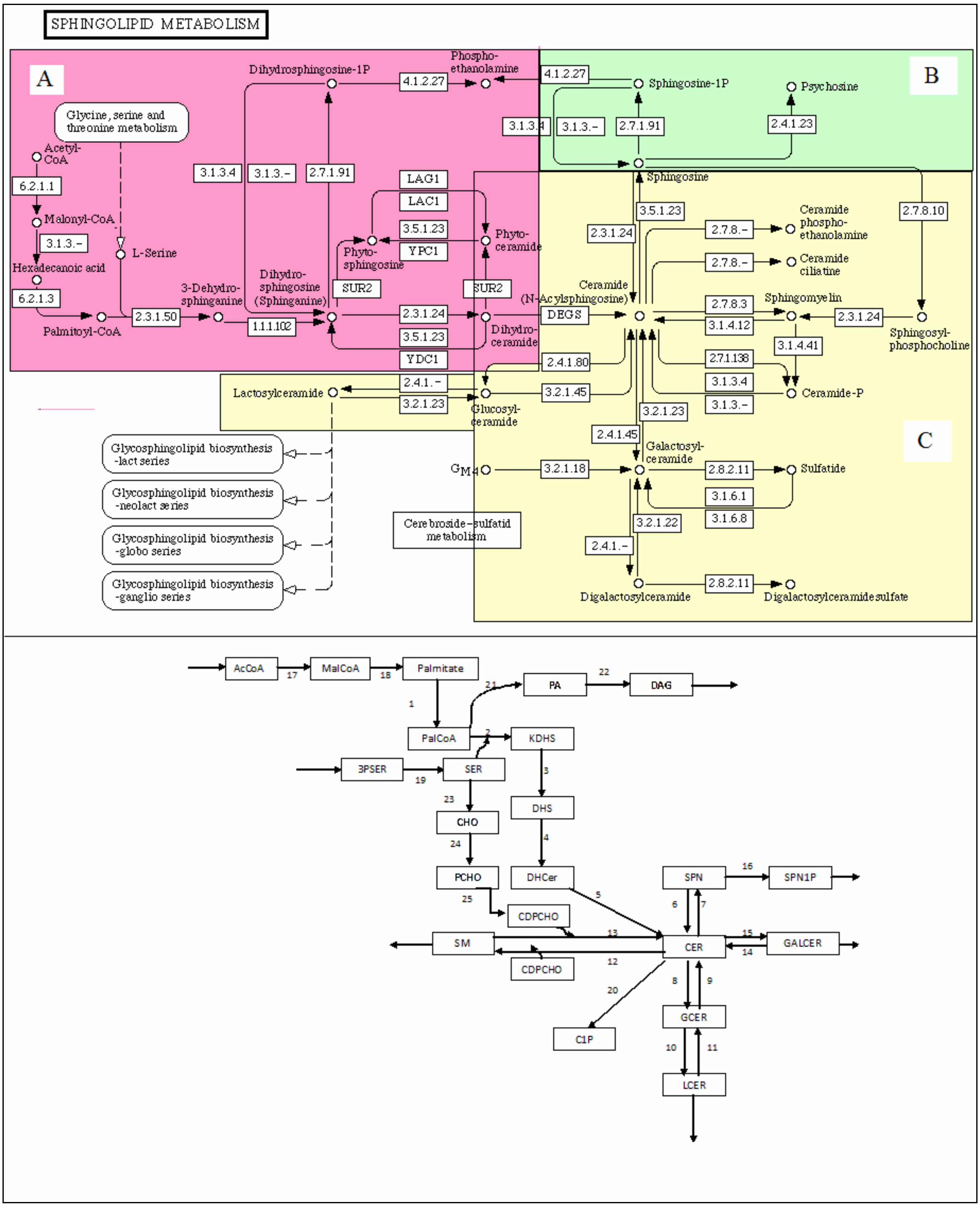

Figure 4.8. Final form of the reconstructed sphingolipid metabolism of 25 reactions

Table 4.8. The enzymes catalyzing the reactions in sphingolipid metabolism in *G. lamblia*

#	Gene	SwissPROT/ Accesion Number	Gene ID	Reactions	References
1	Long chain fatty acid CoA ligase 5	A8BC93	GL50803_17170	1	Morrison et al, 2007
2	Serine palmitoyltransferase 2	A8BTC0	GL50803_14374	2	Morrison et al, 2007
3	Hypothetical protein GL50803_13942	A8BIJ0	GL50803_13942	3	Morrison et al, 2007
4	Cysteine desulfurase	A8B326	GL50803_14519	4	Morrison et al, 2007
5	Hypothetical protein GL50803_5939	A8BKJ1	GL50803_5939	5	Morrison et al, 2007
6	Hypothetical protein (GL50803_17174)	A8BCA2	GL50803_17174	6	Morrison et al, 2007
7	Hypothetical protein (GL50803_14242)	A8BIU7	GL50803_14242	7	Morrison et al, 2007
8	Hypothetical protein (GL50803_5939)	A8BKJ1	GL50803_5939	8	Morrison et al, 2007
9	Glycine-, glutamate- ,thienylcyclohexylpiperidine -binding	A8BDW2	GL50803_16818	9	Morrison et al, 2007
10	Cysteine desulfurase	A8B326	GL50803_14519	10	Morrison et al, 2007
11	Multidrug resistance-associated protein 1	A8B3T0	GL50803_28379	11	Morrison et al, 2007
12	Hypothetical protein GL50803_35341	A8BAV7	GL50803_35341	12	Morrison et al, 2007
13	Acid sphingomyelinase-like phosphodiesterase 3b precursor	A8BRU8	GL50803_8360	13	Morrison et al, 2007
14	Ceramide glucosyltransferase	A8BXJ1	GL50803_11642	14	Morrison et al, 2007
15	Protein 21.1	A8BQR2	GL50803_24194	15	Morrison et al, 2007
16	Hypothetical protein (GL50803_20517)	A8B3G5	GL50803_20517	16	Morrison et al, 2007
17	Hypothetical protein (GL50803_14242)	A8BIU7	GL50803_14242	17	Morrison et al, 2007
18	Hypothetical protein (GL50803_2167) partial mRNA	A8B4J6	GL50803_2167	18	Morrison et al, 2007
19	Hypothetical protein (GL50803_14242)	A8BIU7	GL50803_14242	19	Morrison et al, 2007
20	Lysophosphatidic acid acyltransferase	A8BGW5	GL50803_14403	20	Morrison et al, 2007
21	Kinase, CMGC SRPK	A8BKE0	GL50803_17335	21	Morrison et al, 2007
22	Kinase, CMGC SRPK	A8BKE0	GL50803_17335	22	Morrison et al, 2007
23	Kinase, CMGC DYRK	A8BKE0	GL50803_17335	23	Morrison et al, 2007
24	Hypothetical protein GL50803_17427	A8BD82	GL50803_17427	24	Morrison et al, 2007
25	Ethanolamine kinase	A8BU50	GL50803_4596	25	Morrison et al, 2007

Table 4.9. Reactions considered in Sphingolipid Metabolism

Rxn No	Reactions	Organism	Catalyzing enzyme/ EC number	Related Gene
r1	ATP + Palm + CoA -> AMP + DP + PalCoA	sce	Palmitoyl-CoA synthase/ 6.2.1.3	FAA1
r2	PalCoA + SER -> KDHS + CO2 + CoA	sce	serine C-palmitoyltransferase/ 2.3.1.50	LCB1
r3	KDHS + H + NADPH -> NADP + DHS	sce	3-Dehydrosphinganine reductase/1.1.1.102	TSC10
r4	FA + DHS -> DHCer + CoA + H	sce	Ceramide-1 synthase /2.3.1.24	LAC1
r5	O_2 + H + DHCer -> CER + H2O	mmu	Oxidoreductase/1.14.-.-	Degs1
r6	SPN + AcCoA -> CER + CoA	hsa	ceramide synthase	LASS1
r7	CER + H2O -> FA + SPN	mmu	N-acylsphingosine amidohydrolase /3.5.1.23	Asah1
r8	CER + UDPG -> GCER + UDP	mmu	UDP-glucose ceramide glucosyltransferase/2.4.180	Ugcg
r9	H2O + GCER -> CER + GLC	mmu	acid beta glucosidase/3.2.1.45	Gba
r10	GCER + UDPGAL -> LCER + UDP	mmu	fucosyltransferase 4/2.4.1.-	Fut4
r11	H2O + LCER -> bGLAC + GCER	mmu	galactosidase, beta 1/ 3.2.1.23	Glb1
r12	H + CER + CDPCHO -> SM +CMP	mmu	Ceramide choline phosphotransferase /2.7.8.3	Sgms1
r13	CMP + SM -> CER + CDPCHO + H	mmu	Sphingomyelin phosphodiesterase/3.1.4.12	Smpd1
r14	H2O + GALCER ->CER + bGLAC	mmu	galactosidase, beta 1/ 3.2.1.23	Glb1
r15	UDPGAL + CER -> UDP +GALCER	hsa	UDP-glycosyltransferase/ 2.4.1.45	Ugt8a
r16	SPN +ATP -> SPN1P + ADP	mmu	Sphingosine Kinase/ 2.7.1.91	Sphk1
r17	AcCoA + ATP + CO2 -> ADP + H + MalCoA + P	sce	Acetyl-Coenzyme A Carboxylase/6.2.2.1	ACC1
r18	AcCoA + 7 MalCoA + 14 NADPH + 7 H -> Palm + 7 CO2 + 14 NADP + 8 CoA + 6 H2O	sce	Fatty Acid Synthetase/ 6.2.1.3	FAT1
r19	3PS + H2O -> P + SER + H	sce	Phosphoserine phosphatase/ 3.1.3.3	SER2
r20	ATP + CER -> C1P + ADP	mmu	ceramide kinase/2.7.1.138	Cerk
r21	PalCoA +G3P -> CoA + PA	mmu	1-acylglycerol-3-phosphate O-acyltransferase /2.3.1.51	Agpat1
r22	H2O + PA -> 1 DAG + 1 P	mmu	Lipid phosphate phosphohydrolase 2/3.1.3.4	DPP1
r23	PC + SER -> PS + CHO	sce	phosphatidylserine synthase/2.7.8.8	Pss1
r24	ATP + 1 CHO -> ADP + PCHO	mmu	choline kinase/2.7.1.32	Chkl
r25	PCHO + CTP -> CDPCHO + DP	hsa	phosphate Cytidyltransferase1,Choline, alpha isoform/2.7.7.15	Pcyt1a

4.2.2. Flux Balance Analysis

FBA results are first investigated using the 20 reaction model system and then including the additional reactions (25 reaction pathway) to see the effect of DPP1 gene on the sphingolipid pathway. The effects of different objective functions are studied for both models and the results are presented in Appendix C. The present model is a small system and complete in its own right (analogous to a separate module) and gives profound insights into sphingolipid metabolism.

<u>4.2.2.1. Model system with 20 reactions.</u> The pathway was constructed with 20 reactions through 20 proteins involving 37 metabolites and 26 external metabolites.

The stoichiometric matrix for this system is of size 37 × 46. The resulting vector **v** (for details, see Materials and Methods) has 46 fluxes, including 26 exchange fluxes:

$$v=[v_1 \;\; v_2 \ldots v_{20} \;\; b_1 \;\; b_2 \ldots b_{26}]^T \qquad 4.1$$

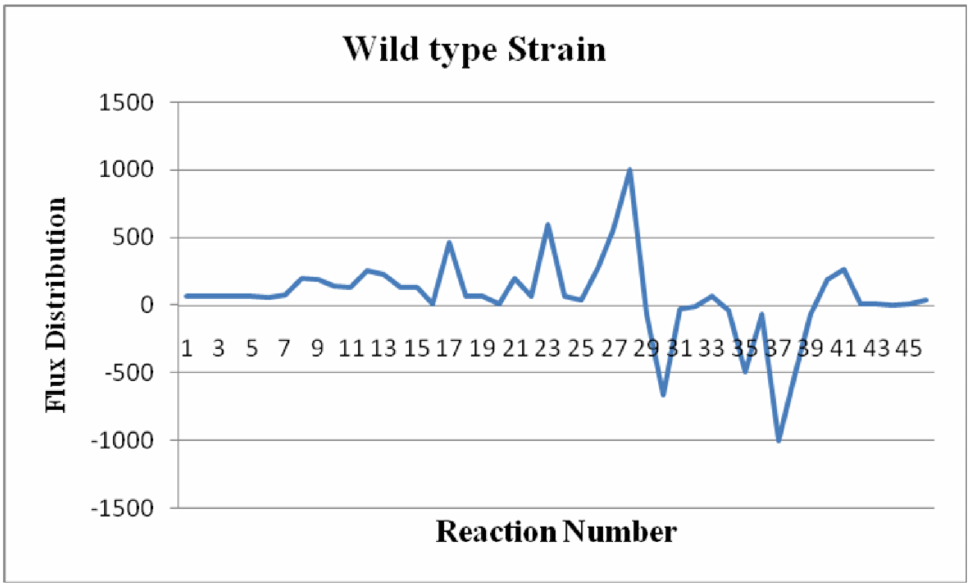

Figure 4.9. Flux distributions for *G. lamblia* without gene deletion (20 reaction model system with objective function of r1 maximization)

In FBA, after an objective function is integrated to the system, the problem is translated to a linear programming (LP) problem as in Equation 3.1 (Sv=0) (listed in Materials and Methods). The solution of the LP problem, using objective functions and specifying the fluxes of all the internal and exchange reactions yields flux distributions. The flux distribution for *G. lamblia* using the maximization of palmitate, the initial metabolite of sphingolipid pathway, was shown in Figure 4.9. the fluxes are increasing for the reactions 8-9 and 12-13 which are glycosylceramide and sphingomyelinsynthesis reactions. The peak at the 17th reaction is because of the AcCoA uptake to the system.

The system is also analysed for several objective functions to find out the optimum flux distribution in sphingolipid metabolism in *G. lamblia*. Since ceramide is known to be the central metabolite for sphingolipid metabolism functioning in anti-poliferative responses such as apoptosis, growth arrest, and/or senescence, it is gaining an increasing attention as a tumor suppressor lipid (Futerman and Hannun, 2004). Five directions having connection with ceramide were focused in the sphingolipid metabolism: GlcCer, S1P, C1P, GalCer and LCer. The maximization of each of these ceramide related products was tested as the objective function. We also considered double objective functions such as LCer and S1P or LCer and C1P or ceramide and S1P or ceramide and C1P productions to reveal how flux is distributed considering the maximization of these metabolites. The results of the flux distributions for different objective functions are presented in Appendix C.2.

Among all the investigated objective functions, the distribution of the system was biologically more meaningful for r1 maximization, i.e. maximum uptake of palmitate. For other objective functions, i.e. maximization of any component (complex sphingolipids) the system only favors the related component.

<u>4.2.2.2. Model System with 25 reactions.</u> The model pathway constructed here, though involving 24 proteins, has 45 metabolites participating in 25 reactions with high interconnectivity, and thus benefits from a systematic FBA.

The stoichiometric matrix for this system is of size 45 × 55 with 25 internal and 30 external reactions, and 15 internal and 30 external metabolites. The resulting vector **v** has 55 fluxes, including 30 exchange fluxes:

$$v=[v_1 \ \ v_2 \ldots v_{25} \ \ b_1 \ \ b_2 \ldots b_{30}]^T \qquad 4.2$$

For FBA studies, in general, the objective functions aim the optimal production of biomass. In the present study, however, the optimal production of ceramide was accomplished at maximum uptake of palmitate. In our 25 reaction model system, each product maximization results in all the net fluxes of other components except the maximized product to become zero. On the other hand, r1 maximization, which favors the maximum uptake of palmitate, gives a proper distribution of fluxes and production of ceramide under the given conditions.

For the chosen objective function, r1 maximization, the general flux distribution in wild type strain is shown in Figure 4.10. The two major peaks at reactions 12–13 correspond to the production of sphingomyelin, and to the uptake of acetyl-CoA which had a fixed value for the system. The external reactions are the reactions between 25-55. The exchange fluxes for the so-called external metabolites are also very high, since they are either utilized or produced in large quantities in the pathway.

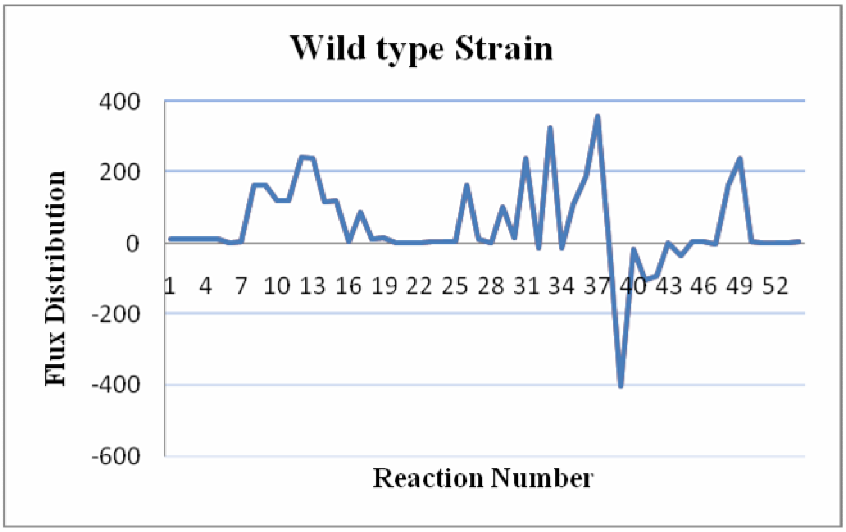

Figure 4.10. Flux distributions for *G. lamblia* without gene deletion 25 reaction pathway (r1 maximization)

The effect of each gene in sphingolipid metabolism was next investigated by deleting it in silico and analyzing the flux profile.

4.2.3. Perturbations : *in silico* gene deletions

The perturbations carried out on the pathway using FBA were the *in silico* deletions of the genes encoding the enzymes catalyzing the reactions. Each of the 24 genes and hence their gene products was systematically deleted from the pathway, one at a time, and its effect on the flux distribution was analysed. The results belonging to the deletion mutants are discussed using the objective function of the maximization of palmitate consumption, i.e. r1 maximization.

When the results of the gene deletion studies obtained using different objective functions are analyzed, it is seen that this particular objective function (r1 maximization) is able to reflect the biological situation better than the other considered objective functions. Since the present model is a small system, any other product maximization causes the flux distribution to favor only that product. Hence, for the rest of the analyses, we have restricted the discussion to the gene deletion results obtained using r1 maximization.

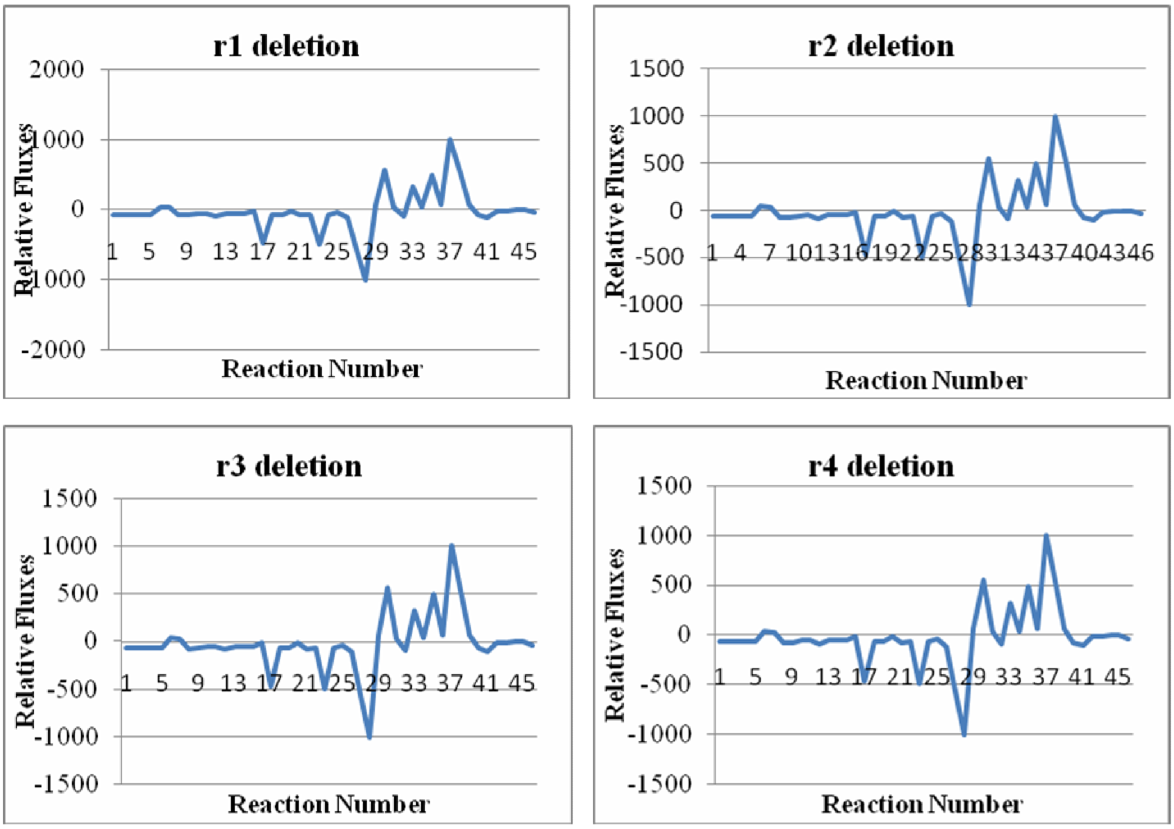

Figure 4.11. Effect of the deletion of the genes encoding the enzymes catalyzing the reactions r1-r4 in 20 reaction model

A similar pattern of flux differences was observed for the deletion of the genes encoding the enzymes catalyzing reactions 1 to 4 (Figure 4.11). For the mentioned reactions this was an expected result because for this part of the pathway there was no branching and such a linear path resulted in the same flux distribution. The fluxes shown in Figure 4.11 are given relative to the fluxes of the wild type strain. If the data on Appendix C3 are investigated the net fluxes (secretion of complex sphingolipids to external medium) were found to become zero for the reactions 1-5 in each gene deletion model. For the mutants, the flux distribution was not so different than the wild type strain except the negative peaks related to reactions 17 and 22. Reaction 17 is the first reaction of the linear pathway, which is the conversion of acetyl-CoA to Malonyl-CoA. Although the fluxes related with the linear part of the pathway decrease as much as the amount of fluxes in wildtype, the range of change for reaction 17 is high because it has a flux which is seven times higher than the flux of linear part of the pathway because of the reaction stoichiometry, and this creates a high range negative peak for the related reaction.

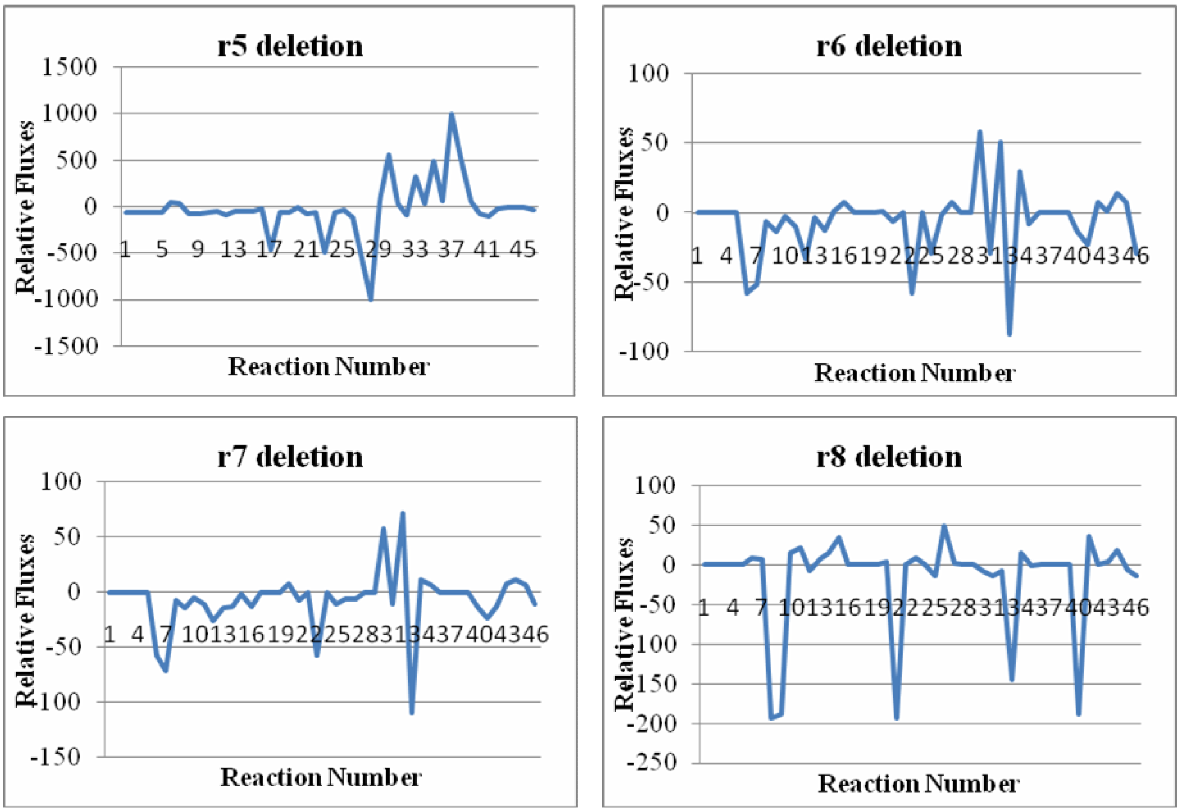

Figure 4.12. Effect of the deletion of the genes encoding the enzymes catalyzing the reactions r5-r8 in 20 reaction model

As related with the reaction 17, acetyl-CoA uptake also decreases in a similar amount, giving the negative peak for the external reaction numbered as 22. The following peaks in the figures represent the exchange fluxes. As it can be seen from Figure 4.12, for the deletion of the gene encoding the enzyme catalyzing reaction 5, the flux pattern is the same as the case of the gene deletions of reactions r1 to r4 since it is another step in the linear part of the pathway. For the mutants of r6 and r7 deletion, there are negative peaks related with the reactions 6 and 7 as expected. The range of flux changes decreases for the case of enzyme inhibitions of reactions 6 and 7. For the mutant related with reaction 8, which is catalysed by Glc-Cer enzyme, the flux distribution is not so different than the wild type, except some major negative peaks at r8 and r9. There are some increases in the fluxes of reactions 13, 14 and 15, which are related with ceramide and galactosyl ceramide syntheses.

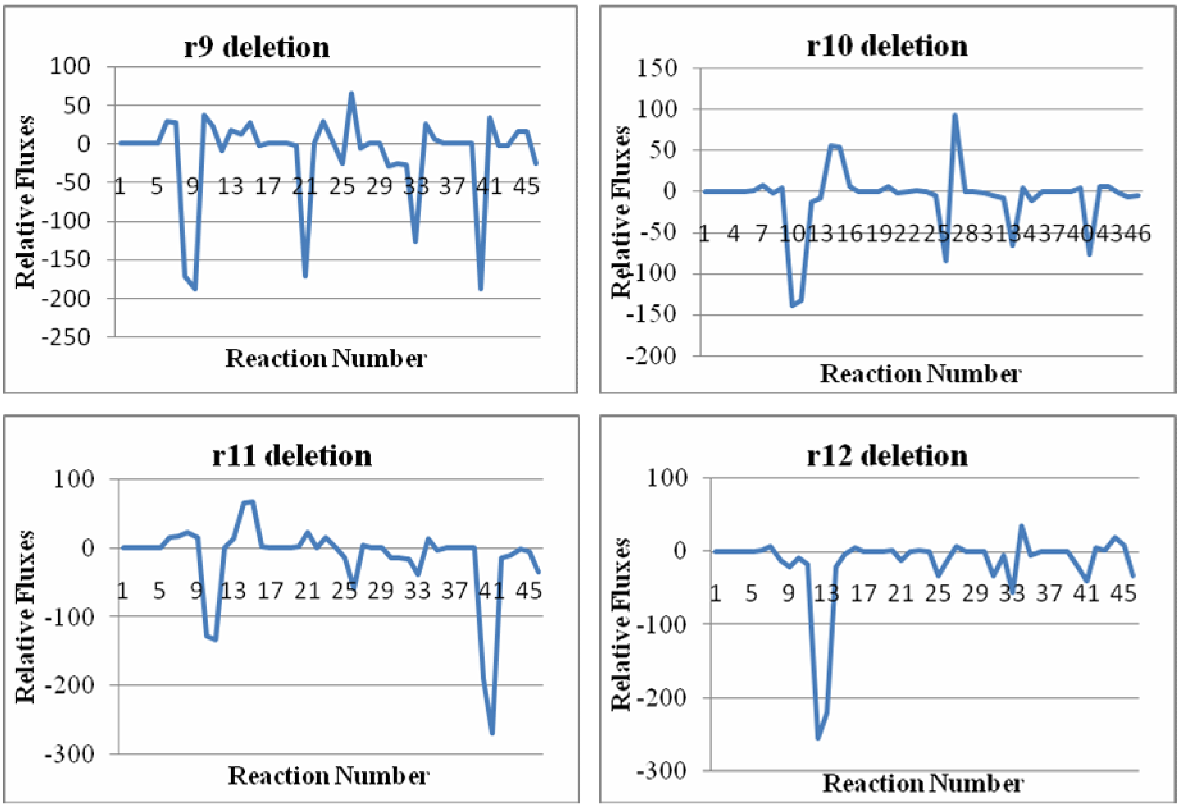

Figure 4.13. Effect of the deletion of the genes encoding the enzymes catalyzing the reactions r9-r12 in 20 reaction model

As it can be seen from Figure 4.13, the mutant related with the deletion of the gene encoding the enzyme catalyzing reaction 9 has the same pattern as the case of the deletion of reaction 8. The main difference is the peaks of reactions 6 and 12 which are sphingosine and sphingomyelin synthesis reactions. The flux differences relative to the wildtype strain was lower in mutant created by deletion of reaction 8 than the mutant of reaction 9, representing higher production of the compounds galactosylceramide and sphingomyelin in case of the deletion of reaction 8. The deletion of reactions 10 and 11 resulted in similar flux patterns since they are reverse of each other and are lactosylceramide and glycosylceramide synthesis reactions. There is an increase in the fluxes favoring ceramide synthesis (reaction 14) for deletion of reaction 10 and galactosylceramide synthesis (reaction 15) for deletion of reaction 11. For the deletion of reaction 12 the flux profile is close to the wild type strain except the negative peak of reactions 12 and 13 which are sphingomyelin synthesis (reaction 12) and ceramide synthesis (reaction 13) reactions.

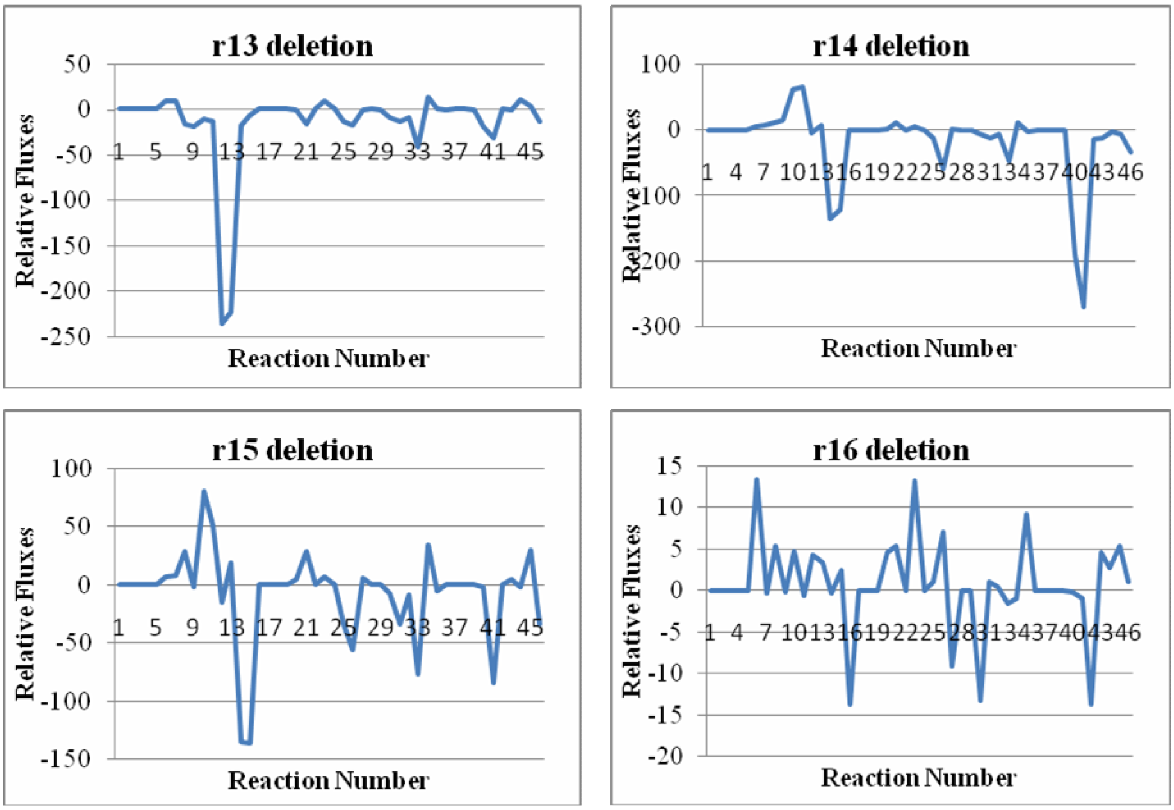

Figure 4.14. Effect of the deletion of the genes encoding the enzymes catalyzing the reactions r13-r16 in 20 reaction model

Figure 4.14 represents the relative fluxes in case of the deletion of the genes encoding the enzymes catalyzing the reactions through 13 to 16, related with the ceramide (reactions 13 and 14), galactosylceramide (reaction 15) and sphingosine-1-phosphate (reaction 16) synthesis. The deletion of reaction 13 gives a similar flux pattern to the deletion of reaction 12 as it is its reverse reaction. For the deletion of reactions 14 and 15 there is an increase in the flux value of the reactions 10 and 11. The mutant related with the deletion of reaction 15 results in higher synthesis of lactosylceramide (reaction 10) while the mutant related with the deletion of reaction 14 favors the synthesis of ceramide (reaction 11). From Figure 4.10 it is seen that the range of change in fluxes are very small for the mutant related with the deletion of reaction 16, meaning that there is no significant change compared to the wild type strain.

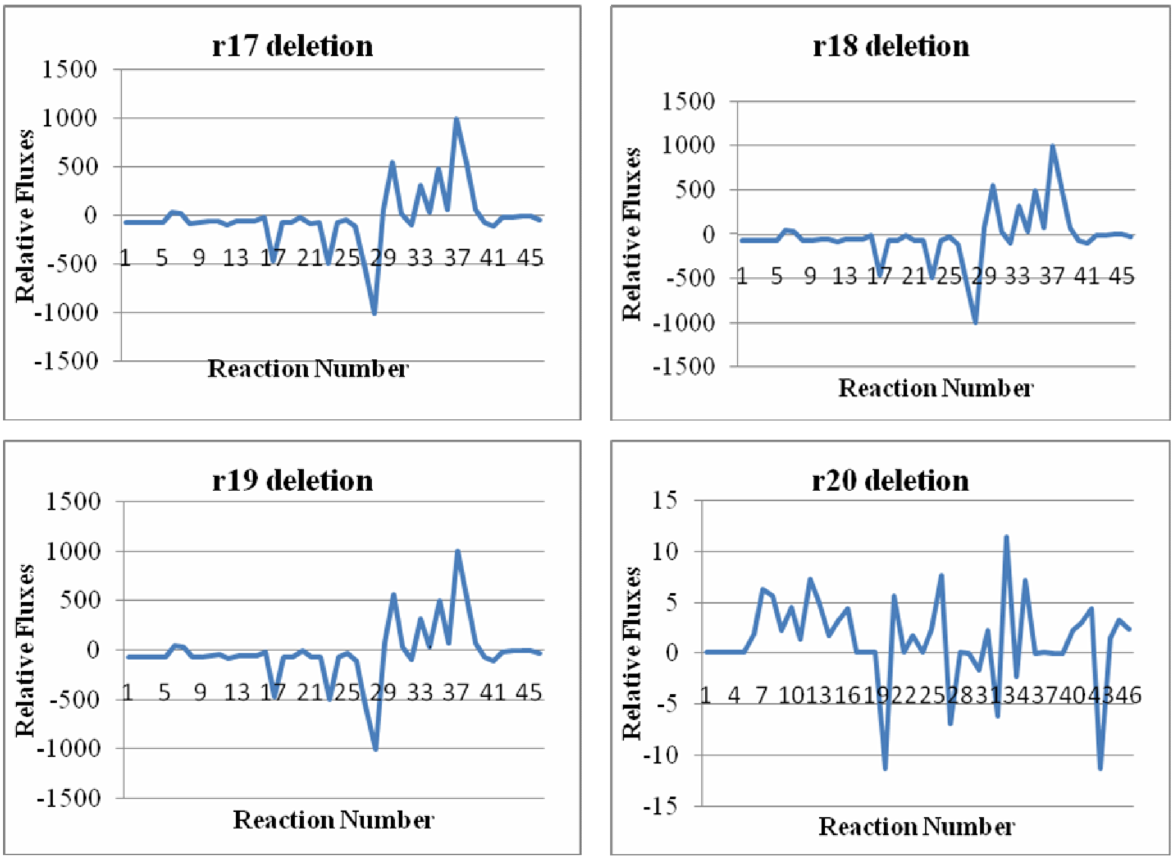

Figure 4.15. Effect of the deletion of the genes encoding the enzymes catalyzing the reactions r17-r20 in 20 reaction model

For the deletions of reactions 17, 18 and 19 which belong to the linear part of the pathway the mutants show similar patterns as the other mutants related with the reactions 1 to 5 (Figure 4.15). The deletion of reaction 20 (ceramide-1-phosphate synthesis) gives similar results as the deletion of reaction 16 (sphingosine-1-phosphate synthesis). This mutant also has similar flux profiles with that of the wildtype strain.

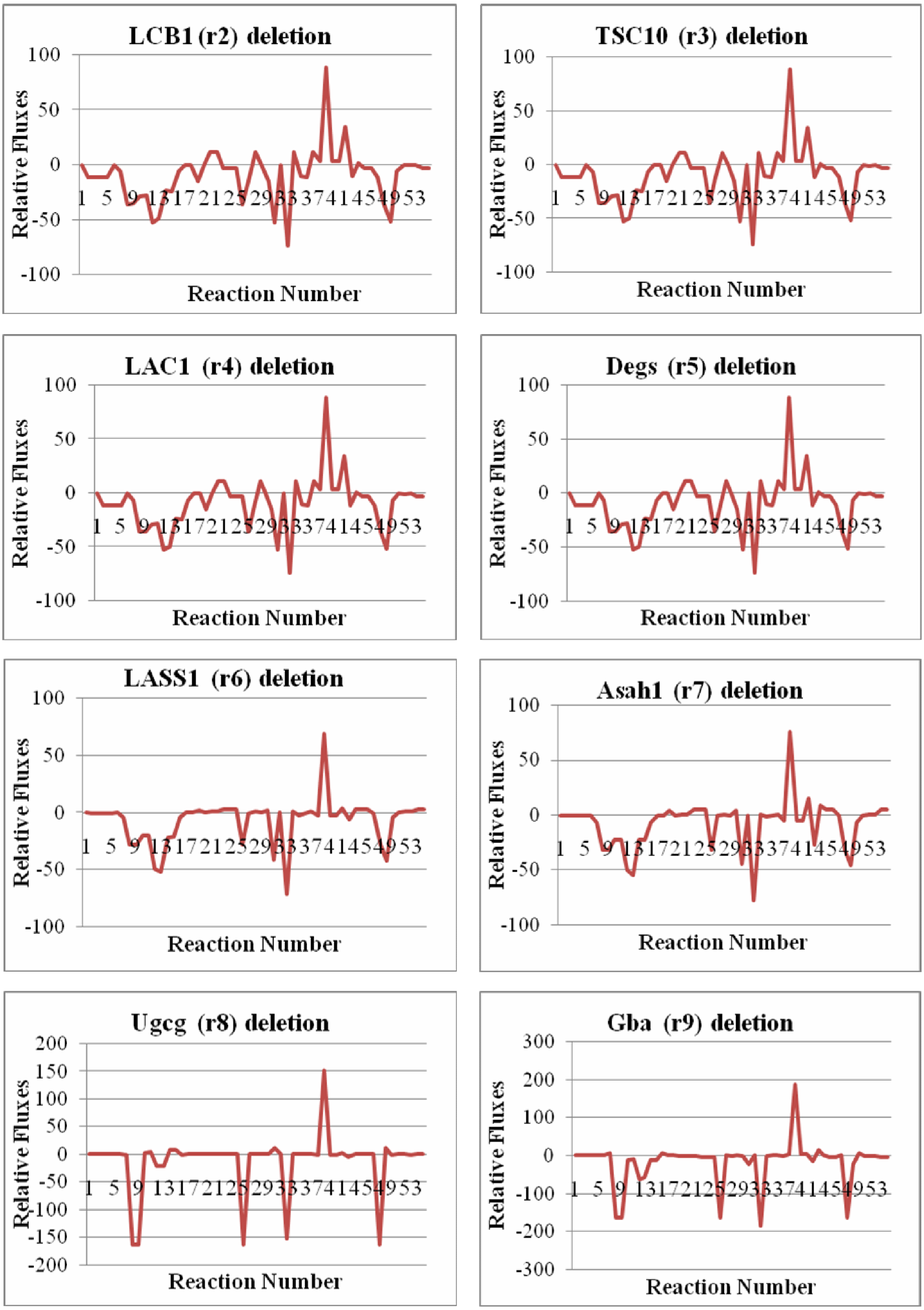

Figure 4.16. Effect of the deletion of the genes encoding the enzymes catalyzing the reactions r2-r9 in 25 reaction model

Next, a similar perturbation study was performed using the model system with 25 reactions. As seen from Figure 4.16, the linear part of the model pathway corresponding to the deletion of the reactions 2-5 has the same pattern of the flux changes (the AcCoA uptake rate was here fixed as 100). For the deletion of the reactions 6 and 7, the response of the system is similar, i.e. fluxes of ceramide pathway reactions are decreasing.

The deletion mutants related with reactions 8 and 9 also show similar patterns of flux changes as the previously investigated model system of 20 reactions. In the case of the deletion of reaction 8 which is glucosylceramide synthase catalysed reaction, the sphingomyelin synthesis was affected negatively (recation 12). (See the data, Appendix C.3.). Other reactions were not altered, so this deletion does not affect the rest of the system.

The effects of the deletion of the genes encoding the enzymes catalyzing the reactions from 10 to 18 can be seen in Figure 4.17. The range of the flux changes is similar for all deletions. For the deletions of the reactions of 10,11,14 and 16, the fluxes related with ceramide synthesis are decreasing. The deletion of sphingomyelin (reaction 12 and 13) related reactions gave flux profiles very close to the wildtype strain except the negative peak on the related reactions. The change in the reactions 17 to 25 cannot be seen in these figures obviously, since the flux ranges related with these reactions are small compared to the rest of the system. For the deletions of reactions 15, 17 and 18, there are positive peaks representing the increase of the fluxes of sphingosine related reactions (reactions 6 and 7).

Figure 4.18 shows the relative flux distributions of *in silico* mutants related with the deletion of the reactions 19 to 25. The deletion of the reactions 19, 21, 23, 24 and 25 gives similar flux profiles with negative peaks on ceramide related reactions. The mutant related with the deletion of the reaction 22, which is the synthesis of diacylglycerol catalysed by DPP1 gene, results in similar flux values with that of the wild type strain. When the relative flux values in the figure were examined, the ranges are very close to zero meaning close results to that of wildtype strain. One should note here that the amounts of fluxes are also small and that particular deletion does change the system only at small amounts. However, positive peaks are observable for ceramide related reactions.

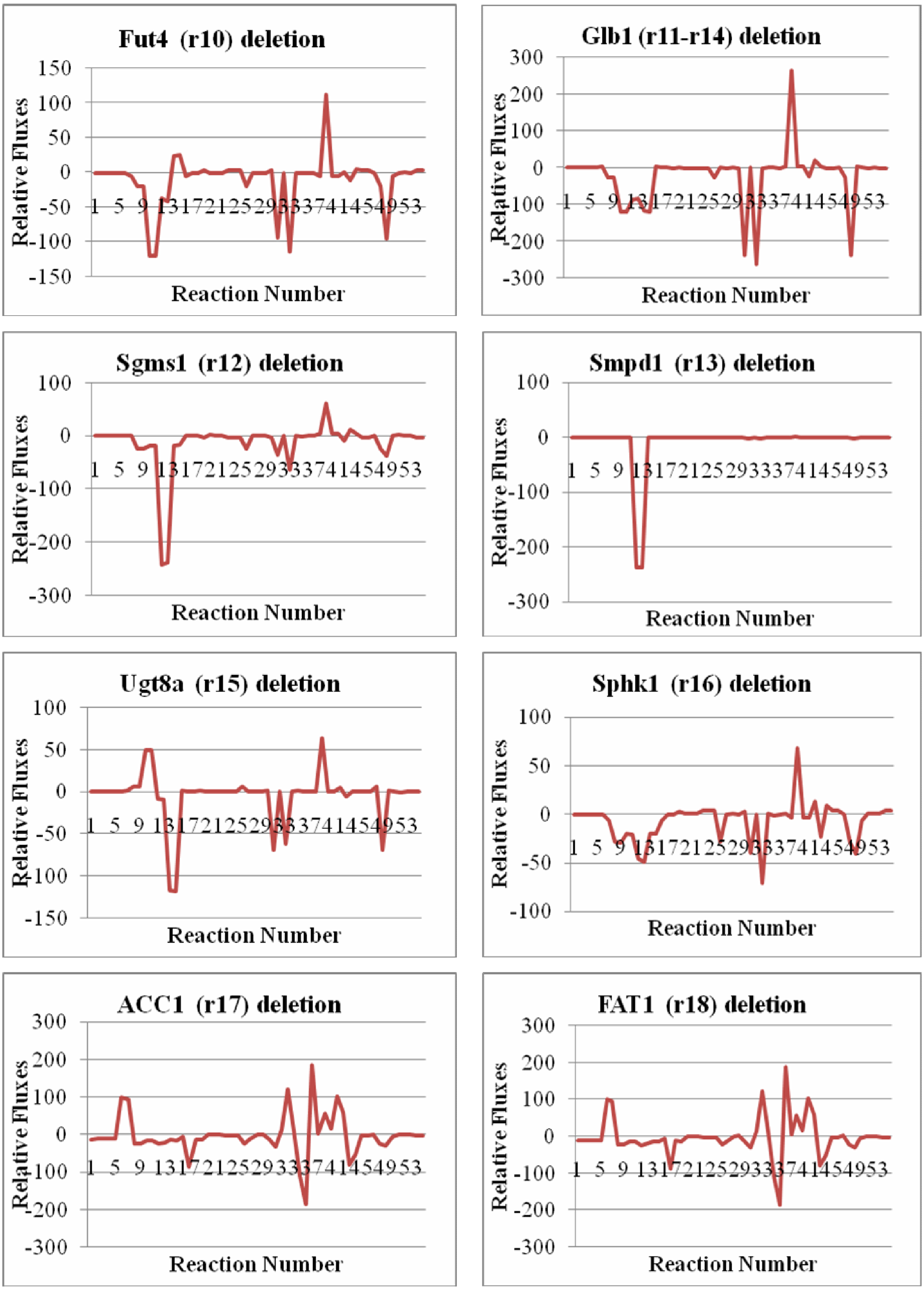

Figure 4.17. Effect of the deletion of the genes encoding the enzymes catalyzing the reactions r10-r18 in 25 reaction model

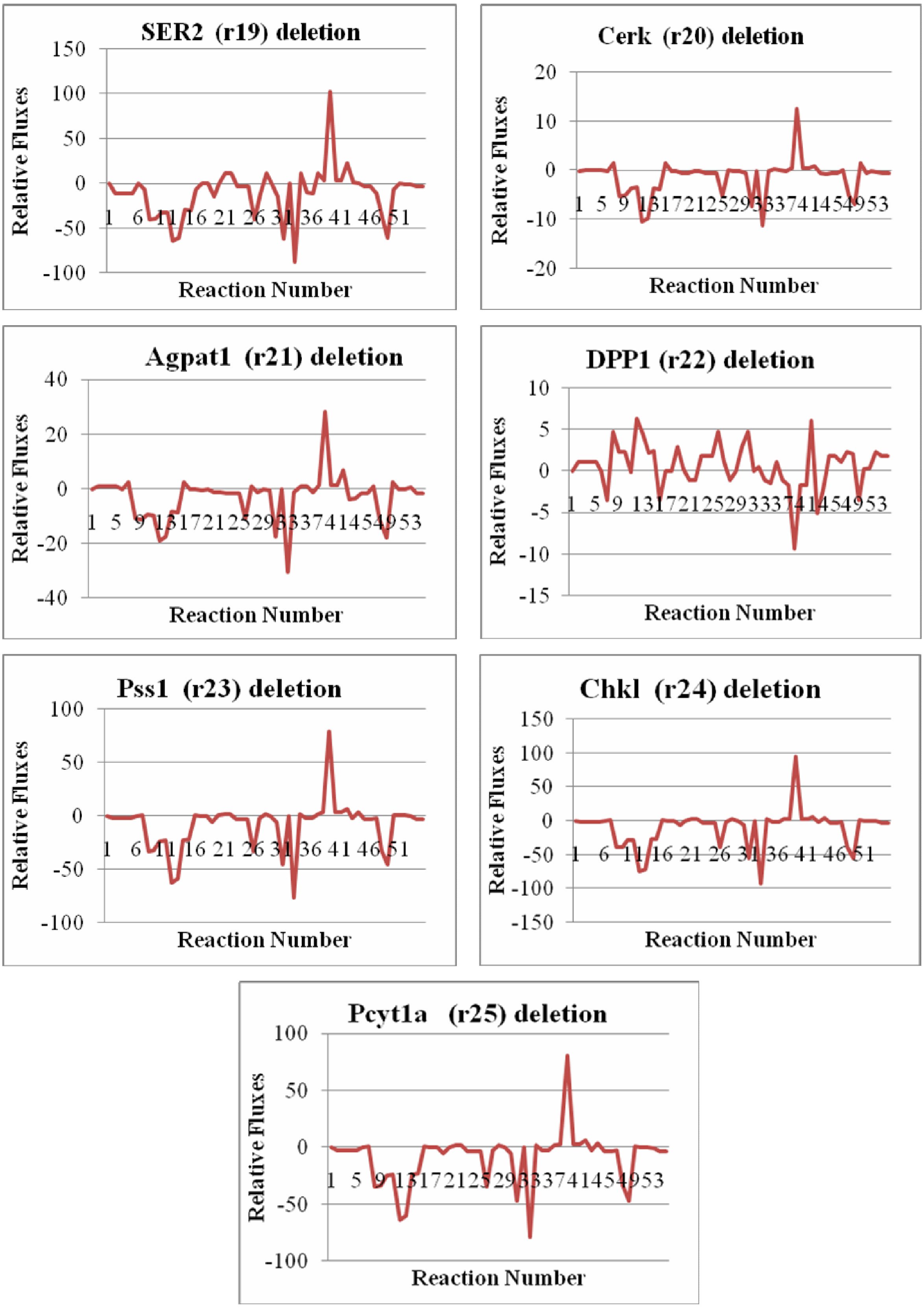

Figure 4.18. Effect of the deletion of the genes encoding the enzymes catalyzing the reactions r19-r25 in 25 reaction model

For the deletion of reaction 20 which is ceramide-1-phosphate synthesis, the flux ranges range were again so small giving similar profile for Cerk Δ mutant as the wildtype strain and the flux pattern is similar to other cases participated in Figure 4.18.

Ceramide being a center metabolite and effective for the productions of all complex sphingolipids is an important metabolite, so the flux distributions surrounding ceramide give peaks (as seen in the figures of Figure 4.18) and that can be explained by the high regulatory role of this metabolite.

4.2.4. Investigation of Drug Target Enzymes

The studies on lipid metabolism show that the Giardia genome contains enzymes capable of fatty acid extension (limited) and sphingomyelin assembly, as well as phospholipid headgroup exchange and modification (Morrison *et al*., 2007). That may explain the high flux rates of sphingomyelin synthesis calculated by FBA and the existence of complex sphingolipids in *G.lamblia*.

Our sequence analysis studies show that most of the sequence similarities result in hypothetical genes without any known functions of them in *G. lamblia*. However, some experimental studies suggest that the key enzymes of sphingolipid metabolism may be conserved in *G. lamblia* despite the high degree of evolutionary divergence. Sequence studies carried out before indicated the existence of serine palmitoyltransferase enzyme catalyzing the condensation reaction between serine and palmitoyl coenzyme CoA to synthesize 3-Ketosphingosine in *G. lamblia*. Moreover, GlcCer is known to transfer glucose from UDP-glucose to a ceramide acceptor molecule, and sphingomyelinase like phosphodiesterase (gSmase) enzymes hydrolyze sphingomyelin to ceramide in *Giardia* (Hernandez *et al.*, 2008). GlcCer synthesis is also a key point in synthesis of complex sphingolipids (Sonda *et. al*., 2008).

In our previous studies (Kavun, 2007) the enzymes encoded by the genes of *Ugcg* and *DPP1* were found to be potential targets for drugs used to induce apoptosis by increasing ceramide levels. However, *DPP1* gene has no homologues in the *Giardia* proteome.

In the present FBA study, upon *in silico* deletion of the gene encoding the drug target enzyme, Ugcg or DPP1, the flux of that reaction was set to zero. It can be seen from Table 4.10 and Figure 4.19 that the fluxes on ceramide producing reactions (reactions 5, 6, 9, 13 and 14) are increasing for these two mutants. These increases are around 2 to 10 % of those of the wildtype strain.

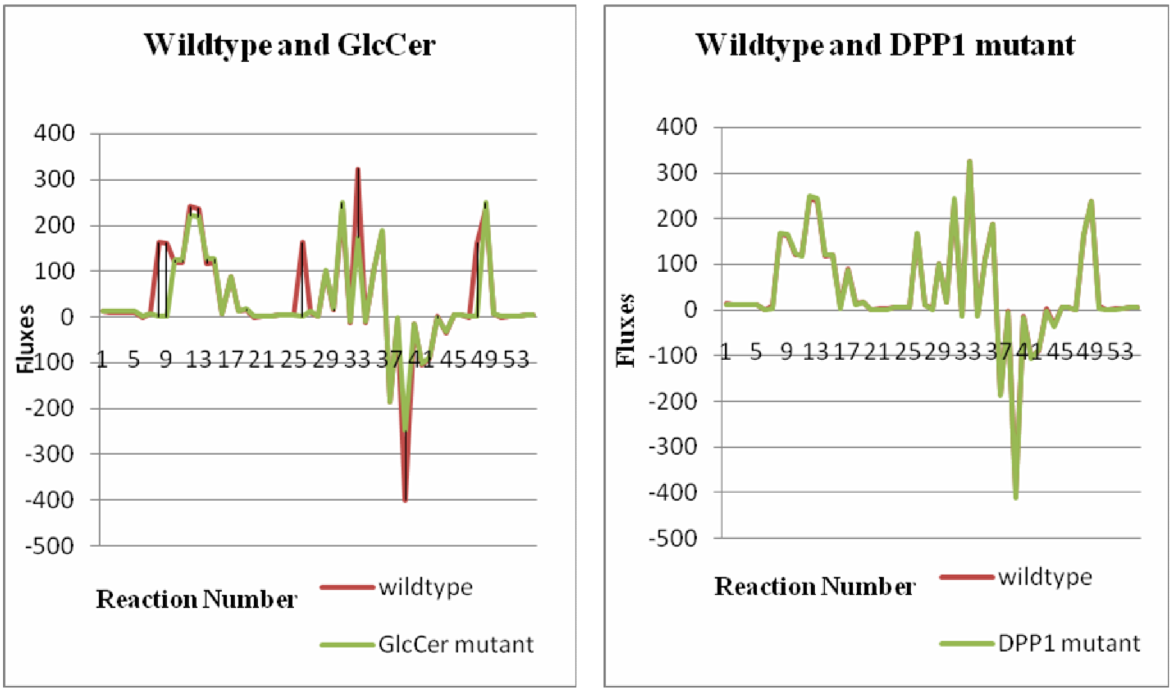

4.19. Comparision of wildtype strain with GlcCer mutant and DPP1 mutant in 25 reaction pathway for r1 maximization

In GlcCer mutant, complex sphingolipids synthesized from ceramide are decreasing except galactosylceramide meaning less ceramide conversion to other sphingolipids (Table 4.11). Experimental studies related to *Ugcg* show that its inhibition compromised the cell division indicating an increase in ceramide levels (Sonda *et al.*, 2008). Our results show a similar effect upon deletion of *Ugcg* gene*,* consistent with the experimental results. The production of sphingosine-1-phosphate which is considered to be a product opposing in function to ceramide, i.e. playing important roles in anti-apoptotic responses by inducing cell proliferation, was favorably decreased in the case of GlyCer mutant (Table 4.11).

In DPP1 mutant, phosphorylated products are produced in larger amounts whereas other complex sphingolipids such as galactosyl ceramide and lactosyl ceramide were in very small amounts compared to the wildtype strain (Table 4.11).

Table 4.10. Fluxes of 25 reaction model system (r1 maximization AcCoA uptake fixed to 100)

Reaction no	Fluxes of Wild type strain (mM/ml.s)	Fluxes of Glc Cer Δ mutant (mM/ml.s)	Fluxes of DPP1 Δ mutant (mM/ml.s)
1	12.5	12.5	12.5
2	11.3892	11.5344	12.5
3	11.3892	11.5344	12.5
4	11.3892	11.5344	12.5
5	11.3892	11.5344	12.5
6	0	0	0
7	6.3917	6.021	2.9026
8	163.155	0	167.8214
9	162.6288	0	164.9705
10	119.3332	122.7313	121.5717
11	118.807	122.7313	118.7207
12	241.3913	220.8248	247.671
13	238.0375	216.9797	242.5559
14	117.4884	124.7293	119.6341
15	118.1317	125.9886	120.5776
16	6.3917	6.021	2.9026
17	87.5	87.5	87.5
18	12.5	12.5	12.5
19	14.743	15.3795	17.6151
20	0.4743	0.409	0.6878
21	1.1108	0.9656	0
22	1.1108	0.9656	0
23	3.3538	3.8451	5.1151
24	3.3538	3.8451	5.1151
25	3.3538	3.8451	5.1151

Very significant differences cannot be observed (Figure 4.15) for the fluxes in the case of deletions of the reactions producing diacylglycerol and glycosylceramide because these products are synthesized in small amounts compared to all the fluxes in the sphingolipid pathway.

Nevertheless, the FBA results of both mutants are in agreement with the previous experimental (Sonda *et al.*, 2008) and theoretical (Kavun, 2007) findings that they can be used as drug targets for apoptotic responses.

Table 4.11. Fluxes of complex sphingolipids (25 reaction model system, r1 maximization, AcCoA uptake fixed to 100)

Metabolite	Flux in Wild type strain (mM/ml.s)	Flux in Glc Cer Δ mutant (mM/ml.s)	Flux in DPP1 Δ mutant (mM/ml.s)
'SPN1P'	6.3311	5.8514	22.21
'C1P'	6.4991	6.439	14.9688
'GALCER'	28.3478	34.0564	6.2422
'LCER'	0.2833	0	0.0414
'SM'	25.2052	20.3198	23.2041

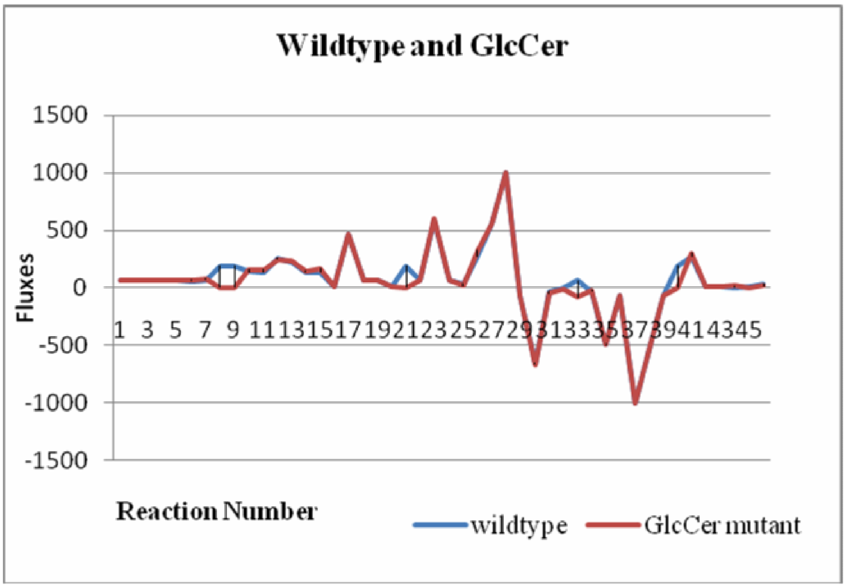

Figure 4.20. Comparison of flux profiles of wildtype strain with that of GlcCer mutant using 20 reaction model

Table 4.12. Fluxes of 20 reaction model system (r1 maximization)

Reaction no	Wild type (mM/ml.s)	GlcCer Δ (mM/ml.s)
1	66.7	66.7
2	66.7	66.7
3	66.7	66.7
4	66.7	66.7
5	66.7	66.7
6	58	65.8
7	71.8	78.9
8	193.9	0
9	188.3	0
10	139.6	154.5
11	133.9	154.5
12	256.2	247.9
13	222	228.6
14	134.7	150
15	136.3	169.9
16	13.8	13.1
17	466.7	466.7
18	66.7	66.7
19	66.7	66.7
20	11.4	14.3
'SPN1P'	13.8	13.1
'C1P'	11.4	14.3
'GALCER'	1.6	19.9
'LCER'	5.7	0
'SM'	34.2	19.3

The flux distribution of the wildtype strain and GlcCer mutant was also investigated using the 20 reaction small model system (Figure 4.20 and Table 4.12). Ceramide synthesis reactions 5, 6, 13 and 14 are obviously increasing as shown in Table 4.12. GlcCer deletion also favors galactosylceramide synthesis, when the net fluxes were considered. However the production of other complex sphingolipids are found to decrease. In conclusion, similar effects are obtained as the 25 reaction model system.

5. CONCLUSIONS AND RECOMMENDATIONS

5.1. Conclusions

Through the study the quantification and qualification of sphingolipids in *S. cerevisiae* experimentally and in *Giardia lamblia* by simulation studies were accomplished. The deletion mutants of two main genes, which are *Ugcg* responsible of encoding Glucosylceramide synthase enzyme in *G. lamblia* and DPP1 gene responsible of encoding DAPP phosphatase in *Saccharomyces cerevisiae* and *G. lamblia,* were used to investigate the effects of drugs inducing apoptosis in sphingolipid metabolism.

In the experimental part of the study, yeast cells (wild type along with *dpp1*Δ deletion mutant) were grown in YPD medium batchwise and the concentrations of sphingolipid metabolites were measured by HPLC. It was observed that the production of D-Cer was increased in the mutant strain and a distinct increase in dihydrosphingosine favoring the increase of ceramide production was also noted. Other complex sphingolipids, MIPC and $M(IP)_2C$, were similarly found to increase.

In the simulation part of the study, being responsible of diarrhea, the organism *Giardia Lamblia* was taken into consideration and the effects of anti-Giardia drugs inhibiting glucosylceramide synthase (*Ugcg)* and DAPP phosphatase enzymes were investigated using *in silico* deletion mutants of the genes encoding these drug target enzymes.

Flux Balance analysis was used for obtaining the flux distribution in sphingolipid metabolism. Since there was not enough information for this pathway in *Giardia*, the enzymes catalyzing the sphingolipid reactions were found by sequence analysis (PSI-BLAST) using the known genes in *Sacchromyces cerevisiae, Mus musculus and Homo sapiens.* Two different pathway models were constructed with 20 reactions and 25 reactions. Both model systems gave similar results.

When the *in silico* deletion mutants simulating the anti-Giardia drug effects are investigated, both enzyme deletions (Ugcg or DPP1) result in higher fluxes of ceramide synthesis. These increases are around 2 to 10 % of those of the wildtype strain. Our simulation study aggree with the experimental results reported by Sonda et al., 2008 for glucosylceramide synthase enzyme. The production of sphingosine-1-phosphate which induces cell proliferation as an anti-apoptotic metabolite, was favorably decreased in the case of GlyCer mutant. In DPP1 mutant, phosphorylated products and ceramide are produced in larger amounts whereas other complex sphingolipids such as galactosyl ceramide and lactosyl ceramide were in very small amounts compared to the wildtype strain.

Beside these two drug target enzymes, the inhibition of each enzyme catalyzing the reactions in sphingolipid metabolic pathway was investigated individually by *in silico* deletions of the genes encoding these enzymes. When the enzymes catalyzing the *de novo* reactions of the pathway were inhibited *in silico*, no production of any complex sphingolipids was observed. For 25 reaction model system, the deletion of the enzyme catalyzing any of the reactions r6, r8, r9, r10 or r22 resulted in decreases in the amount of sphingosine -1-phosphate, whereas the deletion of the enzyme catalyzing any of the reactions r11, r12 and r22 resulted in increases of the fluxes related to ceramide synthesis. The deletion of the enzyme catalyzing any of the reactions r6, r7, r8, r10, r13, r15, r16 and r22 showed higher sphingomyelin production than that of the wildtype strain. Sphingomyelin is mostly considered to be interactive with ceramide which is responsible for important cell activities as cell signaling and growing, proliferation and apoptosis. For 20 reaction model system, the deletion of the enzymes catalyzing the reactions r10, r11, r16 or r20 resulted in increases of ceramide levels.

While the usefulness of FBA for large systems with high network connectivities and redundancy is well established, its application for specific pathways, which can be considered as simpler systems, has not yet been well explored in the literature. The study reported here illustrates the usefulness of FBA even for simple individual pathways. The effects of the perturbations to a system even of this size can be observed which indicate the benefit from systematic studies such as FBA to get meaningful results. Moreover, FBA provides a handle to identify essential genes in the pathway, irrespective of the size of the system, in a systematic, efficient, and much simplified manner. An advantage of considering specific pathways individually is that the objective functions for optimisation can be better defined, with specific biological relevance, to generate hypotheses useful for designing molecular biology studies quite readily. It must be noted that at the present time our understanding of systems, and hence their reconstructions in general, is not sufficient to generate knowledge that can replace biochemical or genetic experiments. However, an *in silico* framework for predicting gene essentiality and complementing experimental data where available, has the additional advantage of enabling studies under various environmental conditions such as low nutrition or oxidative stress, or even presence of drugs, which are difficult to perform experimentally.

5.2. Recommendations

Constructing the pathway models forms an important step towards understanding the underlying molecular mechanisms of diseases, and facilitates rational approaches to drug design. Therefore, a careful study of reactions taking place in the metabolism of interest is required. Unfortunately, the lipid metabolism of *Giardia lamblia* has not been elucidated yet. Our findings along with literature information suggest that even with the high degree of evolutionary divergence between *G. lamblia* and other higher eukaryotes, the key enzymes of sphingolipid biosynthesis may still exist in this primordial organism. An extensive experimental research is necessary for unraveling the genes and the encoded enzymes catalyzing the lipid reactions in *Giardia* species. Only after that, one can extend the model reactions used in simulation studies like FBA and hence improve the results obtained from such theoretical studies.

APPENDIX A: CALIBRATION CURVES AND STANDARDS

A.1. Calibration Curves

A.1.1. Calibration Curve and Equation for C8-Cer

The constructed calibration curves were used to calculate the experimental values of sphingolipids.

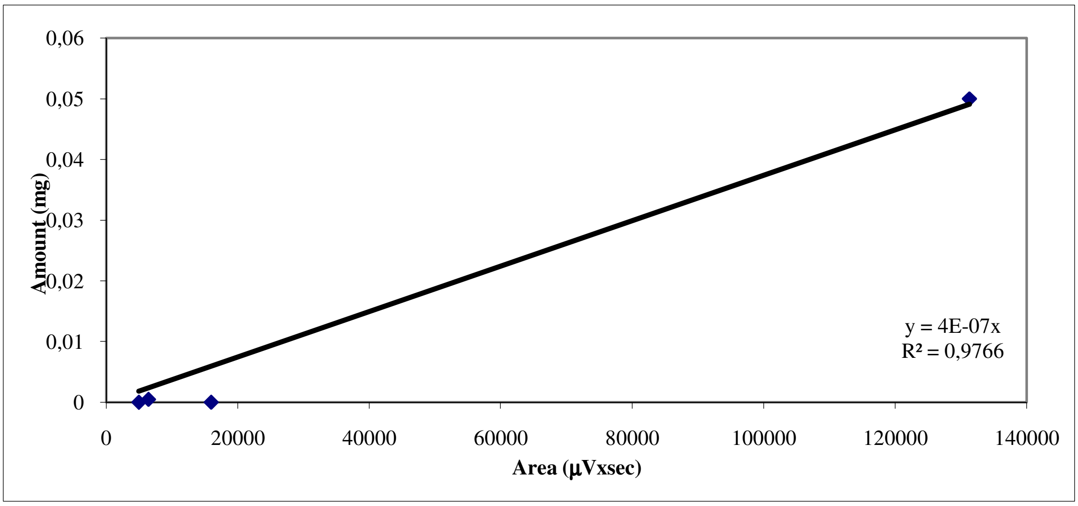

Figure A.1. Calibration curve for C8-Cer

From Figure A.1, it is seen that the calibration curve was constructed as the best fitted trend line type according to the highest R^2 value. The x-axis is the area in µV x sec while the y-axis was the amount of injected C8-Cer in mg. The equation of the calibration curve resulting in a linear one was as follows:

$$y = 4\times10^{-7}\,x \qquad \text{(A.1)}$$

A.1.2. Calibration Curve and Equation for C2-Cer

The constructed calibration curve for C2-Cer was given on Figure A.2 as a second order polynomial one.

The x-axis is the area in µV x sec while the y-axis was the amount of injected C2-Cer in mg.

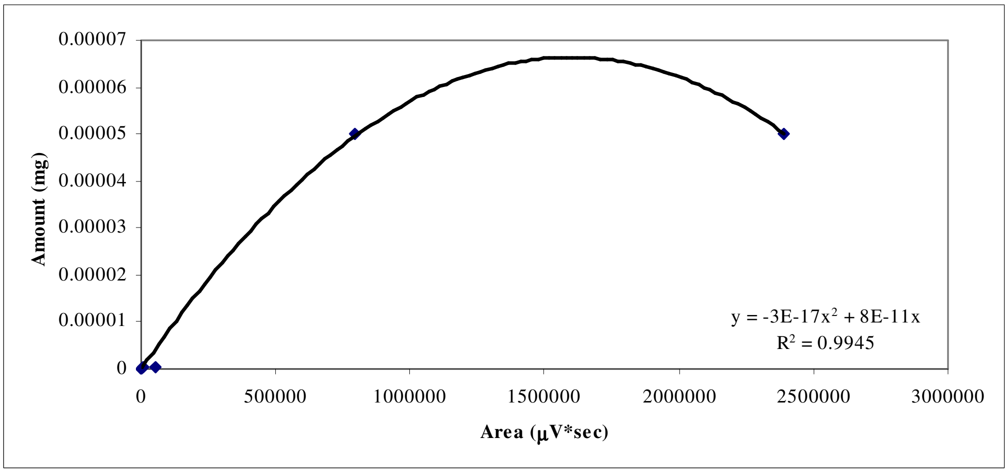

Figure A.2. Calibration curve for C2-Cer

The equation for the calibration curve was as follows:

$$y = -3\times10^{-17}x^2 + 8\times10^{-11}x \tag{A.2}$$

A.1.3. Calibration Curve and Equation for P- Cer

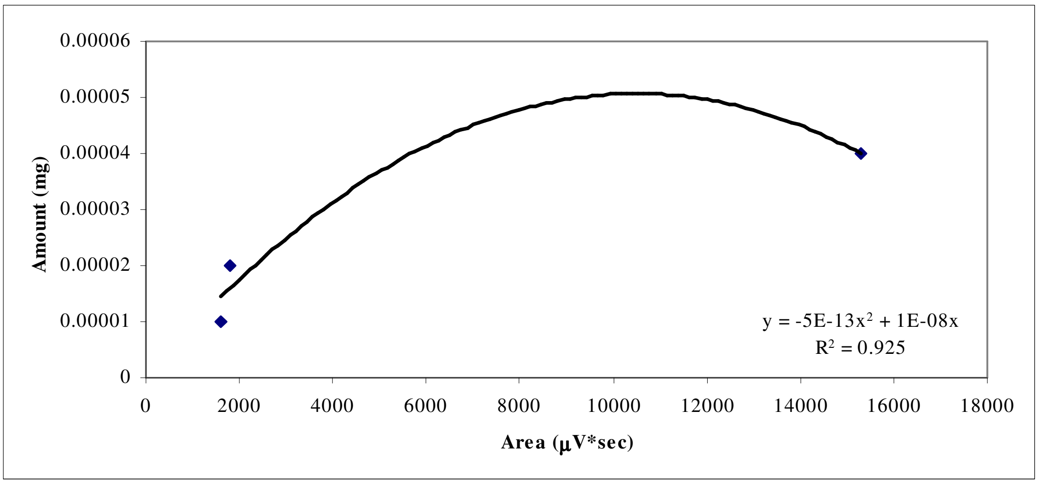

Figure A.3. Calibration curve for P-Cer

Calibration curve used for P-Cer was a second order polynomial equation as can be seen from Figure A.4. The equation of this calibration curve was as follows:

$$y = -5\times10^{-13}x^2 + 10^{-8}x \tag{A.3}$$

A.1.4. Calibration Curve and Equation for PHS

The equation of this calibration curve is as follows:

$$y = -10^{-12}x^2 + 2\times10^{-8}x \quad (A.4)$$

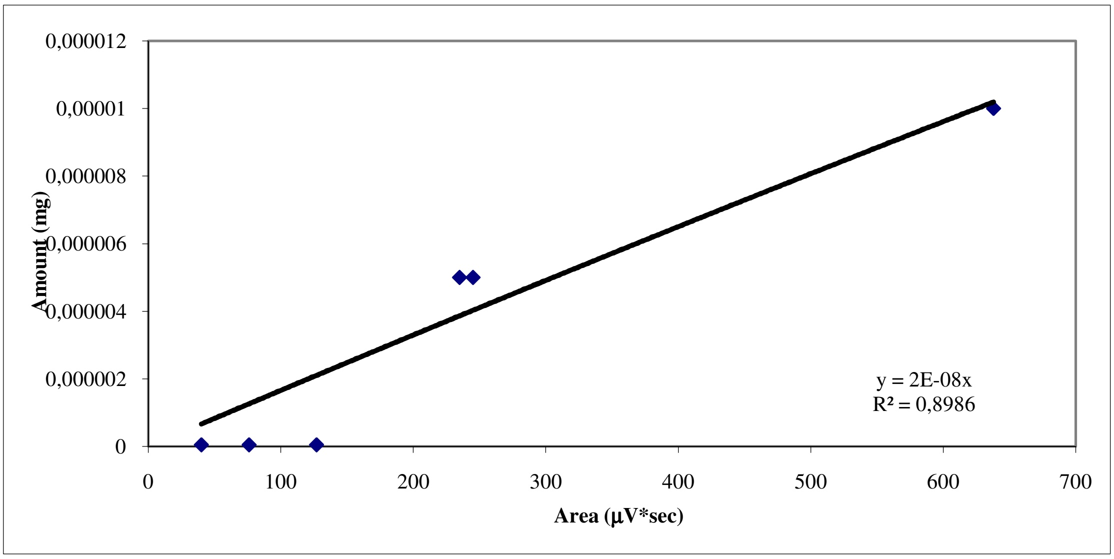

Figure A.4. Calibration curve for PHS

A.1.5. Calibration Curve and Equation for C18-DHS

As it is seen from Figure A.6, the calibration curve constructed is a second order polynomial one. The equation of this calibration curve is as follows:

$$y = -7\times10^{-13}x^2 + 8\times10^{-9}x \quad (A.5)$$

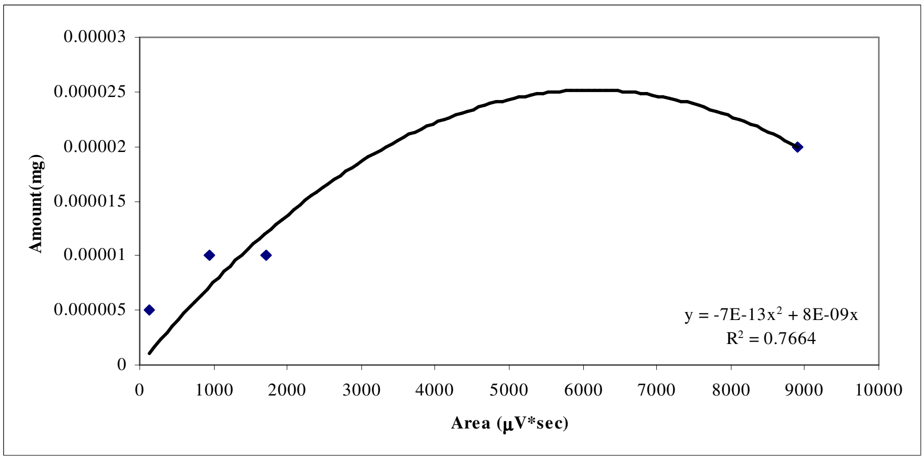

Figure A.5. Calibration curve for C18-DHS

A.2. Standards

A.2.1. Calibration Curve and Equation for C8-Cer

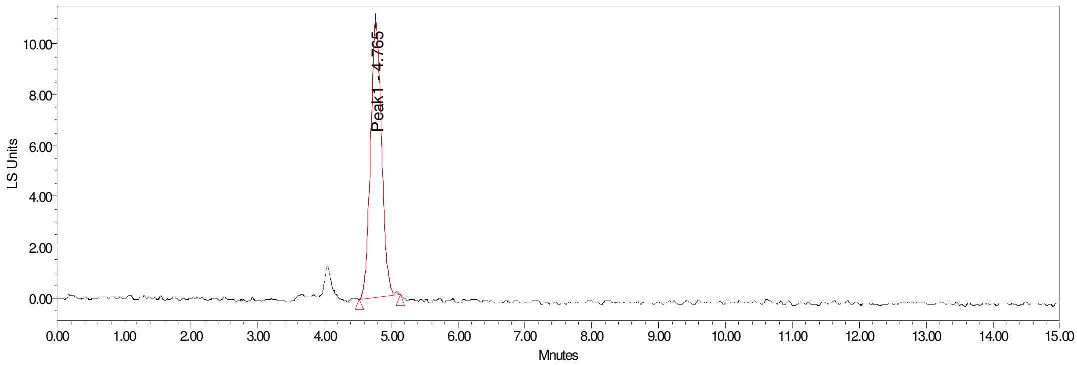

Figure A.6. Autoscaledc hromatogramo f C8-Cer

The residence time for C8-Cer was about 4.7 min. As shown in Figure A.6. for 0.05 mg/ml (0.00012 mM) C8-Cer. However, from previous study carried out by Esra Börklü it was seen that during the multiple injections, the retention time differed from 4 min to 4.8 min, it can be because of instantaneous flowrate changes in the mobile phase.

A.2.2. Calibration Curve and Equation for C2-Cer

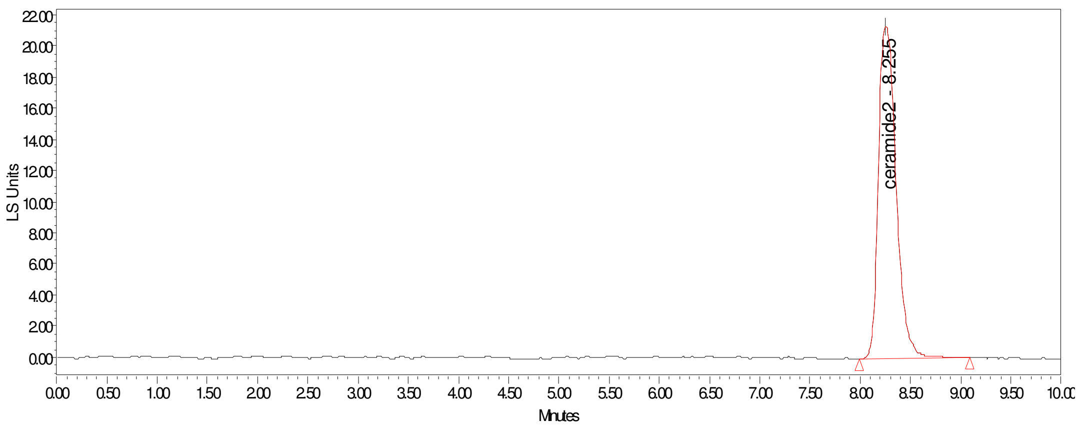

Figure A.7. Autoscaled chromatogram of C2-Cer

The residence time for C2-Cer was about 8.2 min. as shown in Figure A.7. However, from previous study it was seen that during the multiple injections, the retention time differed from 7.9 min to 8.6 min.

A.2.3. Calibration Curve and Equation for P- Cer

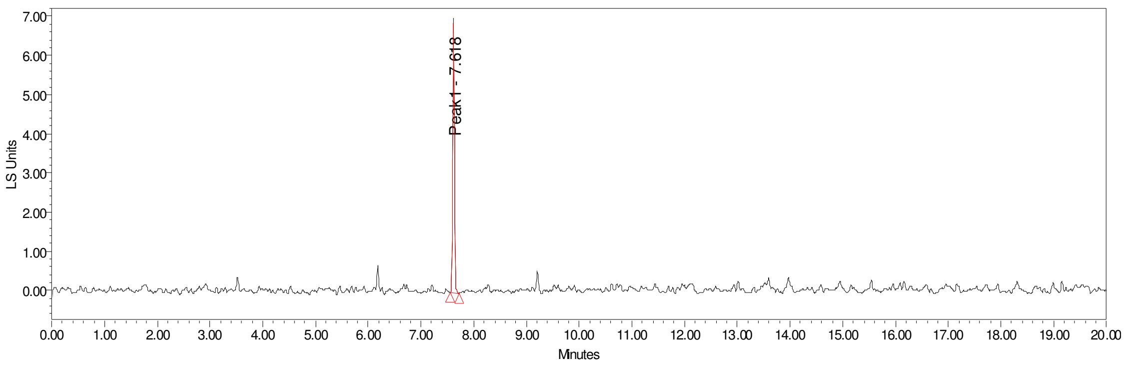

Figure A.8. Autoscaled chromatogram of P-Cer

From the chromatogram given in Figure A.8, it is seen t hat the retention time for C_2 phytoceramide is about 7.6 min. With differentiation of 7.6 to 8 minutes from multiple injections.

A.2.4. Calibration Curve and Equation for PHS

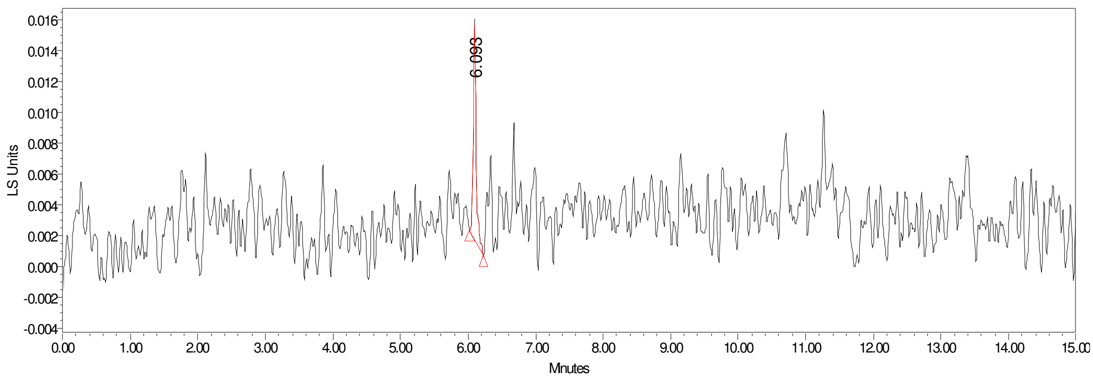

Figure A.9. Autoscaled chromatogram of PHS

For PHS the residence time is about 6 min (Figure A.9- of 0.00005m g/ml (8.6 l0-8m M) PHS). However, during the multiple injections it was seen that it differed from 5.8 min to 6.8 min.

A.2.5. Calibration Curve and Equation for C18-DHS

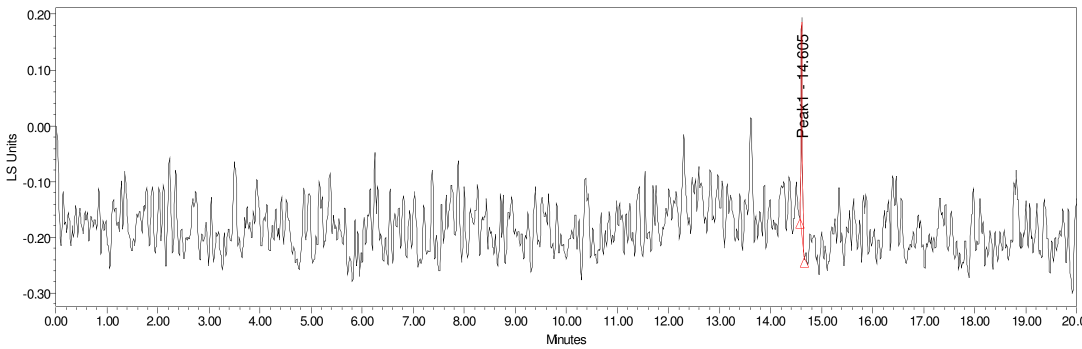

Figure A.10. Autoscaled chromatogram of C18-DHS

The residence time for Cl8-DHS is about 14 min., as it can be seen on Figure A.10 for 0.01m g/ml (1.8 10-5 mM) Cl8-DHS. However, during the multiple injections, it was seen that it differed from 14 min to 16 min.

APPENDIX B: BLAST RESULTS

B.1. BLAST Results of *Sacchromyces Cerevisiae*

B.1.1. Enzymes Catalyzing the Reactions of Sphingolipid Metabolism in *Sacchromyces Cerevisiae*

The enzymes are taken from Genome Scale model of *Sacchromyces Cerevisiae.*

Table B.1. Enzymes Catalyzing the Reactions of Sphingolipid Metabolism in Sacchromyces Cerevisiae

Rxn #	**Reaction**	**EC**	**Gene Name**	**Orf Name**
r1	palmitoyl-CoA synthase	6.2.1.3	FAA1	YOR317W
r2	Glycerol-3-Phosphate Acyltransferase	2.3.1.15	GPT1	YBL011W
r3	phosphatidate phosphatase	3.1.3.4	DPP1	YDR284C
r4	CDP-DAG syhthase	2.7.7.41	CDS1	YBR029C
r5	Phosphatidylinositol synthase	2.7.8.11	PIS1	YPR113W
r6	Inositol-1-Phosphate Synthase	5.5.1.4	INO1	YJL153C
r7	Phosphatidylinositol kinase	2.7.1.137	VPS34	YLR240W
r8	Phosphatidylserine Synthase	2.7.8.8	CHO1	YER026C
r9	Phosphoserine Phosphatase	3.1.3.3	SER2	YGR208W
r10	Serine Hydroxymethyl Transferase	2.1.2.1	SHM1	YLR058C
r11	serine C-palmitoyltransferase	2.3.1.50	LCB1	YMR296C
r12	Acyl-CoA-Binding Protein	FAS1, FAS2	ACB1	YGR037C
r13	3-Dehydrosphinganine reductase		TSC10	YBR265W
r14	sphingoid base-phosphate phosphatase (sphinganine 1-phosphatase)		LBP1	YJL134W
r15	sphingolipid long chain base kinase (sphinganine)	2.7.1.91	LCB4	YOR171C
r16	Phosphatidylserine Decarboxylase	4.1.1.65	PSD1	YNL169C
r17	sphinganine phosphate lyase		DPL1, BST1	YDR294C
r18	phytosphingosine phosphate lyase			
r19	sphingoid base-phosphate phosphatase (phytosphingosine 1-phosphate)		LCB3, YSR2, LBP1	YJL134W
r20	sphingolipid long chain base kinase (phytosphingosine)	2.7.1.91	LCB4	YOR171C
r21	Phytosphingosine synthesis, 4-hydroxylase, YDR297W	1.14.-.-	SUR2, SYR2	YDR297W

Table B.1. Enzymes Catalyzing the Reactions of Sphingolipid Metabolism in Sacchromyces Cerevisiae (continues)

r22	Dihydroceramide Alkaline Ceramidase (YPL087w)	3.5.1.23-ydc1	YDC1	YPL087W
r23	Ceramide-1 synthase (26C), YKL008C, YHL003C, YMR298W	2.3.1.24	LAC1, DGT1, LAG1, LIP1	YKL008C, YHL003C, YMR298W
r24	Ceramide-2 synthase (26C)	2.3.1.24	LAG1	YHL003C
r25	Phytoceramide Alkaline Ceramidase (YBR18w)	3.5.1.23-ypc1	YPC1	YBR18W
r26	Ceramide-1 hydroxylase (26C)			
r27	GPI remodelase		GUP1	YGL084c
r28	Inositol Phosphosphingolipid Phospholipase C	3.1.4.3	ISC1	YER019W
r29	Inositol phosphorylceramide synthase (ceramide-1, 26C), YS		CSH1	YBR161W
r30	Inositol phosphoryceramide synthase (ceramide-2, 26C), YS		CSH1	YBR161W
r31	Inositol Phosphosphingolipid Phospholipase C	3.1.4.3	ISC1	YER019W
r32	Diacylglycerol-Ethanolamine Phosphotransferase	2.7.8.1	EPT1	YHR123W
r33	Phosphoethanolamıne Cytıdylyltransferase	2.7.7.14	MUQ1	YGR007W
r34	Acetyl-Coenzyme A Synthetase	6.2.1.1	ACS1	YAL054C
r35	Acetyl-Coenzyme A Carboxylase	6.4.1.2	ACC1	YLR153C
r36	Fatty Acid Synthetase		FAT1	YBR041W
r37	very long chain fatty acid synthase	YLR372W	SUR4	YLR372W
r38	very long chain fatty acid synthase	YBR041W	FAT1	YBR041W
r39	Transport of ipc-ceramide-1 to PM			
r40	Transport of ipc-ceramide-2 to PM			
r41	mannose-inositol phosphorylceramide synthase (ceramide-1, 26C), YS			
r42	mannose-inositol phosphorylceramide synthase (ceramide-2, 26C), YS			
r43	Inositol Phosphosphingolipid Phospholipase C	3.1.4.3	ISC1	YER019W
r44	Transport of MIPC-ceramide-1 to PM			
r45	Transport of MIPC-ceramide-2 to PM			
r46	Inositol Phosphosphingolipid Phospholipase C	3.1.4.3	ISC1	YER019W
r47	Inositol Phosphosphingolipid Phospholipase C	3.1.4.3	ISC1	YER019W
r48	Inositol Phosphosphingolipid Phospholipase C	3.1.4.3	ISC1	YER019W
r49	Transport of M(IP)2C-ceramide-1 to PM			
r50	Transport of M(IP)2C-ceramide-2 to PM			
r51	mannose-(inositol-P)2-ceramide synthase (ceramide-1, 26C), YS		IPT1	YDR072C
r52	mannose-(inositol-P)2-ceramide synthase (ceramide-2, 26C), YS		IPT1	YDR072C
r53	inositol producing and missing rxn		INM1	YHR046C

B.1.2. BLAST Results of *Sacchromyces Cerevisiae* and *Giardia Lamblia* (taxid:184922)

BLAST results for *Sacchromyces Cerevisiae* and *Giardia Lamblia* (taxid:184922) are represented in Table B.2. Gene sequences were queried by Ncbi BLAST Tool. The treshold for e values is determined as 0.1. Those enzymes which have e values greater than the treshold value are not considered as a part of sphingolipid metabolism for *Giardia lamblia*. Some genes are absent even for Sacchromyces Cerevisiae. The enzymes, which are specific for fungi as yeasts and give high e values meaning very low similarity, were not considered for Giardia species.

Table B.2. BLAST Results of *Sacchromyces Cerevisiae* and *Giardia Lamblia*

	Giardia L. Blast		**Giardia L. Blast**	
	protein- protein blast	**e value**	**nucleot. blast**	**e value**
1	Long chain fatty acid CoA ligase 5	1E-53	Long chain fatty acid CoA ligase 5	0.027
2	Cleavage and polyadenylation specificity specificity factor	0.76	Hypothetical protein	1.3
3	Protein 21.1	2.4	Dynein heavy chain	0.46
4	Phosphatidate cytidylyltransferase	1E-16	Kinesin-13	2.7
5	CDP-diacylglycerol-inositol 3-phosphatidyltransferase	7E-21	Hypothetical protein	0.37
6	Inositol-3-phosphate synthase	7E-101	Ser/Thr phosphatase 2C, putative	3.2
7	Phosphoinositide-3-kinase, class 3	5E-26	Kinase, VPS15	0.43
8	Hypothetical protein GL50803_17427	0.00003	Hypothetical protein	0.46
9	High cysteine membrane protein VSP-like	0.17	Kinase, CMGC DYRK	0.043
10	SOF1 protein	0.037	Hypothetical protein	0.8
11	Serine palmitoyltransferase 2	7E-28	Kinase, NEK	0.022
12	Hypothetical protein GL50803_31998	0.25	Long chain fatty acid CoA ligase	0.48
13	Hypothetical protein GL50803_13942	0.061	ClpB protein	0.54
14	Methionyl-tRNA synthetase	1	ABC transporter, ATP-binding protein	2.4
15	hypothetical	0.3	Nitric oxide synthase	0.087
16	Phosphatidylserine decarboxylase proenzyme	3E-13	Hypothetical protein	1.9
17	Cysteine desulfurase	0.041	No significant similarity found	
19	Methionyl-tRNA synthetase	1	ABC transporter, ATP-binding protein	2.4
20	hypothetical	0.3	Nitric oxide synthase	0.087
21	Gamma tubulin ring complex	1.6	Tenascin-X precursor	0.004
22	Hypothetical protein GL50803_112932	0.035	Coiled-coil protein	0.53

Table B.2. BLAST Results of *Sacchromyces Cerevisiae* and *Giardia Lamblia* (continues)

23	Hypothetical protein GL50803_5939	0.00003	Hypothetical protein (GL50803_90122)	0.71
24	Hypothetical protein GL50803_5939	0.00003	Hypothetical protein (GL50803_90122)	0.71
25	Hypothetical protein GL50803_112932	0.16	Kinase, NEK (GL50803_114937)	0.53
26				
27	Hypothetical protein GL50803_10238	3.2	Hypothetical protein (GL50803_4789)	3.3
28	Hypothetical protein GL50803_12146	0.87	ABC transporter, ATP-binding protein	0.066
29	VSP	2.3	VSP with INR	2.2
30	VSP	2.3	VSP with INR	2.2
31	Hypothetical protein GL50803_12146	0.87	ABC transporter, ATP-binding protein	0.066
32	CDP-diacylglycerol-glycerol-3-phosphate 3-phosphatidyltransferase	0.35	NOD3 protein, putative	39509
33	Tubulin tyrosine ligase	0.17	Ubiquitin-conjugating enzyme	1.9
34	Long chain fatty acid CoA ligase 5	0.006	UDP-glucose 4-epimerase	0.35
35	Acetyl-CoA carboxylase/pyruvate	0.042	Aminoacyl-histidine dipeptidase	0.31
36	Long chain fatty acid CoA ligase 5	0.006	Long chain fatty acid CoA ligase 5	0.027
37	Kinesin-13	0.45	Mlh1-like protein	0.58
38	Long chain fatty acid CoA ligase 5	0.006	Long chain fatty acid CoA ligase 5	0.027
43	Hypothetical protein GL50803_12146	0.87	ABC transporter, ATP-binding protein	0.066
44				
45				
46	Hypothetical protein GL50803_12146	0.87	ABC transporter, ATP-binding protein	0.066
47	Hypothetical protein GL50803_12146	0.87	ABC transporter, ATP-binding protein	0.066
48	Hypothetical protein GL50803_12146	0.87	ABC transporter, ATP-binding protein	0.066
49				
50				
51	DNA damage repair protein	1.2	Hypothetical protein (GL50803_38432)	3.1
52	DNA damage repair protein	1.2	Hypothetical protein (GL50803_38432)	3.1
54	Hypothetical protein GL50803_9353	0.002		

B.1.3. BLAST Results of *Sacchromyces Cerevisiae* and *Giardia* (taxid:5740)

For different taxonomies of Giardia different BLAST results were found. As it is seen from following tables Giardia lamblia gave the best results among all Giardia species.

Table B.3. BLAST Results of *Sacchromyces Cerevisiae* and *Giardia* (taxid:5740)

	Giardia Blast		**Giardia Blast**	
	protein- protein blast	**e value**	**nucleot. blast**	**e value**
1	Long chain fatty acid CoA ligase 5	0.006	Long chain fatty acid CoA ligase 5	0.032
2	Cleavage and polyadenylation specificity factor, 73 kDa subunit	0.82	No significant similarity found	
3	Hypothetical protein GL50803_37452	6.4	No significant similarity found	
4	CDP-diacylglycerol synthase	1E-17	No significant similarity found	
5	CDP-diacylglycerol-inositol 3-phosphatidyltransferase	7E-21	No significant similarity found	
6	Inositol-3-phosphate synthase	8E-101	No significant similarity found	
7	Phosphoinositide-3-kinase, class 3	5E-26	No significant similarity found	
8	Hypothetical protein GL50803_17427	0.00003	No significant similarity found	
9	High cysteine membrane protein VSP-like	0.18	Kinase, CMGC DYRK	0.052
10	SOF1 protein	0.04	No significant similarity found	
11	Serine palmitoyltransferase 2	7E-28	No significant similarity found	
12	Hypothetical protein GL50803_31998	0.27	Long chain fatty acid CoA ligase, putative	0.58
13	Hypothetical protein GL50803_13942	0.066	No significant similarity found	
14	Methionyl-tRNA synthetase	1.1	No significant similarity found	
15	Hypothetical protein GL50803_9157	0.33	No significant similarity found	
16	phosphatidylserine decarboxylase	3E-13	No significant similarity found	
17	Cysteine desulfurase	0.044	No significant similarity found	
19	Methionyl-tRNA synthetase	1.1	No significant similarity found	
20	Oxidoreductase, short chain dehydrogenase/reductase family	5E-25	No significant similarity found	
21	Gamma tubulin ring complex	1.7	No significant similarity found	
22	Hypothetical protein GL50803_112932	0.037	No significant similarity found	
23	Hypothetical protein GL50803_5939	0.00003	No significant similarity found	
25	Hypothetical protein GL50803_112932	0.17	Giardia lamblia ATCC 50803 Kinase, NEK	0.64
27	Hypothetical protein GL50803_10238	3.4	Hypothetical protein (GL50803_4789)	4
28	Hypothetical protein GL50803_12146	0.94	Giardia lamblia ATCC 50803 ABC transporter, ATP-binding protein	0.08
29	VSP	2.5	No significant similarity found	
30	VSP	2.5	No significant similarity found	
31	Hypothetical protein GL50803_12146	0.94	Giardia lamblia ATCC 50803 ABC transporter, ATP-binding protein	0.08
32				
33	Tubulin tyrosine ligase	0.18	No significant similarity found	

Table B.3. BLAST Results of *Sacchromyces Cerevisiae* and *Giardia* (taxid:5740) (continues)

34	Long chain fatty acid CoA ligase 5	0.006	No significant similarity found	
35	putative acetyl-CoA carboxylase/pyruvate carboxylase fusion protein	0.045	No significant similarity found	
36	Long chain fatty acid CoA ligase 5	0.006	Long chain fatty acid CoA ligase 5	0.032
43	Hypothetical protein GL50803_12146	0.94	Giardia lamblia ATCC 50803 ABC transporter, ATP-binding protein	0.08
46	Hypothetical protein GL50803_12146	0.94	Giardia lamblia ATCC 50803 ABC transporter, ATP-binding protein	0.08
47	Hypothetical protein GL50803_12146	0.94	Giardia lamblia ATCC 50803 ABC transporter, ATP-binding protein	0.08
48	Hypothetical protein GL50803_12146	0.94	Giardia lamblia ATCC 50803 ABC transporter, ATP-binding protein	0.08

B.1.4. BLAST Results of *Sacchromyces Cerevisiae* and *Giardia Intestinalis* (taxid:5741)

As it is seen from Table B.4, BLAST results of *Giardia intestinalis* is not different from those of *Giardia lamblia*. Some ezymes, e.g. oxidoreductases, CDP-diacylglycerol synthase, inositol-3-phosphate synthase, phosphoinositide-3-kinase, serine palmitoyltransferase and phosphatidylserine decarboxylase, gave high resemblence for both species.

Table B.4. BLAST Results of *Sacchromyces Cerevisiae* and *Giardia Intestinalis* (taxid:5741)

	Giardia Intestinalis Blast		**Giardia Intestinalis Blast**	
	protein- protein blast	**e value**	**nucleot. blast**	**e value**
1	Long chain fatty acid CoA ligase 5	0.006	Long chain fatty acid CoA ligase 5	0.032
2	Cleavage and polyadenylation specificity factor, 73 kDa subunit	0.82	No significant similarity found	
3	Hypothetical protein GL50803_37452	6.4	No significant similarity found	
4	CDP-diacylglycerol synthase	1E-17	Hypothetical protein	0.93
5	CDP-diacylglycerol-inositol 3-phosphatidyltransferase	7E-21	Hypothetical protein	0.44
6	Inositol-3-phosphate synthase	8E-101	Inositol-3-phosphate synthase	0.000001
7	Phosphoinositide-3-kinase, class 3	5E-26	Hypothetical protein	0.52
8	Hypothetical protein GL50803_17427	0.00003	No significant similarity found	
9	High cysteine membrane protein VSP-like	0.18	Kinase, CMGC DYRK	0.051
10	SOF1 protein	0.04	No significant similarity found	
11	Serine palmitoyltransferase 2	7E-28	No significant similarity found	
12	Hypothetical protein GL50803_31998	0.27	No significant similarity found	
13	Hypothetical protein GL50803_13942	0.066	No significant similarity found	
14	Methionyl-tRNA synthetase	1.1	No significant similarity found	
15	Hypothetical protein GL50803_9157	0.33	No significant similarity found	
16	phosphatidylserine decarboxylase	3E-13	No significant similarity found	
17	Cysteine desulfurase	0.044	No significant similarity found	
19	Methionyl-tRNA synthetase	1.1	No significant similarity found	
20	Oxidoreductase, short chain dehydrogenase/reductase family	5E-25	No significant similarity found	
21	Gamma tubulin ring complex	1.7	No significant similarity found	
22	Hypothetical protein GL50803_112932	0.037	No significant similarity found	
23	Hypothetical protein GL50803_5939	0.00003	No significant similarity found	

Table B.4. BLAST Results of *Sacchromyces Cerevisiae* and *Giardia Intestinalis* (taxid:5741) (continues)

25	Hypothetical protein GL50803_112932	0.17	No significant similarity found	
27	Hypothetical protein GL50803_10238	3.4	No significant similarity found	
28	Hypothetical protein GL50803_12146	0.94	Giardia lamblia ATCC 50803 ABC transporter, ATP-binding protein	0.08
29	VSP	2.5	No significant similarity found	
30	VSP	2.5	No significant similarity found	
31	Hypothetical protein GL50803_12146	0.94	Giardia lamblia ATCC 50803 ABC transporter, ATP-binding protein	0.08
33	Tubulin tyrosine ligase	0.18	No significant similarity found	
34	Long chain fatty acid CoA ligase 5	0.006	No significant similarity found	
35	putative acetyl-CoA carboxylase/pyruvate carboxylase fusion protein	0.045	No significant similarity found	
36	Long chain fatty acid CoA ligase 5	0.006	Long chain fatty acid CoA ligase 5	0.032
43	Hypothetical protein GL50803_12146	0.94	Giardia lamblia ATCC 50803 ABC transporter, ATP-binding protein	0.08
46	Hypothetical protein GL50803_12146	0.94	Giardia lamblia ATCC 50803 ABC transporter, ATP-binding protein	0.08
47	Hypothetical protein GL50803_12146	0.94	Giardia lamblia ATCC 50803 ABC transporter, ATP-binding protein	0.08
48	Hypothetical protein GL50803_12146	0.94	Giardia lamblia ATCC 50803 ABC transporter, ATP-binding protein	0.08

B.1.5. BLAST Results of *Sacchromyces Cerevisiae* and *Giardia Muris* (taxid:5742)

As can be seen from Table B.5, *Giardia Muris* results are different than those of *Giardia lamblia* and *intestinalis*, e values were high meaning low resemblence.

Table B.5. BLAST Results of *Sacchromyces Cerevisiae* and *Giardia Muris* (taxid:5741)

	Giardia Muris Blast		**Giardia Muris Blast**	
	protein- protein blast	**e value**	**nucleot. blast**	**e value**
1	beta-giardin	0.61	No significant similarity found	
2	elongation factor 1 alpha	0.3	No significant similarity found	
3	variant-specific surface protein 02	0.036	No significant similarity found	
4	unknown	0.5	Giardia muris variant-specific surface protein 06 gene	0.23
5	elongation factor 1 alpha	0.017	Giardia muris variant-specific surface protein 04 gene	4.7
6	elongation factor 1 alpha	0.24	Giardia muris variant-specific surface protein 06 gene	3.3
7	elongation factor 1 alpha	2	G.muris ribosomal RNA operon DNA encoding 16S, 23S and 5.8S ribosomal rNA	1.6
8	variant-specific surface protein 01	1.4	No significant similarity found	
9	variant-specific surface protein 06	1.1	No significant similarity found	
10	beta-giardin	3	No significant similarity found	
11	variant-specific surface protein 05	1.1	No significant similarity found	
12	variant-specific surface protein 03	0.37	No significant similarity found	
13	cysteine protease	0.72	No significant similarity found	
14	variant-specific surface protein 02	0.032	No significant similarity found	
15	elongation factor 1 alpha	5.4	No significant similarity found	
16	elongation factor 1 alpha	0.52	No significant similarity found	
17	beta-giardin	4.2	No significant similarity found	
19	variant-specific surface protein 02	0.032	No significant similarity found	
20	cysteine protease	2.8	No significant similarity found	
21	No significant similarity found		No significant similarity found	
22	variant-specific surface protein 04	2.3	No significant similarity found	
25	triose phosphate isomerase	2.8	No significant similarity found	
28	variant-specific surface protein 06	4.3	No significant similarity found	
29	cysteine protease	1.9	No significant similarity found	
30	cysteine protease	1.9	No significant similarity found	
31	variant-specific surface protein 06	4.3	No significant similarity found	
33	variant-specific surface protein 04	0.53	No significant similarity found	
34	variant-specific surface protein 05	0.72	No significant similarity found	
35	cysteine protease	2.7	No significant similarity found	
36	beta-giardin	0.61	No significant similarity found	

Table B.5. BLAST Results of *Sacchromyces Cerevisiae* and *Giardia Muris* (taxid:5741) (continues)

43	variant-specific surface protein 06	4.3	No significant similarity found	
46	variant-specific surface protein 06	4.3	No significant similarity found	
47	variant-specific surface protein 06	4.3	No significant similarity found	
48	variant-specific surface protein 06	4.3	No significant similarity found	

B.1.6. BLAST Results of *Sacchromyces Cerevisiae* and *Giardia Lamblia Virus* (taxid:29255)

Table B.6. BLAST Results of *Sacchromyces Cerevisiae* and *Giardia Virus* (taxid:29255)

	Giardia Lamblia virus Blast		**Giardia Lamblia Virus Blast**	
	protein- protein blast	**e value**	**nucleot. blast**	**e value**
1	capsid protein	4.7	No significant similarity found	
2	gag-pol fusion protein	1.6	No significant similarity found	
3	No significant similarity found		No significant similarity found	
4	gag-pol fusion protein	1.3	Giardia canis virus from China	0.91
5	gag-pol fusion protein	4.7	Giardia canis virus from China	0.44
6	capsid protein	7.5	Giardia canis virus from China	1.1
7	No significant similarity found		Gardiavirus genomic sequence	1.8
8	gag-pol fusion protein	7.6	No significant similarity found	
9	No significant similarity found		No significant similarity found	
10	capsid protein	6.6	No significant similarity found	
11	gag-pol fusion protein	0.68	No significant similarity found	
12	gag-pol fusion protein	0.72	No significant similarity found	
13	gag-pol fusion protein	0.79	No significant similarity found	
14	No significant similarity found		No significant similarity found	
15	No significant similarity found		No significant similarity found	
16	gag-pol fusion protein	2.4	No significant similarity found	
17	capsid protein	3.5	No significant similarity found	
18				
19	No significant similarity found		No significant similarity found	
20	ORF2; gag-pol fusion protein	0.27	No significant similarity found	
21	gag-pol fusion protein	0.13	No significant similarity found	
22	gag-pol fusion protein	4.1	No significant similarity found	
25	ORF2; gag-pol fusion protein	0.14	No significant similarity found	
27	ORF2; gag-pol fusion protein	3.8	Giardia canis virus from China, complete genome	1.1
28	gag-pol fusion protein	1.2	Giardia canis virus from China	0.96
29	gag-pol fusion protein	1	No significant similarity found	
30	gag-pol fusion protein	1	No significant similarity found	
31	gag-pol fusion protein	1.2	Giardia canis virus from China	0.96
33	gag-pol fusion protein	2.7	No significant similarity found	
34	gag-pol fusion protein	1.9	No significant similarity found	
35	gag-pol fusion protein	0.59	No significant similarity found	
36	capsid protein	4.7	No significant similarity found	
43	gag-pol fusion protein	1.2	Giardia canis virus from China	0.96
46	gag-pol fusion protein	1.2	Giardia canis virus from China	0.96
47	gag-pol fusion protein	1.2	Giardia canis virus from China	0.96
48	gag-pol fusion protein	1.2	Giardia canis virus from China	0.96
54	ORF2; gag-pol fusion protein	7.3		

B.2. BLAST Results of *Mus Musculus*

B.2.1. Enzymes Catalyzing the Reactions of Sphingolipid Metabolism in *Mus Musculus*

The enzymes related with the sphingolipid metabolism in *M. Musculus* (Sheikh et al., 2005).

Table B.7. Enzymes catalyzing the Reactions of Sphingolipid Metabolism in *Mus musculus*

Reaction no	EC number		Enzyme Name
Inositol phosphate metabolism			
		Pik3C2g	phosphatidylinositol 3-kinase, C2 domain Containing, gamma polypeptide
1	2.7.1.137	Pik3Ca	phosphatidylinositol 3-kinase, CatalytiC, alpha polypeptide
2	2.7.1.137	Pik3Cd	phosphatidylinositol 3-kinase CatalytiC delta polypeptide
3	2.7.1.137	Pik3Cg	phosphoinositide-3-kinase, CatalytiC, gamma polypeptide
4	2.7.1.68	Pipk5k3	phosphatidylinositol-4-phosphate 5-kinase, type III
5	2.7.1.68	Pip5k2a	phosphatidylinositol-4-phosphate 5-kinase, type II, alpha
6	3.1.4.11	PlCb3	phospholipase C, beta 3
7	2.7.1.-	Akt1	thymoma viral proto-onCogene 1
8	2.7.1.-	Akt2	thymoma viral proto-onCogene 2
9	3.1.3.25	Impa2	inositol (myo)-1(or 4)-monophosphatase 2
10	3.1.3.25	Impa1	inositol (myo)-1(or 4)-monophosphatase 1
11	3.1.3.25	Impa1	inositol (myo)-1(or 4)-monophosphatase 1
12	3.1.3.57	Inpp1	inositol polyphosphate-1-phosphatase
13	3.1.3.57	Inpp1	inositol polyphosphate-1-phosphatase
14	5.5.1.4	1300017C10Rik	RIKEN CDNA 1300017C10 gene
15	3.1.3.56	INP	inositol-polyphosphate 5-phosphatase
16	3.1.3.56	INP	inositol-polyphosphate 5-phosphatase
Sphingophospholipid biosynthesis			
17	3.1.4.12	Smpd1	sphingomyelin phosphodiesterase 1, aCid lysosomal
18	3.1.4.12	Smpd2	sphingomyelin phosphodiesterase 2, neutral
19	3.1.4.12	Opn4	opsin 4 (melanopsin)
20	3.1.4.12	Smpd3	sphingomyelin phosphodiesterase 3, neutral
21		CCP	ceramide choline phosphotransferase

Table B.7. Enzymes catalyzing the Reactions of Sphingolipid Metabolism in *Mus musculus* (continues)

Phospholipid degradation			
22	3.1.4.4	PLD1	Phospholipase D1
23	3.1.4.4	Pld2	phospholipase D2
Sphingoglycolipid metabolism			
24	2.3.1.50	SptlC1	serine palmitoyltransferase, long chain base subunit 1
25	2.3.1.50	SptlC2	serine palmitoyltransferase, long chain base subunit 2
26	1.1.1.102		3-Dehydrosphinganine reductase
27	1.3.99.-		
28			sphinganine N-acyltransferase
29	3.5.1.23	Asah1	N-acylsphingosine amidohydrolase 1
30	2.4.1.80	UgCg	UDP-glucose ceramide glucosyltransferase
31	3.2.1.45	Gba	aCid beta gluCosidase
32	3.2.1.23	Glb1	galactosidase, beta 1
33	3.2.1.23	Glb1	galactosidase, beta 1
34	3.2.1.23	Glb1	galactosidase, beta 1
35	3.2.1.23	Glb1	galactosidase, beta 1
36	2.4.1.-	Fut4	fucosyltransferase 4
37	2.4.1.-	Galgt2	UDP-N-acetyl-alpha-D-galactosamine:(N-acetylneuraminyl)-galactosyl-N-acetylglucosaminylpolypeptide-beta-1, 4-N-acetylgalactosaminyltransferase
38	2.4.1.- 2.4.1.22 2.4.1.90 2.4.1.38	Ggtb	beta-1,4-galactosyltransferase / lactose synthase / N-acetyllactosamine synthase / beta-N-acetylglucosaminylglycopeptide beta-1,4-galactosyltransferase
39		SGL1	
40	2.4.1.-	B4galt5	UDP-Gal:betaGlcNAc beta 1,4-galactosyltransferase, polypeptide 5
41	2.4.1.92	Galgt1	UDP-N-acetyl-alpha-D-galactosamine:(N-acetylneuraminyl)-galactosylglucosylceramide-beta-1, 4-N-acetylgalactosaminyltransferase
42	2.4.1.92	Galgt1	UDP-N-acetyl-alpha-D-galactosamine:(N-acetylneuraminyl)-galactosylglucosylceramide-beta-1, 4-N-acetylgalactosaminyltransferase
43	2.4.1.92	Galgt1	UDP-N-acetyl-alpha-D-galactosamine:(N-acetylneuraminyl)-galactosylglucosylceramide-beta-1, 4-N-acetylgalactosaminyltransferase
44	2.4.99.8	Siat8a	sialyltransferase 8 (alpha-2, 8-sialytransferase) A
45	2.4.99.-	Siat5	sialyltransferase 5
46	3.2.1.18	Neu1	neuraminidase 1
47	3.2.1.18	Neu2	neuraminidase 2
48		SGL2	
49		SGL3	
50		SGL4	
51		SGL5	

Table B.7. Enzymes catalyzing the Reactions of Sphingolipid Metabolism in *Mus musculus* (continues)

52		SGL6	
53		SGL7	
54		SGL8	
55		SGL9	
56		SGL10	
57		SGL11	
58	2.7.1.-	Akt1	thymoma viral proto-onCogene 1
59	3.2.1.22	Gla	galaCtosidase, alpha
60	4.1.2.27	Sgpl1	sphingosine phosphate lyase 1
61	2.4.99.9	Siat9	sialyltransferase 9 (CMP-NeuAC:laCtosylCeramide alpha-2,3-sialyltransferase)
62	2.4.99.9	Siat9	sialyltransferase 9 (CMP-NeuAC:laCtosylCeramide alpha-2,3-sialyltransferase)
63	2.4.99.9	Siat9	sialyltransferase 9 (CMP-NeuAC:laCtosylCeramide alpha-2,3-sialyltransferase)
64	3.2.1.52	Hexa	hexosaminidase A
65	3.2.1.52	Hexb	hexosaminidase B

B.2.2. BLAST Results of *Mus Musculus* and *Giardia Lamblia* (taxid:184922)

The BLAST results of *Mus Musculus* and *Giardia Lamblia* are given in Table B.8. Some results are missing since there was no information about those genes.

Table B.8. The BLAST results of *Mus Musculus* and *Giardia Lamblia*

	Giardia L.		**Giardia L.**	
	P-blast	**e value**	**N-Blast**	**e-value**
1	Phosphoinositide-3-kinase, catalytic, alpha polypeptide	4E-28	Hypothetical protein (GL50803_87970) partial mRNA	0.091
2	Phosphoinositide-3-kinase, catalytic, alpha polypeptide	1E-35	Phosphatidylinositol 4-kinase (GL50803_16558) partial mRNA	0.004
3	Phosphoinositide-3-kinase, catalytic, alpha polypeptide	4E-33	Phosphoinositide-3-kinase, catalytic, alpha polypeptide	0.00002
4	Phosphoinositide-3-kinase, catalytic, alpha polypeptide	3E-37	Hypothetical protein (GL50803_17008) partial mRNA	0.54
5	TCP-1 chaperonin subunit gamma	1E-19	Hypothetical protein (GL50803_16544)	3.5
7	AAA family ATPase	1.3	Hypothetical protein (GL50803_8586)	0.17
8	Kinase, AGC PKA	4E-65	Kinase, AGC PKA	0.81

Table B.8. The BLAST results of *Mus Musculus* and *Giardia Lamblia* (continues)

9	Kinase, AGC PKA	4E-65	Kinase, NEK (GL50803_16279) mRNA, complete cds	0.0001
10	Hypothetical protein GL50803_9353	0.00005	Splicing factor U2AF subunit, putative (GL50803_16554) partial mRNA	0.49
11	Hypothetical protein GL50803_9353	0.003	Hypothetical protein (GL50803_18722) partial mRNA	0.038
12	Hypothetical protein GL50803_9353	0.003	Hypothetical protein (GL50803_18722) partial mRNA	0.038
13	Hypothetical protein GL50803_9353	0.003	Hypothetical protein (GL50803_9072) partial mRNA	0.055
14	Hypothetical protein GL50803_9353	0.003	Hypothetical protein (GL50803_9072) partial mRNA	0.055
16	Type II inositol-1,4,5-trisphosphate 5-phosphatase prc.	7E-17	Hypothetical protein (GL50803_23389)partial mRNA	0.18
17	Type II inositol-1,4,5-trisphosphate 5-phosphatase precursor	7E-17	Hypothetical protein (GL50803_23389) partial mRNA	0.18
18	Acid sphingomyelinase-like phosphodiesterase 3b precursor	1E-16	Hypothetical protein (GL50803_113970) partial mRNA	0.025
19	Hypothetical protein GL50803_97698	0.45	Ser/Thr protein kinase (GL50803_37353)	0.20
20	Hypothetical protein GL50803_22573	2.0	Hypothetical protein (GL50803_8627) partial mRNA	0.00004
21	Hypothetical protein GL50803_102184	1.3	Mannose-1-phosphate guanyltransferase (GL50803_16598) partial mRNA	3.9
22	Hypothetical protein GL50803_35341	0.12	Cyst wall protein 1 (GL50803_5638) partial mRNA	0.71
23	Protein 21.1	0.76	Heat-shock protein, putative (GL50803_16412)	0.15
24	Hypothetical protein GL50803_90434	0.23	Syntaxin 16 (GL50803_3869) mRNA, complete cds	1.6
25	Serine palmitoyltransferase 1	5E-37	Hypothetical protein (GL50803_10675) partial mRNA	0.019
26	hemagglutinin protein-like protein (GL50803_8982) partial mRNA	0.27	Serine palmitoyltransferase 2	1E-76
29	Kinesin-4	1.1	Kelch repeat-containing protein (GL50803_15054) partial mRNA	2.3
30	Hypothetical protein GL50803_5768	4.6	Exonuclease (GL50803_14763) mRNA, complete cds	0.67
31	No significant similarity found		Protein 21.1 (GL50803_94662) mRNA, complete cds	0.87
32	No significant similarity found		Hypothetical protein (GL50803_38948) partial mRNA	1.1
33	No significant similarity found		Hypothetical protein (GL50803_38948) partial mRNA	1.1
34	No significant similarity found		Hypothetical protein (GL50803_38948) partial mRNA	1.1
35	No significant similarity found		Hypothetical protein (GL50803_38948) partial mRNA	1.1
36	Coatomer gamma subunit	1.2	Hypothetical protein (GL50803_2167) partial mRNA	0.005
38	Mucin-like protein	2.4	Protein 21.1 (GL50803_9720) mRNA, complete cds	0.18

Table B.8. The BLAST results of *Mus Musculus* and *Giardia Lamblia* (continues)

40	Hypothetical protein GL50803_14997	0.63	Hypothetical protein (GL50803_6455) partial mRNA	0.66
44	Hypothetical protein GL50803_34882	2.9	Hypothetical protein (GL50803_24528) partial mRNA	0.17
46	Kinase, NEK	5.1	Alanine aminotransferase, putative (GL50803_16363) partial mRNA	0.20
47	Hypothetical protein GL50803_8468	0.69	Ciliary dynein heavy chain 11 (GL50803_42285) partial mRNA	0.053
58	Kinase, AGC PKA	4E-65	Hypothetical protein (GL50803_6581) partial mRNA	0.23
59	Hypothetical protein GL50803_37350	3.5	Hypothetical protein (GL50803_103175) partial mRNA	0.20
60	Transducin	0.88	Hypothetical protein (GL50803_41451) partial mRNA	0.97
64	Hypothetical protein GL50803_16321	0.39	Kinase, CAMKK (GL50803_96363) mRNA, complete cds	0.074
65	Splicing factor-like protein, putative	0.58	Transcription regulatory protein SNF2 (GL50803_16143)	0.26

APPENDIX C: FBA RESULTS

C.1. Results related to 20 reaction pathway

C.1.1. Wildtype Results with Different Objective Functions

Table C.1. Objective functions of Complex Sphingolipid Maximizations

Reaction No	No Obj	LCER Max	C1P Max	GALCER Max	SM Max	SPN1P Max	CER max	GCER Max
1	10.9862	12.5	12.5	12.5	12.5	12.5	12.5	12.5
2	10.9862	12.5	12.5	12.5	12.5	12.5	12.5	12.5
3	10.9862	12.5	12.5	12.5	12.5	12.5	12.5	12.5
4	10.9862	12.5	12.5	12.5	12.5	12.5	12.5	12.5
5	10.9862	12.5	12.5	12.5	12.5	12.5	12.5	12.5
6	12.1103	0	0	0	0	0	0	0
7	16.0736	0	0	0	0	12.5	0	0
8	136.1065	197.0514	235.8378	192.2484	248.3879	184.346	256.5743	228.1538
9	132.5923	184.5514	235.8378	192.2484	248.3879	184.346	256.5743	215.6538
10	96.8927	144.3739	170.0536	136.2267	179.397	131.859	186.1028	158.6204
11	93.3785	131.8739	170.0536	136.2267	179.397	131.859	186.1028	158.6204
12	182.6145	256.3366	329.9293	264.0652	354.3393	253.061	364.1718	299.0432
13	182.6082	256.3366	329.9293	264.0652	341.8393	253.061	364.1718	299.0432
14	93.8078	133.1114	169.2159	133.955	178.5163	131.599	185.7722	157.5864
15	95.5159	133.1114	169.2159	146.455	178.5163	131.599	185.7722	157.5864
16	3.9632	0	0	0	0	12.5	0	0
17	76.9034	87.5	87.5	87.5	87.5	87.5	87.5	87.5
18	10.9862	12.5	12.5	12.5	12.5	12.5	12.5	12.5
19	10.9862	12.5	12.5	12.5	12.5	12.5	12.5	12.5
20	1.7944	0	12.5	0	0	0	0	0

Table C.2. Objective functions of Combinations of Complex Sphingolipid Maximizations

Reaction No	SPN Max	CER+C1P	CER+SPN1P	LCER+SPN1P	r1max	AccoA max	r1andCERmax
1	12.5	12.5	12.5	12.5	12.5	0	12.5
2	12.5	12.5	12.5	12.5	12.5	0	12.5
3	12.5	12.5	12.5	12.5	12.5	0	12.5
4	12.5	12.5	12.5	12.5	12.5	0	12.5
5	12.5	12.5	12.5	12.5	12.5	0	12.5
6	0	0	0	0	0	1000	0
7	12.5	0	11.1136	9.7301	6.4316	1000	0
8	228.8874	184.5599	172.6216	154.7265	175.3987	0	246.1646
9	228.8874	184.5599	172.6216	151.9567	172.4791	0	246.1646
10	164.9521	133.2526	124.4729	111.232	125.7802	0	178.3278

Table C.2. Objective functions of Combinations of Complex Sphingolipid Maximizations (continues)

11	164.9521	133.2526	124.4729	108.4621	122.8606	0	178.3278
12	315.5448	253.4699	235.1734	206.3171	237.35	340.3812	346.3745
13	315.5448	253.4699	235.1734	206.3171	237.2292	340.3812	346.3745
14	164.4278	132.592	123.7186	107.7344	123.0829	0	177.988
15	164.4278	132.592	123.7186	107.7344	124.5308	0	177.988
16	0	0	11.1136	9.7301	6.4316	0	0
17	87.5	87.5	87.5	87.5	87.5	0	87.5
18	12.5	12.5	12.5	12.5	12.5	0	12.5
19	12.5	12.5	12.5	12.5	12.5	0	12.5
20	0	12.3612	0	0	1.5801	0	4.5271

C.1.2. Deletion Results of r1 maxmization as Objective Function

Table C.3. Results of 20 reaction pathway as r1 maximization

Reaction No		r1 del	r2 del	r3 del	r4 del	r5 del	r6 del	r7 del	r8 del
1	66.7	0	0	0	0	0	66.6667	66.6667	66.7
2	66.7	0	0	0	0	0	66.6667	66.6667	66.7
3	66.7	0	0	0	0	0	66.6667	66.6667	66.7
4	66.7	0	0	0	0	0	66.6667	66.6667	66.7
5	66.7	0	0	0	0	0	66.6667	66.6667	66.7
6	58	100.3091	100.3112	100.5129	100.5129	100.5129	0	0	65.8
7	71.8	100.3091	100.3112	100.5129	100.5129	100.5129	20.9614	0	78.9
8	193.9	116.3269	116.3296	116.5842	116.5842	116.5842	187.8381	186.1737	0
9	188.3	116.3269	116.3296	116.5842	116.5842	116.5842	174.9463	174.2505	0
10	139.6	82.1766	82.1787	82.3546	82.3546	82.3546	136.9661	134.4647	154.5
11	133.9	82.1766	82.1787	82.3546	82.3546	82.3546	124.0744	122.5416	154.5
12	256.2	169.367	169.3704	169.7545	169.7545	169.7545	223.5282	229.9813	247.9
13	222	169.367	169.3704	169.7545	169.7545	169.7545	218.8807	206.932	228.6
14	134.7	82.4091	82.4105	82.5746	82.5746	82.5746	121.6444	121.7885	150
15	136.3	82.4091	82.4105	82.5746	82.5746	82.5746	137.5761	134.6019	169.9
16	13.8	0	0	0	0	0	20.9614	0	13.1
17	466.7	0	0	0	0	0	466.6667	466.6667	466.7
18	66.7	0	0	0	0	0	66.6667	66.6667	66.7
19	66.7	0	0	0	0	0	66.6667	66.6667	66.7
20	11.4	0	0	0	0	0	12.2344	18.8808	14.3
'UDPG'	193.9	116.3269	116.3296	116.5842	116.5842	116.5842	187.8381	186.1737	0
'O2'	66.7	0	0	0	0	0	66.6667	66.6667	66.7
'AcCoA'	591.4	100.3091	100.3112	100.5129	100.5129	100.5129	533.3333	533.3333	599.1
'3PS'	66.7	0	0	0	0	0	66.6667	66.6667	66.7
'CDPCHO'	34.2	0	0	0	0	0	4.6475	23.0493	19.3
'UDPGAL'	275.9	164.5857	164.5891	164.9292	164.9292	164.9292	274.5421	269.0666	324.5
'ATP'	558.5	0	0	0	0	0	566.5291	552.2141	560.7

Table C.3. Results of 20 reaction pathway as r1 maximization (continues)

'NADPH'	1000	0	0	0	0	0	1000	1000	1000
'CO2'	-66.6	0	0	0	0	0	-66.6667	-66.6667	-66.7
'CoA'	-658.1	-100.309	-100.311	-100.513	-100.513	-100.513	-600	-600	-665.7
'H'	-32.4	0	0	0	0	0	-62.0192	-43.6174	-47.4
'FA'	-5.1	-100.309	-100.311	-100.513	-100.513	-100.513	45.7052	66.6667	-12.3
'H2O'	62	381.2216	381.23	382.0262	382.0262	382.0262	-25.0401	-48.0862	-83.2
'CMP'	-34.2	0	0	0	0	0	-4.6475	-23.0493	-19.3
'ADP'	-491.9	0	0	0	0	0	-499.863	-485.548	-494.1
'DP'	-66.6	0	0	0	0	0	-66.6667	-66.6667	-66.7
'NADP'	-1000	0	0	0	0	0	-1000	-1000	-1000
'P'	-533.3	0	0	0	0	0	-533.333	-533.333	-533.3
'AMP'	-66.6	0	0	0	0	0	-66.6667	-66.6667	-66.7
'GLC'	188.3	116.3269	116.3296	116.5842	116.5842	116.5842	174.9463	174.2505	0
'bGLAC'	268.6	164.5857	164.5891	164.9292	164.9292	164.9292	245.7188	244.33	304.5
'SPN1P'	13.8	0	0	0	0	0	20.9614	0	13.1
'C1P'	11.4	0	0	0	0	0	12.2344	18.8808	14.3
'GALCER'	1.6	0	0	0	0	0	15.9317	12.8134	19.9
'LCER'	5.7	0	0	0	0	0	12.8917	11.9232	0
'SM'	34.2	0	0	0	0	0	4.6475	23.0493	19.3

C.2. Results related to 25 reaction pathway

C.2.1. Deletion Results of r1 maximization as Objective Function

Table C.4. Deletion Results of 25 reaction pathway with r1 maximization (r1 to r8)

Reaction No		r2 del	r3del	r4del	r5del	r6 del	r7 del	r8 del
r1	12.5	12.5	12.5	12.5	12.5	12.5	12.5	12.5
r2	11.3892	0	0	0	0	10.5057	10.852	11.5344
r3	11.3892	0	0	0	0	10.5057	10.852	11.5344
r4	11.3892	0	0	0	0	10.5057	10.852	11.5344
r5	11.3892	0	0	0	0	10.5057	10.852	11.5344
r6	0	0	0	0	0	0	0	0
r7	6.3917	0	0	0	0	1.6569	0	6.021
r8	163.155	127.2042	127.2236	127.2236	127.2236	135.4568	132.0584	0
r9	162.6288	127.2042	127.2236	127.2236	127.2236	134.3539	131.232	0
r10	119.3332	90.6435	90.657	90.657	90.657	99.3817	96.8387	122.7313
r11	118.807	90.6435	90.657	90.657	90.657	98.2788	96.0123	122.7313
r12	241.3913	188.7193	188.7525	188.7525	188.7525	192.0572	191.7981	220.8248
r13	238.0375	188.7193	188.7525	188.7525	188.7525	186.2691	183.5034	216.9797
r14	117.4884	94.1503	94.1683	94.1683	94.1683	95.6834	94.715	124.7293
r15	118.1317	94.1503	94.1683	94.1683	94.1683	97.0829	96.0518	125.9886
r16	6.3917	0	0	0	0	1.6569	0	6.021
r17	87.5	87.5	87.5	87.5	87.5	87.5	87.5	87.5
r18	12.5	12.5	12.5	12.5	12.5	12.5	12.5	12.5
r19	14.743	0	0	0	0	16.2937	19.1467	15.3795
r20	0.4743	0	0	0	0	0.5582	0.3941	0.409
r21	1.1108	12.5	12.5	12.5	12.5	1.9943	1.648	0.9656
r22	1.1108	12.5	12.5	12.5	12.5	1.9943	1.648	0.9656
r23	3.3538	0	0	0	0	5.788	8.2947	3.8451
r24	3.3538	0	0	0	0	5.788	8.2947	3.8451
r25	3.3538	0	0	0	0	5.788	8.2947	3.8451
'UDPG'	163.155	127.2042	127.2236	127.2236	127.2236	135.4568	132.0584	0
'O2'	11.3892	0	0	0	0	10.5057	10.852	11.5344
'G3P'	1.1108	12.5	12.5	12.5	12.5	1.9943	1.648	0.9656
'AcCoA'	100	100	100	100	100	100	100	100
'3PS'	14.743	0	0	0	0	16.2937	19.1467	15.3795
'UDPGAL'	237.465	184.7937	184.8252	184.8252	184.8252	196.4646	192.8905	248.72
'AMP'	-12.5	-12.5	-12.5	-12.5	-12.5	-12.5	-12.5	-12.5
'H2O'	323.3912	249.498	249.5488	249.5488	249.5488	252.2497	246.05	171.7579
'CO2'	-11.3892	0	0	0	0	-10.5057	-10.852	-11.5344
'ATP'	110.2197	100	100	100	100	108.0032	108.6888	110.275
'NADPH'	186.3893	175	175	175	175	185.5056	185.852	186.5344

Table C.4. Deletion Results of 25 reaction pathway with r1 maximization (r1 to r8) (continues)

'NADP'	-186.389	-175	-175	-175	-175	-185.506	-185.852	-186.534
'CMP'	-3.3538	0	0	0	0	-5.7881	-8.2947	-3.8451
'UDP'	-400.62	-311.998	-312.049	-312.049	-312.049	-331.921	-324.949	-248.72
'DP'	-15.8538	-12.5	-12.5	-12.5	-12.5	-18.2881	-20.7947	-16.3451
'P'	-103.354	-100	-100	-100	-100	-105.788	-108.295	-103.845
'CoA'	-91.6517	-57.2431	-57.235	-57.235	-57.235	-88.1518	-76.7054	-89.5043
'H'	1.9153	-9.0427	-9.0473	-9.0473	-9.0473	-3.996	-24.8369	-2.3659
'FA'	-34.752	-33.7142	-33.7177	-33.7177	-33.7177	-31.5907	-25.8991	-33.3754
'PC'	3.3538	0	0	0	0	5.788	8.2947	3.8451
'CTP'	3.3538	0	0	0	0	5.7881	8.2947	3.8451
'DAG'	-1.1108	-12.5	-12.5	-12.5	-12.5	-1.9944	-1.648	-0.9656
'GLC'	162.6288	127.2042	127.2236	127.2236	127.2236	134.3539	131.232	0
'bGLAC'	236.2955	184.7937	184.8252	184.8252	184.8252	193.9621	190.7273	247.4606
'SPN1P'	6.3917	0	0	0	0	1.6569	0	6.021
'C1P'	0.4743	0	0	0	0	0.5582	0.3941	0.409
'GALCER'	0.6433	0	0	0	0	1.3996	1.3367	1.2593
'LCER'	0.5262	0	0	0	0	1.1029	0.8264	0
'SM'	3.3538	0	0	0	0	5.788	8.2947	3.8451
'PS'	3.3538	0	0	0	0	5.788	8.2947	3.8451

Table C.5. Deletion Results of 25 reaction pathway with r1 maximization (r9 to r16)

Reaction No	r9 del	r10 del	r11 del	r12 del	r13 del	r14 del	r15 del	r16 del
r1	12.5	12.5	12.5	12.5	12.5	12.5	12.5	12.5
r2	12.0659	11.3988	12.1349	10.7006	11.4796	11.8425	11.6834	10.6533
r3	12.0659	11.3988	12.1349	10.7006	11.4796	11.8425	11.6834	10.6533
r4	12.0659	11.3988	12.1349	10.7006	11.4796	11.8425	11.6834	10.6533
r5	12.0659	11.3988	12.1349	10.7006	11.4796	11.8425	11.6834	10.6533
r6	0	0	0	0	0	0	0	0
r7	11.8793	1.4172	11.494	6.8701	6.4017	8.9239	7.0078	0
r8	0.0594	143.7006	142.1328	138.5673	162.5595	155.0583	169.5762	134.7942
r9	0	143.7006	142.0392	137.4946	162.0139	154.4674	168.9546	133.7945
r10	108.524	0	0.0936	101.2919	118.8259	156.4683	167.8576	99.3046
r11	108.4646	0	0	100.2192	118.2803	155.8774	167.236	98.3048
r12	179.7467	204.8577	187.9252	0	3.4563	212.2137	232.6579	195.9236
r13	179.7464	197.2248	187.6092	0	0	210.394	228.964	188.8453
r14	105.5828	142.2263	139.7803	99.2056	116.9095	0	0	97.2902
r15	105.6353	144.1874	139.8719	100.4172	117.5153	0.2069	0	98.3164
r16	11.8793	1.4172	11.494	6.8701	6.4017	8.9239	7.0078	0
r17	87.5	87.5	87.5	87.5	87.5	87.5	87.5	87.5
r18	12.5	12.5	12.5	12.5	12.5	12.5	12.5	12.5
r19	12.0663	19.0316	12.451	10.7006	14.9359	13.6622	15.3773	17.7316

Table C.5. Deletion Results of 25 reaction pathway with r1 maximization (r9 to r16) (continues)

r20	0.0743	0.3876	0.1398	1.5462	0.4702	0.3011	0.3602	1.5491
r21	0.4341	1.1012	0.3651	1.7994	1.0204	0.6575	0.8166	1.8467
r22	0.4341	1.1012	0.3651	1.7994	1.0204	0.6575	0.8166	1.8467
r23	0.0004	7.6328	0.316	0	3.4563	1.8197	3.6938	7.0783
r24	0.0004	7.6328	0.316	0	3.4563	1.8197	3.6938	7.0783
r25	0.0004	7.6328	0.316	0	3.4563	1.8197	3.6938	7.0783
'UDPG'	0.0594	143.7006	142.1328	138.5673	162.5595	155.0583	169.5762	134.7942
'O2'	12.0659	11.3988	12.1349	10.7006	11.4796	11.8425	11.6834	10.6533
'G3P'	0.4341	1.1012	0.3651	1.7994	1.0204	0.6575	0.8166	1.8467
'AcCoA'	100	100	100	100	100	100	100	100
'3PS'	12.0663	19.0316	12.451	10.7006	14.9359	13.6622	15.3773	17.7316
'UDPGAL'	214.1593	144.1874	139.9655	201.7091	236.3413	156.6752	167.8576	197.621
'AMP'	-12.5	-12.5	-12.5	-12.5	-12.5	-12.5	-12.5	-12.5
'H2O'	139.2952	209.6794	206.8596	259.8883	321.6026	234.9034	261.0253	252.6613
'CO2'	-12.0659	-11.3987	-12.1349	-10.7006	-11.4796	-11.8425	-11.6834	-10.6533
'ATP'	111.9539	109.4377	111.9497	108.4164	110.3281	111.0446	111.0618	108.6274
'NADPH'	187.0658	186.3988	187.135	185.7006	186.4796	186.8425	186.6834	185.6533
'NADP'	-187.066	-186.399	-187.135	-185.701	-186.48	-186.843	-186.683	-185.653
'CMP'	-0.0003	-7.6329	-0.316	0	-3.4562	-1.8197	-3.6939	-7.0783
'UDP'	-214.219	-287.888	-282.098	-340.276	-398.901	-311.734	-337.434	-332.415
'DP'	-12.5003	-20.1329	-12.816	-12.5	-15.9563	-14.3196	-16.1938	-19.5783
'P'	-100	-107.633	-100.316	-100	-103.456	-101.82	-103.694	-107.078
'CoA'	-105.182	-90.7914	-102.727	-100.496	-92.0936	-93.9669	-87.3801	-78.1197
'H'	15.3222	-8.0853	11.0984	13.8151	1.8533	3.0235	-3.7854	-20.8088
'FA'	-34.0859	-29.205	-32.6329	-30.8903	-34.5533	-33.4623	-34.9133	-25.8814
'PC'	0.0004	7.6328	0.316	0	3.4563	1.8197	3.6938	7.0783
'CTP'	0.0003	7.6329	0.316	0	3.4562	1.8197	3.6939	7.0783
'DAG'	-0.4341	-1.1012	-0.3651	-1.7994	-1.0204	-0.6575	-0.8166	-1.8467
'GLC'	0	143.7006	142.0392	137.4946	162.0139	154.4674	168.9546	133.7945
'bGLAC'	214.0473	142.2263	139.7803	199.4248	235.1898	155.8774	167.236	195.5951
'SPN1P'	11.8793	1.4172	11.494	6.8701	6.4017	8.9239	7.0078	0
'C1P'	0.0743	0.3876	0.1398	1.5462	0.4702	0.3011	0.3602	1.5491
'GALCER'	0.0525	1.9611	0.0916	1.2116	0.6059	0.2069	0	1.0261
'LCER'	0.0594	0	0.0936	1.0727	0.5456	0.5909	0.6216	0.9998
'SM'	0.0004	7.6328	0.316	0	3.4563	1.8197	3.6938	7.0783
'PS'	0.0004	7.6328	0.316	0	3.4563	1.8197	3.6938	7.0783

Table C.6. Deletion Results of 25 reaction pathway with r1 maximization (r16 to r20)

Reaction No	r17 del	r18 del	r19 del	r20 del	r21 del	r22del	r23del	r24del	r25del
1	0	0	12.5	12.5	12.5	12.5	12.5	12.5	12.5
2	0	0	0	11.4104	12.5	12.5	9.3061	9.0916	9.3058
3	0	0	0	11.4104	12.5	12.5	9.3061	9.0916	9.3058
4	0	0	0	11.4104	12.5	12.5	9.3061	9.0916	9.3058
5	0	0	0	11.4104	12.5	12.5	9.3061	9.0916	9.3058
6	100	100	0	0	0	0	0	0	0
7	100	100	0	7.8269	8.7886	2.9026	7.3344	7.0522	7.3318
8	138.8029	138.6873	123.2087	157.9042	152.4647	167.8214	130.0664	123.7682	129.2472
9	138.8029	138.6873	123.2087	157.6247	151.4024	164.9705	130.0547	123.7614	129.2362
10	103.1635	103.0802	86.9493	115.745	110.1057	121.5717	95.7987	91.2018	95.2092
11	103.1635	103.0802	86.9493	115.4655	109.0435	118.7207	95.787	91.195	95.1982
12	216.7104	216.513	177.6443	231.0866	222.5127	247.671	179.1892	167.4442	177.7292
13	216.7104	216.513	177.6443	228.306	220.5991	242.5559	179.1892	167.4442	177.7292
14	102.9058	102.8071	88.4423	113.8926	109.3078	119.6341	94.7569	90.1095	94.1613
15	102.9058	102.8071	88.4423	114.416	109.6955	120.5776	95.78	91.1761	95.1907
16	0	0	0	7.8269	8.7886	2.9026	7.3344	7.0522	7.3318
17	0	0	87.5	87.5	87.5	87.5	87.5	87.5	87.5
18	0	0	12.5	12.5	12.5	12.5	12.5	12.5	12.5
19	0	0	0	14.191	14.4136	17.6151	9.3061	9.0916	9.3058
20	0	0	0	0	0.3478	0.6878	0.9369	0.966	0.9335
21	0	0	12.5	1.0896	0	0	3.1939	3.4084	3.1942
22	0	0	12.5	1.0896	0	0	3.1939	3.4084	3.1942
23	0	0	0	2.7806	1.9136	5.1151	0	0	0
24	0	0	0	2.7806	1.9136	5.1151	0	0	0
25	0	0	0	2.7806	1.9136	5.1151	0	0	0
'UDPG'	138.8029	138.6873	123.2087	157.9042	152.4647	167.8214	130.0664	123.7682	129.2472
'O2'	0	0	0	11.4104	12.5	12.5	9.3061	9.0916	9.3058
'G3P'	0	0	12.5	1.0896	0	0	3.1939	3.4084	3.1942
'AcCoA'	100	100	100	100	100	100	100	100	100
'3PS'	0	0	0	14.191	14.4136	17.6151	9.3061	9.0916	9.3058
UDPGAL'	206.0693	205.8873	175.3915	230.161	219.8013	242.1493	191.5787	182.3779	190.3999
'AMP'	0	0	-12.5	-12.5	-12.5	-12.5	-12.5	-12.5	-12.5
'H2O'	444.8722	444.5746	236.1002	312.2694	292.956	323.843	246.8209	231.4349	244.8158
'CO2'	0	0	0	-11.4104	-12.5	-12.5	-9.3061	-9.0916	-9.3058
'ATP'	0	0	100	110.6075	111.05	108.7056	108.2713	108.0182	108.2653
'NADPH'	0	0	175	186.4104	187.5	187.5	184.3061	184.0916	184.3058
'NADP'	0	0	-175	-186.41	-187.5	-187.5	-184.306	-184.092	-184.306
'CMP'	0	0	0	-2.7806	-1.9136	-5.1151	0	0	0
'UDP'	-344.872	-344.575	-298.6	-388.065	-372.266	-409.971	-321.645	-306.146	-319.647
'DP'	0	0	-12.5	-15.2806	-14.4136	-17.6151	-12.5	-12.5	-12.5
'P'	0	0	-100	-102.781	-101.914	-105.115	-100	-100	-100
'CoA'	-33.2908	-33.388	-69.0488	-90.7955	-84.8811	-85.5554	-85.3477	-86.1848	-85.4973

Table C.6. Deletion Results of 25 reaction pathway with r1 maximization (r16 to r20) (continues)

'H'	-79.1557	-79.0893	3.3665	1.4682	-1.9519	-3.149	-0.5352	0.14	-0.4233
'FA'	-87.5535	-87.5227	-34.3177	-35.4713	-38.2829	-36.9284	-30.7577	-30.099	-30.717
'PC'	0	0	0	2.7806	1.9136	5.1151	0	0	0
'CTP'	0	0	0	2.7806	1.9136	5.1151	0	0	0
'DAG'	0	0	-12.5	-1.0896	0	0	-3.1939	-3.4084	-3.1942
'GLC'	138.8029	138.6873	123.2087	157.6247	151.4024	164.9705	130.0547	123.7614	129.2362
'bGLAC'	206.0693	205.8873	175.3915	229.3581	218.3513	238.3549	190.5439	181.3045	189.3594
'SPN1P'	0	0	0	7.8269	8.7886	2.9026	7.3344	7.0522	7.3318
'C1P'	0	0	0	0	0.3478	0.6878	0.9369	0.966	0.9335
'GALCER'	0	0	0	0.5234	0.3877	0.9435	1.0231	1.0666	1.0295
'LCER'	0	0	0	0.2795	1.0623	2.8509	0.0117	0.0068	0.011
'SM'	0	0	0	2.7806	1.9136	5.1151	0	0	0
'PS'	0	0	0	2.7806	1.9136	5.1151	0	0	0

C.2.2. Deletion Results of r2 maximization as Objective Function

Table C.7. Deletion Results of 25 reaction pathway with r2 maximization (r1 to r8)

Reaction No	wildtype	FAA1 (r1)	LCB1 (r2)	TSC10 (r3)	LAC1 (r4)	Degs1 (r5)	LASS1 (r6)	Asah1 (r7)	Ugcg (r8)
r1	66.6667	0	17.8238	17.8268	17.8549	17.8549	66.6667	66.6667	66.6667
r2	66.6667	0	0	0	0	0	66.6667	66.6667	66.6667
r3	66.6667	0	0	0	0	0	66.6667	66.6667	66.6667
r4	66.6667	0	0	0	0	0	66.6667	66.6667	66.6667
r5	66.6667	0	0	0	0	0	66.6667	66.6667	66.6667
r6	61.0896	126.1115	82.9679	82.9838	83.1282	83.1282	0	0	59.9417
r7	67.4208	126.1115	82.9679	82.9838	83.1282	83.1282	19.9373	0	65.7932
r8	175.8969	134.5703	121.6854	121.7045	121.9343	121.9343	179.4725	184.8019	0
r9	175.6136	134.5703	121.6854	121.7045	121.9343	121.9343	170.2813	170.0963	0
r10	127.5006	99.4571	86.2394	86.2528	86.4176	86.4176	131.4346	136.3542	140.2954
r11	127.2172	99.4571	86.2394	86.2528	86.4176	86.4176	122.2435	121.6487	140.2954
r12	252.0779	220.1416	182.2357	182.2654	182.6243	182.6243	244.043	237.0868	240.0954
r13	226.8727	220.1416	182.2357	182.2654	182.6243	182.6243	221.8779	228.5726	219.7756
r14	116.5484	102.2614	88.48	88.4974	88.655	88.655	126.2214	112.9453	131.3969
r15	144.8963	102.2614	88.48	88.4974	88.655	88.655	126.5137	148.0218	165.4533
r16	6.3311	0	0	0	0	0	19.9373	0	5.8514
r17	466.6667	0	124.7665	124.7878	124.9842	124.9842	466.6667	466.6667	466.6667
r18	66.6667	0	17.8238	17.8268	17.8549	17.8549	66.6667	66.6667	66.6667
r19	91.8719	0	0	0	0	0	88.8318	75.1809	86.9865
r20	6.4991	0	0	0	0	0	15.0809	8.3704	6.439
r21	0	0	17.8238	17.8268	17.8549	17.8549	0	0	0
r22	0	0	17.8238	17.8268	17.8549	17.8549	0	0	0

Table C.7. Deletion Results of 25 reaction pathway with r2 maximization (r1 to r8) (continues)

r23	25.2052	0	0	0	0	0	22.1651	8.5143	20.3198
r24	25.2052	0	0	0	0	0	22.1651	8.5143	20.3198
r25	25.2052	0	0	0	0	0	22.1651	8.5143	20.3198
'UDPG'	175.8969	134.5703	121.6854	121.7045	121.9343	121.9343	179.4725	184.8019	0
'O2'	66.6667	0	0	0	0	0	66.6667	66.6667	66.6667
'G3P'	0	0	17.8238	17.8268	17.8549	17.8549	0	0	0
'AcCoA'	594.423	126.1115	225.5582	225.5984	225.9673	225.9673	533.3333	533.3333	593.2751
'3PS'	91.8719	0	0	0	0	0	88.8318	75.1809	86.9865
'UDPGAL'	272.3968	201.7185	174.7195	174.7502	175.0726	175.0726	257.9483	284.376	305.7487
'AMP'	-66.6667	0	-17.8238	-17.8268	-17.8548	-17.8548	-66.6667	-66.6667	-66.6667
'H2O'	45.3386	462.4003	290.2539	290.3042	290.8606	290.8606	-5.818	-53.4621	-108.861
'CO2'	-66.6666	0	0	0	0	0	-66.6666	-66.6667	-66.6667
'ADP'	-504.702	0	-124.766	-124.7878	-124.984	-124.984	-523.85	-483.551	-499.277
'ATP'	571.3689	0	142.5902	142.6147	142.8391	142.8391	590.5166	550.2179	565.9436
'NADPH'	1000	0	249.533	249.5756	249.9684	249.9684	1000	1000	1000
'NADP'	-1000	0	-249.533	-249.5756	-249.968	-249.968	-1000	-1000	-1000
'CMP'	-25.2052	0	0	0	0	0	-22.1651	-8.5142	-20.3198
'UDP'	-448.294	-336.289	-296.405	-296.4547	-297.007	-297.007	-437.421	-469.178	-305.749
'DP'	-91.8719	0	-17.8238	-17.8269	-17.8549	-17.8549	-88.8318	-75.1809	-86.9864
'P'	-558.539	0	-142.59	-142.6146	-142.839	-142.839	-555.499	-541.848	-553.653
'H'	-117.077	0	0	0	0	0	-110.997	-83.6952	-107.306
'FA'	-0.7541	-126.112	-82.968	-82.9838	-83.1282	-83.1282	46.7294	66.6667	0.8734
'CoA'	-661.09	-126.112	-225.558	-225.5984	-225.967	-225.967	-600	-600	-659.942
'PC'	25.2052	0	0	0	0	0	22.1651	8.5143	20.3198
'CTP'	25.2052	0	0	0	0	0	22.1651	8.5142	20.3198
'DAG'	0	0	-17.8238	-17.8268	-17.8548	-17.8548	0	0	0
'GLC'	175.6136	134.5703	121.6854	121.7045	121.9343	121.9343	170.2813	170.0963	0
'bGLAC'	243.7657	201.7185	174.7195	174.7502	175.0726	175.0726	248.4649	234.594	271.6923
'SPN1P'	6.3311	0	0	0	0	0	19.9373	0	5.8514
'C1P'	6.4991	0	0	0	0	0	15.0809	8.3704	6.439
'GALCER'	28.3478	0	0	0	0	0	0.2923	35.0765	34.0564
'LCER'	0.2833	0	0	0	0	0	9.1911	14.7056	0
'SM'	25.2052	0	0	0	0	0	22.1651	8.5143	20.3198
'PS'	25.2052	0	0	0	0	0	22.1651	8.5143	20.3198

Table C.8. Deletion Results of 25 reaction pathway with r2 maximization (r9 to r16)

Reaction No	Gba (r9)	Fut4 (r10)	Glb1 (r11)	Smpd1 (r12)	Sgms1 (r13)	Glb1 (r14)	Ugt8a (r15)	SGPP1 (r16)
r1	66.6667	66.6667	66.7	66.7	66.6667	66.7	66.6667	66.6667
r2	66.6667	66.6667	66.7	66.7	66.6667	66.7	66.6667	66.6667
r3	66.6667	66.6667	66.7	66.7	66.6667	66.7	66.6667	66.6667
r4	66.6667	66.6667	66.7	66.7	66.6667	66.7	66.6667	66.6667
r5	66.6667	66.6667	66.7	66.7	66.6667	66.7	66.6667	66.6667
r6	73.0462	61.1671	69.9	52.4	62.9863	66.3	64.6858	64.2031
r7	84.4072	61.8018	75.3	70.9	69.4804	75.6	69.4893	64.2031
r8	13.447	183.3947	194.6	186.7	177.6101	186.8	204.7413	173.8813
r9	0	183.3947	182.7	173.6	177.2729	185.9	164.4138	173.691
r10	154.5409	0	11.9	138	128.8184	184.4	203.2822	125.9958
r11	141.0939	0	0	125	128.4812	183.5	162.9547	125.8055
r12	261.2045	240.1807	243	0	28.8293	258.9	245.9359	249.2819
r13	229.8443	224.4753	238.3	0	0	226.5	227.952	226.4716
r14	143.5074	165.3437	166.3	121.6	119.0382	0	0	110.7523
r15	144.7174	211.9631	208.3	140.6	143.2522	15.2	0	149.0669
r16	11.361	0.6347	5.4	18.5	6.4941	9.3	4.8035	0
r17	466.6667	466.6667	466.7	466.7	466.6667	466.7	466.6667	466.6667
r18	66.6667	66.6667	66.7	66.7	66.6667	66.7	66.6667	66.6667
r19	98.0268	82.372	71.4	66.7	95.4959	99.1	84.6506	89.477
r20	9.2886	3.7073	2.6	16.3	6.7922	8.8	3.5517	5.3516
r21	0	0	0	0	0	0	0	0
r22	0	0	0	0	0	0	0	0
r23	31.3601	15.7053	4.7	0	28.8293	32.5	17.984	22.8103
r24	31.3601	15.7053	4.7	0	28.8293	32.5	17.984	22.8103
r25	31.3601	15.7053	4.7	0	28.8293	32.5	17.984	22.8103
'UDPG'	13.447	183.3947	194.6	186.7	177.6101	186.8	204.7413	173.8813
'O2'	66.6667	66.6667	66.7	66.7	66.6667	66.7	66.6667	66.6667
'G3P'	0	0	0	0	0	0	0	0
'AcCoA'	606.3795	594.5005	603.2	585.8	596.3197	599.7	598.0191	597.5365
'3PS'	98.0268	82.372	71.4	66.7	95.4959	99.1	84.6506	89.477
'UDPGAL'	299.2583	211.9631	220.2	278.6	272.0706	199.6	203.2822	275.0626
'AMP'	-66.6666	-66.6667	-66.7	-66.7	-66.6666	-66.7	-66.6667	-66.6667
'H2O'	-66.298	-40.4211	-37.7	24.5	56.4354	10.9	-51.8249	30.5956
'CO2'	-66.6666	-66.6667	-66.7	-66.6	-66.6667	-66.7	-66.6667	-66.6666
'ADP'	-518.676	-486.714	-479.4	-501.4	-508.782	-517.2	-493.006	-494.829
'ATP'	585.343	553.3806	546.1	568.1	575.4488	583.9	559.6725	561.4952
'NADPH'	1000	1000	1000	1000	1000	1000	1000	1000
'NADP'	-1000	-1000	-1000	-1000	-1000	-1000	-1000	-1000
'CMP'	-31.3602	-15.7054	-4.7	0	-28.8293	-32.4	-17.9839	-22.8103
'UDP'	-312.705	-395.358	-414.8	-465.2	-449.681	-386.4	-408.023	-448.944
'DP'	-98.0268	-82.372	-71.4	-66.6	-95.4959	-99.2	-84.6506	-89.4769
'P'	-564.694	-549.039	-538.1	-533.4	-562.163	-565.8	-551.317	-556.144

Table C.8. Deletion Results of 25 reaction pathway with r2 maximization (r9 to r16) (continues)

'H'	-129.387	-98.0773	-76.1	-66.6	-124.325	-131.6	-102.635	-112.287
'FA'	-17.7405	4.8649	-8.6	-4.2	-2.8138	-8.9	-2.8226	2.4635
'CoA'	-673.046	-661.167	-669.8	-652.4	-662.986	-666.3	-664.686	-664.203
'PC'	31.3601	15.7053	4.7	0	28.8293	32.5	17.984	22.8103
'CTP'	31.3602	15.7054	4.7	0	28.8293	32.4	17.9839	22.8103
'DAG'	0	0	0	0	0	0	0	0
'GLC'	0	183.3947	182.7	173.6	177.2729	185.9	164.4138	173.691
'bGLAC'	284.6013	165.3437	166.3	246.6	247.5194	183.5	162.9547	236.5578
'SPN1P'	11.361	0.6347	5.4	18.5	6.4941	9.3	4.8035	0
'C1P'	9.2886	3.7073	2.6	16.3	6.7922	8.8	3.5517	5.3516
'GALCER'	1.21	46.6194	42	18.9	24.214	15.2	0	38.3145
'LCER'	13.447	0	11.9	13	0.3372	0.9	40.3275	0.1903
'SM'	31.3601	15.7053	4.7	0	28.8293	32.5	17.984	22.8103
'PS'	31.3601	15.7053	4.7	0	28.8293	32.5	17.984	22.8103

Table C.9. Deletion Results of 25 reaction pathway with r2 maximization (r17 to r25)

Reaction No	ACC1 (r17)	FAT1 (r18)	SER2 (r19)	Cerk (r20)	Agpat (r21)	DPP1 (r22)	Pss1 (r23)	Chkl (r24)	Pcyt1a (r25)
r1	0	0	12.3457	66.6667	66.6667	66.6667	66.6667	66.6667	66.6667
r2	0	0	0	66.6667	66.6667	66.6667	66.6667	66.6667	66.6667
r3	0	0	0	66.6667	66.6667	66.6667	66.6667	66.6667	66.6667
r4	0	0	0	66.6667	66.6667	66.6667	66.6667	66.6667	66.6667
r5	0	0	0	66.6667	66.6667	66.6667	66.6667	66.6667	66.6667
r6	126.1115	126.294	76.6078	63.1226	54.9823	52.7869	68.2057	68.0684	67.9364
r7	126.1115	126.294	76.6078	69.3005	73.8301	74.9969	101.0875	100.9329	100.7828
r8	134.5703	134.759	111.6501	174.7779	170.8473	172.9631	175.1987	174.8962	174.6046
r9	134.5703	134.759	111.6501	174.5868	169.9846	172.9216	171.5583	171.2475	170.9466
r10	99.4571	99.5935	78.6491	126.8714	122.0823	123.747	128.88	128.6638	128.4555
r11	99.4571	99.5935	78.6491	126.6804	121.2196	123.7055	125.2395	125.015	124.7976
r12	220.1416	220.5769	165.6143	251.8017	249.9556	249.6036	226.9135	226.4269	225.9576
r13	220.1416	220.5769	165.6143	227.7336	221.2969	226.3994	226.9135	226.4269	225.9576
r14	102.2614	102.4084	78.5948	111.7436	117.0598	119.3596	123.1788	122.9508	122.7297
r15	102.2614	102.4084	78.5948	147.9731	124.0925	125.6018	131.2099	130.9983	130.7948
r16	0	0	0	6.1779	18.8478	22.21	32.8818	32.8646	32.8464
r17	0	0	86.4199	466.6667	466.6667	466.6667	466.6667	466.6667	466.6667
r18	0	0	12.3457	66.6667	66.6667	66.6667	66.6667	66.6667	66.6667
r19	0	0	0	90.7349	95.3254	89.8708	66.6667	66.6667	66.6667
r20	0	0	0	0	11.2648	14.9688	22.1134	22.1058	22.0973
r21	0	0	12.3457	0	0	0	0	0	0
r22	0	0	12.3457	0	0	0	0	0	0
r23	0	0	0	24.0682	28.6587	23.2041	0	0	0
r24	0	0	0	24.0682	28.6587	23.2041	0	0	0
r25	0	0	0	24.0682	28.6587	23.2041	0	0	0
'UDPG'	134.5703	134.759	111.6501	174.7779	170.8473	172.9631	175.1987	174.8962	174.6046
'O2'	0	0	0	66.6667	66.6667	66.6667	66.6667	66.6667	66.6667
'G3P'	0	0	12.3457	0	0	0	0	0	0
'AcCoA'	126.1115	126.294	175.3735	596.4559	588.3157	586.1202	601.539	601.4017	601.2698
'3PS'	0	0	0	90.7349	95.3254	89.8708	66.6667	66.6667	66.6667
'UDPGAL'	201.7185	202.0019	157.2439	274.8446	246.1747	249.3488	260.0898	259.6621	259.2503
'AMP'	0	0	-12.3457	-66.6667	-66.6667	-66.6667	-66.6666	-66.6667	-66.6667
'H2O'	462.4003	463.055	283.7734	39.7128	44.0861	47.5211	54.3973	53.4796	52.5901
'CO2'	0	0	0	-66.6667	-66.6667	-66.6667	-66.6666	-66.6667	-66.6667
'ADP'	0	0	-86.4199	-496.913	-525.438	-527.05	-521.662	-521.637	-521.61
'ATP'	0	0	98.7656	563.5795	592.1046	593.7163	588.3285	588.3037	588.277
'NADPH'	0	0	172.8399	1000	1000	1000	1000	1000	1000
'NADP'	0	0	-172.84	-1000	-1000	-1000	-1000	-1000	-1000
'CMP'	0	0	0	-24.0681	-28.6587	-23.2042	0	0	0
'UDP'	-336.289	-336.761	-268.894	-449.623	-417.022	-422.312	-435.289	-434.558	-433.855
'DP'	0	0	-12.3457	-90.7348	-95.3254	-89.8709	-66.6666	-66.6667	-66.6667
'P'	0	0	-98.7656	-557.402	-561.992	-556.538	-533.333	-533.333	-533.333

Table C.9. Deletion Results of 25 reaction pathway with r2 maximization (r17 to r25) (continues)

'H'	0	0	0	-114.803	-123.984	-113.075	-66.6666	-66.6667	-66.6667
'FA'	-126.112	-126.294	-76.6079	-2.6338	-7.1634	-8.3302	-34.4208	-34.2662	-34.1161
'CoA'	-126.112	-126.294	-175.374	-663.123	-654.982	-652.787	-668.206	-668.068	-667.936
'PC'	0	0	0	24.0682	28.6587	23.2041	0	0	0
'CTP'	0	0	0	24.0681	28.6587	23.2042	0	0	0
'DAG'	0	0	-12.3457	0	0	0	0	0	0
'GLC'	134.5703	134.759	111.6501	174.5868	169.9846	172.9216	171.5583	171.2475	170.9466
'bGLAC'	201.7185	202.0019	157.2439	238.424	238.2793	243.0651	248.4183	247.9658	247.5273
'SPN1P'	0	0	0	6.1779	18.8478	22.21	32.8818	32.8646	32.8464
'C1P'	0	0	0	0	11.2648	14.9688	22.1134	22.1058	22.0973
'GALCER'	0	0	0	36.2295	7.0327	6.2422	8.031	8.0476	8.0651
'LCER'	0	0	0	0.1911	0.8627	0.0414	3.6405	3.6487	3.658
'SM'	0	0	0	24.0682	28.6587	23.2041	0	0	0
'PS'	0	0	0	24.0682	28.6587	23.2041	0	0	0

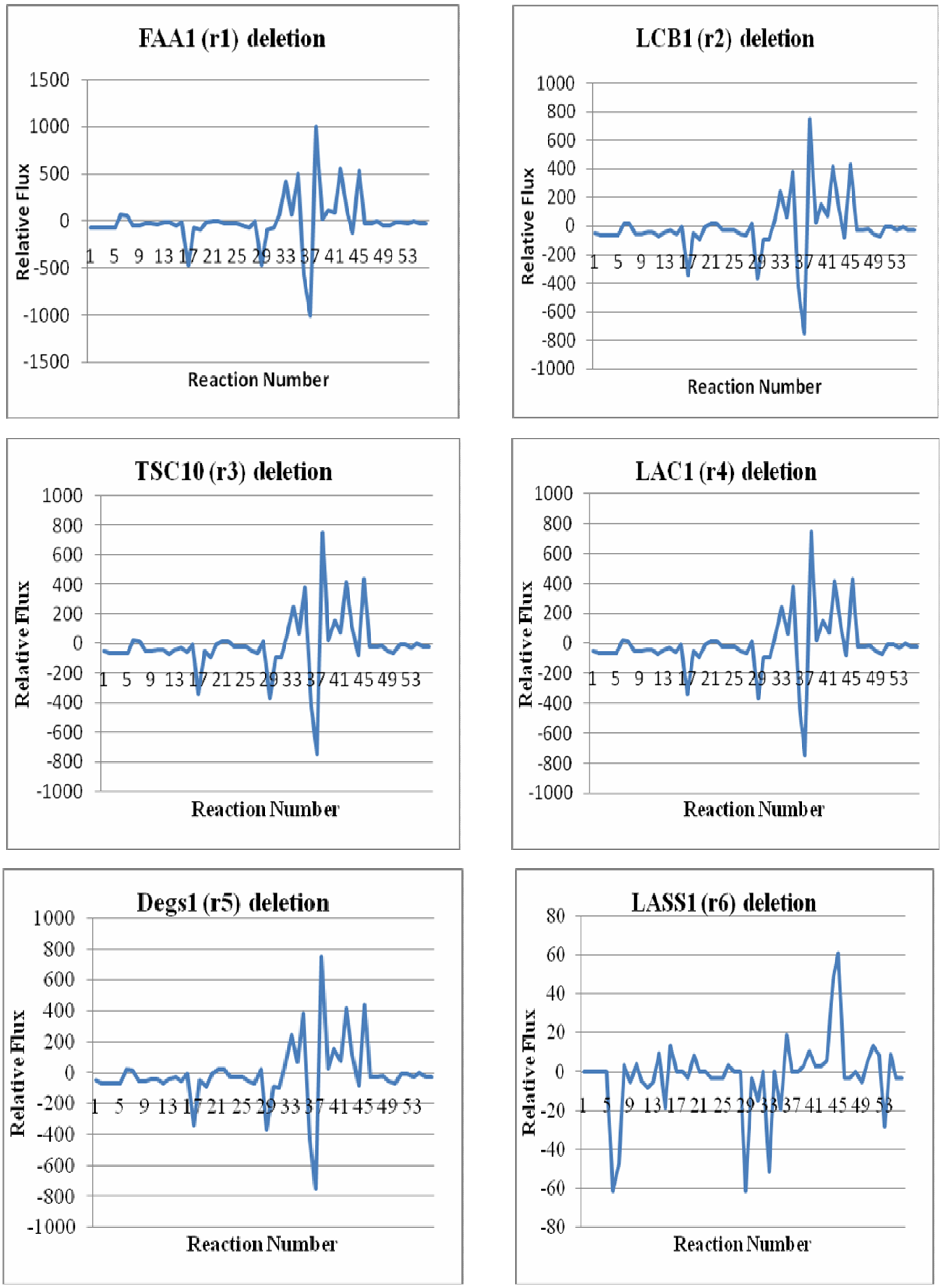

Figure C.1. Deletion results of reactions r1-r6 in 25 reaction pathway with objective function of r2 maximization

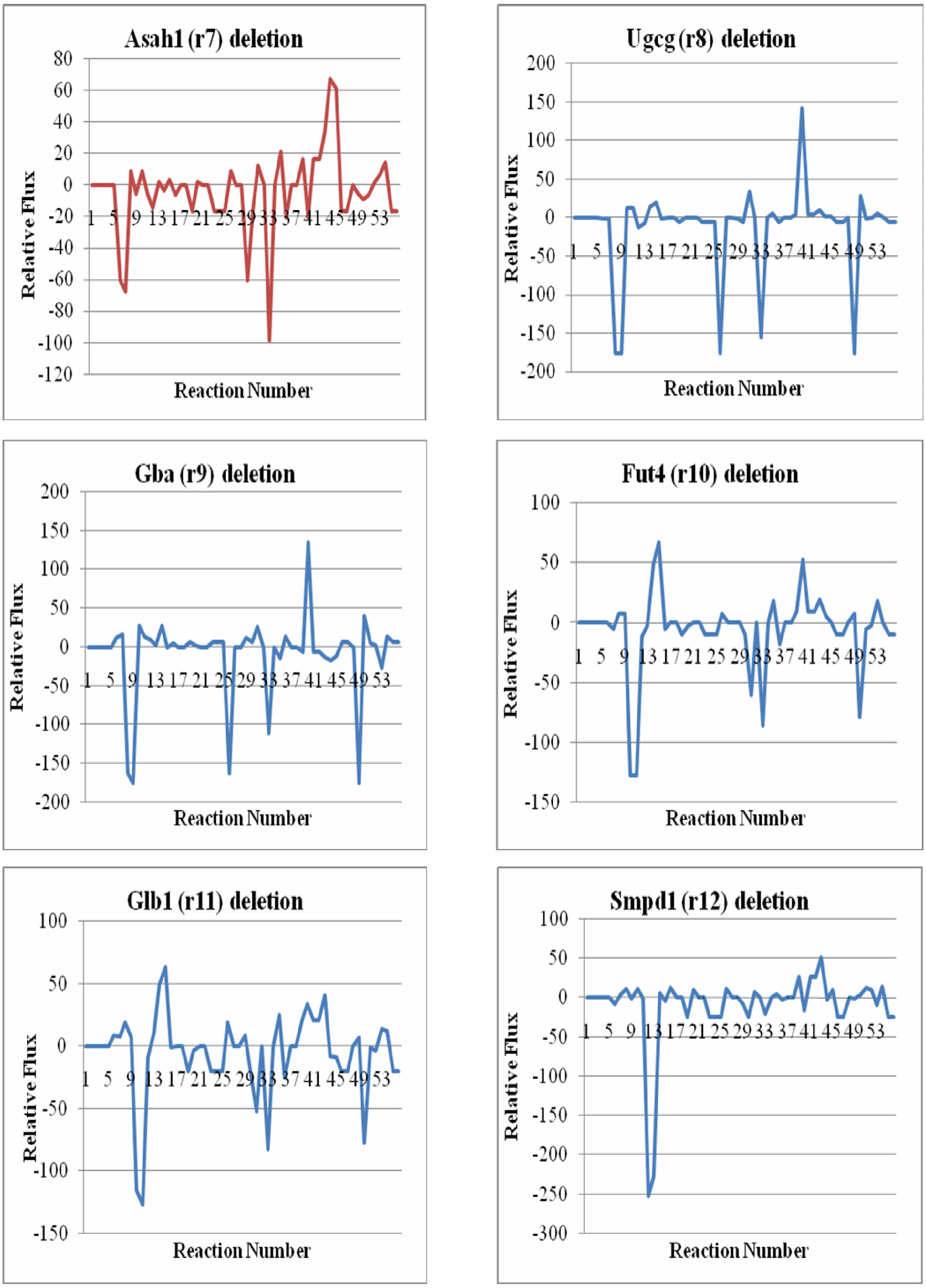

Figure C.2. Deletion results of reactions r9-r12 in 25 reaction pathway with objective function of r2 maximization

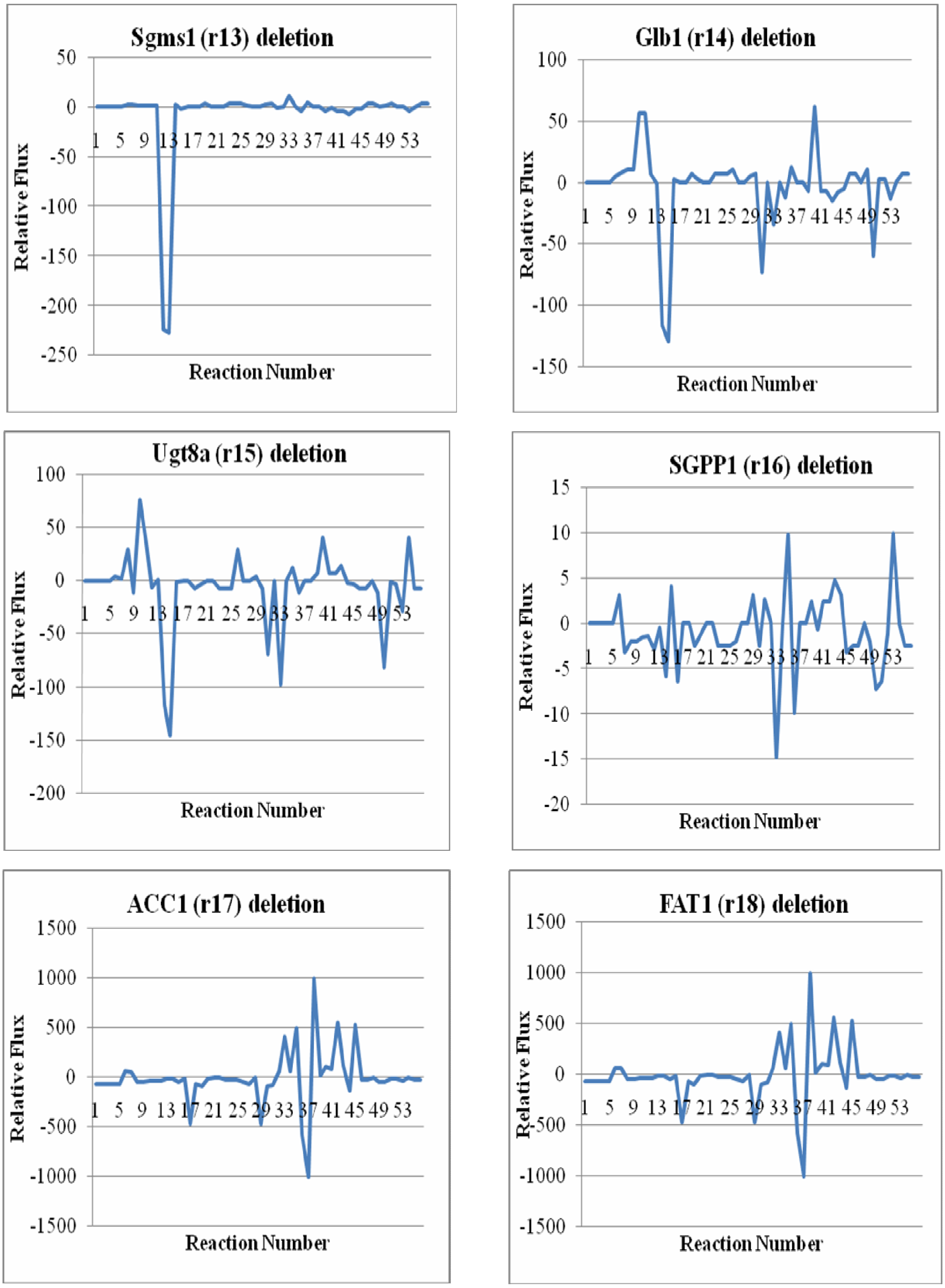

Figure C.3. Deletion results of reactions r12-r18 in 25 reaction pathway with objective function of r2 maximization

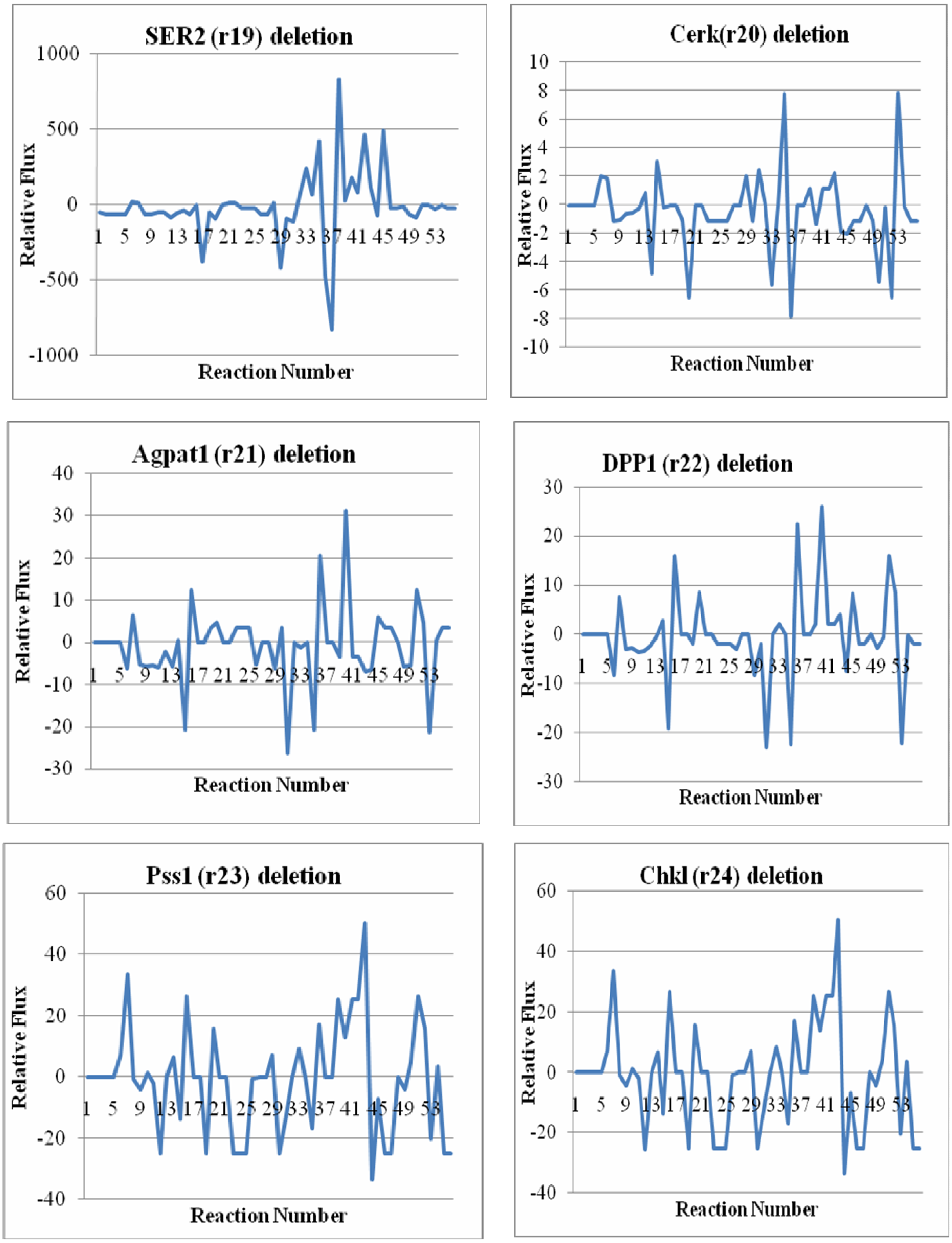

Figure C.4. Deletion results of reactions r19-r24 in 25 reaction pathway with objective function of r2 maximization

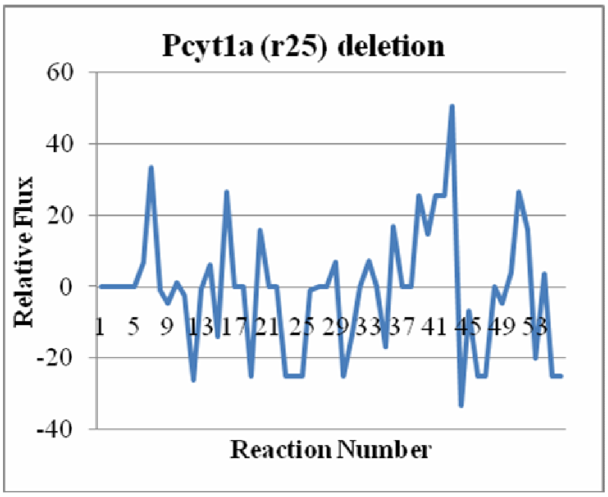

Figure C.5. Deletion results of reaction 25 in 25 reaction pathway with objective function of r2 maximization

APPENDIX D: FBA CODE

```
clear all
tic
global stoich tp err_coeff
tp = 1;
global depo_metnum_match
[rxnno, rxnlist] = textread('sphingolipidpathway.txt','%s
%s','delimiter','\t','commentstyle','shell','headerlines',1);
rxnlist = strtrim(rxnlist);
format compact
disp(sprintf('\nReaction List was read from the file: %d Reactions',length(rxnlist)) )
for i = 1: length(rxnlist)
[reactant(i), prdct(i)] = strread(rxnlist{i},'%s %s', 'delimiter', '>');
end
reactant = reactant';       prdct = prdct';
for i = 1:length(reactant)
reactant{i} = strrep(reactant{i},' -',''); % replace (remove) ' -' and '<-'.
reactant{i} = strrep(reactant{i},'<-','');
end
reactant = strtrim(reactant);
prdct    = strtrim(prdct);


%************   CONSTRUCN OF METABOLITE LIST  ************
metname = func_metlist(rxnlist);
disp( sprintf('Metabolite List was constructed from reaction list: %d Metabolites',
length(metname) ) )
%************  RXN IRREVERSIBILITY INFO: LB/UB  **********
%stores the 1000ormation of rxn reversibility in a binary vector.
j = 1;
for i  = 1:length(rxnlist)
```

```
if length(strfind(rxnlist{i},' -> '))~= 0
rev_1000o(i) = 0; % if IRREV
lb(i) = 0;     ub(i) = 1000;
elseif length(strfind(rxnlist{i}, ' <-> '))~= 0
rev_1000o(i) = 1; % if REV
lb(i) = -1000;  ub(i) = 1000;
else
hata(j) = i;    j = j + 1;
end
end
disp( sprintf(' Number of Irreversible Reactions: %d ',length(find(rev_1000o == 0)) )  )
disp( sprintf(' Number of Reversible Reactions  : %d ',length(find(rev_1000o == 1)) )  )
if j > 1
{'There is an error regarding reaction irreversibility! ...';
'The algorithm will stop...'}
return
end
stoich = zeros(length(metname), length(rxnlist));
%************   STOICH. COEFFS OF REACTANTS AND PRODUCTS  **********
% REACTANTS
for i = 1:length(reactant) %i.e: = 13. % for REACTANTS
if length(strfind(reactant{i}, ' + ')) == 0 %there is ONE reactant
%out1 = strread(reactant{i},'%s','delimiter','+'); % identify the reactant individually
out1 = reactant{i};
[a,b] = coeff_met(out1,metname,i);
stoich(a,i) = b;
else
reactant(i) = strrep(reactant(i),' + ',' @ ');
out = strread(reactant{i},'%s','delimiter','@'); % identify the reactants individually
for nn = 1:length(out)
[a,b] = coeff_met(out(nn),metname,i);
stoich(a,i) = b;
end
```

```
end
% PRODUCTS
if length(strfind(prdct{i}, ' + ')) == 0 %there is ONE reactant
out1 = prdct{i};
[a,b] = coeff_met(out1,metname,i);
stoich(a,i) = -b;
else
prdct(i) = strrep(prdct(i),' + ',' @ ');
out = strread(prdct{i},'%s','delimiter','@'); % identify the reactants individually
for nn = 1:length(out)
[a,b] = coeff_met(out(nn),metname,i);
stoich(a,i) = -b;
end
end
end
stoich_sparse = sparse(stoich);
disp('Matrix conversion for REACTANTS and PRODUCTS were completed ...')
disp( sprintf('STOICHIOMETRIC MATRIX FOR NODUPLIC MODEL IS READY!. :
%d x %d',size(stoich_sparse)))
Inputmet={'UDPG' 'O2' 'AcCoA' '3PS' 'UDPGAL' 'ATP' 'NADPH' 'CO2' 'CoA' 'H' 'FA'
'H2O' 'CMP'  };
Inputmet=Inputmet';
Outputmet={'GLC' 'bGLAC' 'SPN1P' 'C1P' 'GALCER' 'LCER' 'SM' 'AMP' 'ADP' 'DP'
'NADP' 'P' 'UDP' };
Outputmet=Outputmet';
format loose
toc
rxnno;
save MAT stoich_sparse metname lb ub rxnno rev_1000o
save Smtrx stoich
save Inout Inputmet Outputmet
clear all
load MAT
```

```
load Smtrx
load Inout
revirrev = rev_1000o;
[metnum rxnnum] = size(stoich_sparse);
rxnnumm=rxnnum;
for i = 1:length(Inputmet) % uptaken
inputmetxt{i} = [Inputmet{i} 'xt'];
rxnnum = rxnnum + 1;
stoich_sparse(strmatch(Inputmet{i},metname,'exact'),rxnnum) = 1;
lb(rxnnum) = -1000; ub(rxnnum) = 1000;
end
inputmetxt=inputmetxt';
for i = 1:length(Outputmet) % secreted
outputmetxt{i} = [Outputmet{i} 'xt'];
rxnnum = rxnnum + 1;
stoich_sparse(strmatch(Outputmet{i},metname,'exact'),rxnnum) = -1;
lb(rxnnum) = -1000; ub(rxnnum) = 1000;
end
outputmetxt=outputmetxt';
allrxnname = [rxnno; inputmetxt; outputmetxt];
lb(8) = 0 ; ub(8) = 0;
b = zeros(metnum,1);
f1 = zeros(1,length(allrxnname));
f1(1) = -1;% maximization
[x1,obj1,exitflag,output,lambda] = linprog(f1,[],[],stoich_sparse,b,lb',ub');%MOSEK-  OR
MATLAB
x1
obj1
exitflag
output
lambda
check=stoich_sparse*x1;
plot (stoich_sparse*x1)
```

REFERENCES

Adam, R.D., 2001, "Biology of *Giardia lamblia*", Clin Microbiol Rev., Vol. 14, No. 3 pp. 447–475, July.

Ariga, T., D. W. Jarvis, , and R. K. Yu, , Ariga et al, 1998, "Role of sphingolipid-mediated cell death in neurodegenerative diseases", J Lipid Res., Vol. 39, pp. 1-16.

Baumruker, T., and E.E. Prieschl, , 2002, "Sphingolipids and the regulation of the immune response", Seminars in Immunology, Vol. 14, pp. 57-63.

Bertram, M. A., E. A. Meyer, J. D. Lile and S. A. Morse, 1983, "A comparison of isozymes of five axenic *Giardia* isolates". Vol. 69, pp. 793–801.

Blair, R. J., P. F. Weller, 1987, "Uptake and Esterification of Arachidonic Acid by Trophozoites of *Giardia lamblia*", Molecular and Biochemical Parasitology, Vol 25, No. 1, pp. 11–18, August.

Börklü-Yücel, E., 2005, Sphingolipidomics: Qualification and Quantification of Sphingolipids in Yeast, M.S. Thesis, Bogazici University.

Dan, M. and C. C. Wang, 2000, "Role of Alcohol Dehydrogenase E (ADHE) in the Energy Metabolism of *Giardia lamblia*", Molecular and Biochemical Parasitology, Vol.109, pp. 25-36.

Das, S., C. D. Schteingart, A. F. Hofmann, D. S. Reiner, S. B. Aley and F. D. Gillin, 1997, "*Giardia lamblia*: Evidence for Carrier-Mediated Uptake and Release of Conjugated Bile Acids", Experimental Parasitology, Vol. 87, pp. 133-141.

Dickson, R. C. and R. L. Lester, 1999, "Metabolism and Selected Functions of Sphingolipids in the Yeast Saccharomyces cerevisiae" , Biochimica et Biophysica Acta (BBA), Molecular and Cell Biology of Lipids, Vol. 1438, pp. 305-321.

Dickson, R. C. and R. L. Lester, 1999, “Yeast Sphingolipids”, Biochimica et Biophysica Acta, Vol. 1426, pp. 347-357.

Edwards, J.S., B.O. Palsson, 2000, “The *Escherichia coli* MG1655 *in silico* metabolic genotype: its definition, characteristics, and capabilities”, Proc Natl Acad Science, Vol. 97, pp 5528–5533.

Edwards, J.S., M. Covert and B. Palsson, 2002, “Metabolic Modelling of Microbes: The Flux-Balance Approach”, Environmental Microbiology, Vol. 4, pp. 133-140.

Edwards, M. R., P. J. Schofield, W. J. O'Sullivan and M. Costello, 1992, “Arginine Metabolism during Culture of *Giardia intestinalis*”, Molecular and Biochemical Parasitology, Vol. 53, pp. 97-103.

Ellis, J.E., M. A. Wyder, E. L. Jarroll and E. S. Kaneshiro, 1996, “Changes in Lipid Composition during In Vitro Encystation and Fatty Acid Desaturase Activity of *Giardia lamblia*”, Molecular and Biochemical Parasitology, Vol. 81, pp. 13-25.

Farthing, M. J., G. T. Keusch and M. C. Carey, 1985, “Effects of Bile and Bile Salts on Growth and Membrane Lipid Uptake by *Giardia lamblia*, Possible Implications for Pathogenesis of Intestinal Disease”, The Journal of Clinical Investigation, Vol. 76, pp 1727-1732.

Forster, J., I. Famili, P. Fu, B. Palsson and J. Nielsen, 2005, “Genome-Scale Reconstruction of the *Saccharomyces cerevisiae* Metabolic Network”, Vol. 13, pp 244-53

Futerman, A. H. and Y. A. Hannun, 2004, “The Complex Life of Simple Sphingolipids”, EMBO Reports, Vol. 5, pp. 777-782.

Gasch, A. P., P. T. Spellman, C. M. Kao, O. Carmel-Harel, M. B. Eisen, G. Storz, D. Botstein and P.O. Brown, 2000, “Genomic Expression Programs in the Response of

Yeast Cells to Environmental Changes", Molecular Biology of the Cell, Vol. 11, pp. 4241–4257.

Geeraert, L., G.E. Mannaerts, and P.E. Van Veldhoven, 1997, "Conversion of dihydroceramide into ceramide: involvement of a desaturase", Biochemical Journal, Vol. 327, No.63, pp. 125-132.

Gibson, G. R., D. Ramirez, J. Maier, C. Castillo and S. Das, 1999, "*Giardia lamblia*: Incorporation of Free and Conjugated Fatty Acids into Glycerol-based Phospholipids", Experimental Parasitology, Vol. 92, pp. 1–11.

Gillin, F. D., M. J. Gault, A. F. Hofmann, D. Gurantz and J. F. Sauch, 1986, "Biliary Lipids Support Serum-Free Growth of Giardia lamblia", Infection and Immunity, Vol. 53, pp. 641–645.

Gray, M W., 1989, "The Evolutionary Origins of Organelles". Trends Genet., Vol. 5, pp. 294–299.

Hakomori, S., and Y. Igarashi, 1993, "Gangliosides and glycosphingolipids as modulators of cell growth, adhesion, and transmembrane signaling", Journal of Lipid Research, Vol. 23, pp. 147-162.

Hannun, Y.A. and L. M. Obeid, 2002, "The Ceramide-centric Universe of Lipid-mediated Cell Regulation: Stress Encounters of the Lipid Kind", J. Biol. Chem., Vol. 277, Issue 29, pp. 25847-25850.

Hannun, Y. A., C. R. Loomis, A. H. Merrill and R. M. Bell, 1986, "Sphingosine inhibition of protein kinase C activity and of phorbol dibutyrate binding in vitro and in human platelets", J. Biol. Chem. 261: 12604–12609

Heim, S., A. Bauleke, C. Wylegalla, and K.G. Wagner, 1987, "Evidence of phosphatidylinositol and diacylglycerol kinases in suspension cultured plant cells", Plant Science, Vol. 49, pp. 159-165.

Hernandez, Y., M. Shpak and T. T. Duarte, 2008, “Novel Role of Sphingolipid Synthesis Genes in Regulating Giardial Encystation”, Infection and Immunity, Vol. 76, pp. 2939-2949.

Hofmann, A. F. and L. R. Hagey, 2008, “Bile Acids: Chemistry, Pathochemistry, Biology, Pathobiology,and Therapeutics” ,Cell. Mol. Life Sci., Vol. 65, pp. 2461 – 2483.

Huwiler, A., T. Kolter, J. Pfeilschifter and K. Sandhoff, 2000, “Physiology and Pathophysiology of Sphingolipid Metabolism and Signaling”, Biochimica et Biophysica Acta, Vol. 1485, pp. 63–99.

Ichikawa, S., K. Ozawa, and Y. Hirabayashi, 1998, “Molecular Cloning and Characterization of the Mouse Ceramide Glucosyltransferase Gene”, Biochemical and Biophysical Research Communications, Vol. 253, pp. 707-711.

Igarashi, Y., 1997, “Functional roles of sphingosine, sphingosine 1-phosphate, and methylsphingosines: in regard to membrane sphingolipid signaling pathways”, J. Biochem., Vol. 122, pp. 1080-1087.

Iwabuchi, K., Y. Zhang, K. Handa, D. A. Withers, P. Sinay and S. Hakomori, 2000, “Reconstitution of Membranes Simulating Glycosignaling domain and Their Susceptibility to lyso-GM3.”, Journal of Biological Chemistry, Vol. 275, pp. 15174–15181.

Jenkins, G. M., and Y. A. Hannun, 2001, “Role for de Novo Sphingoid Base Biosynthesis in the Heat-induced Transient Cell Cycle Arrest of Saccharomyces cerevisiae”, Journal of Biological Chemistry, Vol. 276, pp. 8574-8581.

Johnson, M., I. Zaretskaya, Y. Raytselis, Y. Merezhuk, S. McGinnis, and T. L. Madden, 2008, NCBI BLAST: A Better Web Iinterface, Nucleic Acids Research, Vol. 36, pp. 1-5.

Kavun, B., “Drug Target Identification in Sphingolipid Metabolism by Computational Systems Biology Tools: MCA & MPA”, 2007.

Kanehisa, M., S. Goto, S. Kawashima, Y. Okuno and M. Hattori, 2003, The KEGG Resource for Deciphering the Genome, Nucleic Acids Research, Vol. 32, pp. 277-280.

Koval, M. and R. E. Pagano, 1991, "Intracellular Transport and Metabolism of Sphingomyelin", Biochimica et Biophysica Acta, Vol. 1082, pp. 113-125.

Koynova, R. and M. Caffrey, 1995, "Phases and Phase Transitions of the Sphingolipids", Biochimica et Biophysica Acta, Vol. 1255, pp. 213-236.

Lester, R. L. and R. C. Dickson, 1993, "Sphingolipids with inositolphosphate-containing head groups", Journal of Lipid Research, Vol. 26, pp. 253-272.

Leevers, S. J., B. Vanhaesebroeck and M. D. Waterfield, 1999, "Signalling through phosphoinositide 3-kinases: the lipids take centre stage", Curr. Opin. Cell Biol., Vol. 11, pp. 219–225.

McNabb, T. J., A. E. Cremesti, P. R. Brown and A. A. Fischl, 1999, "High-performance liquid chromatography/ evaporative light-scattering detector techniques for neutral, polar, and acidic lipid classes : a review of methods and detector models", Vol. 4, pp. 53-70.

Meier, K. D., O. Deloche and H. Reizman, 2006, "Sphingoid Base Is Required for Translation Initiation during Heat Stress in *Saccharomyces cerevisiae*", Mol. Biol Cell., Vol. 17, pp. 1164-1175.

Merrill, A. H. and D. D. Jones, 1990, "An Update of the Enzymology and Regulation of Sphingomyelin Metabolism", Biochimica et Biophysica Acta, Vol. 1044, pp. 1–12.

Michael, C., G. Echten-Deckert, J. Rother, K. Sandhoff, E. Wang and A.H. Merrill, 1997, "Characterization of Ceramide Synthesis, A Dihydroceramide Desaturase Introduces The 4,5-Trans-Double Bond of Sphingosine at the level of Dihydroceramide", Journal of Biological Chemistry, Vol. 272, pp. 22432-22437.

Morrison, H. G., A. G. McArthur and F. D. Gillin, 2007, "Genomic Minimalism in the Early Diverging Intestinal Parasite *Giardia lamblia*", Science, Vol. 17, pp. 1921-1926.

Nagiec, M.M., J. A. Baltisberger, G. B. Wells, R. L. Lester and R. C. Dickson, 1994 , "The LCB2 gene of Saccharomyces and the related LCB1 gene encode subunits of serine palmitoyltransferase, the initial enzyme in sphingolipid synthesis", Proceedings of the National Academy of Sciences U.S.A., Vol. 91, pp. 7899-7902.

O'Brien, J. S., and E. L. Sampson, 1965, "Lipid Composition of the Normal Human Brain: Gray Matter, White Matter, and Myelin", Journal of Lipid Research, Vol. 6, pp. 537-544.

Ogretmen, B., and Y. A. Hannun, 2004, "Biologically Active Sphingolipids in Cancer Pathogenesis and Treatment", Nature Reviews Cancer, Vol. 4, pp. 604–616.

Ohanian, V., and J. Ohanian, 2001, "Sphingolipids in mammalian cell signalling", Biomedical and Life Sciences, Vol. 58, pp. 2053-2068.

Oshiro, J., S. Rangaswamy, X. Chen, G. Han, J.E. Quinn, and G. M. Carma, 2000, "Regulation of the DPP1-encoded diacylglycerol pyrophosphate (DGPP) phosphatase by inositol and growth phase. Inhibition of DGPP phosphatase activity by CDP-Diacylglycerol and activation of phosphatidylserine synthase activity by DGPP", Vol. 275, Issue 52, pp. 40887-40896.

Riboni, L., P. Viani, R. Bassi, A. Prinetti and G. Tettamanti, 1997, "The Role Of Sphingolipids In The Process Of Signal Transduction", Prog. Lipid Res., Vol. 36, No. 2/3, pp. 153-195.

Rother, J., G. Van Echten, G. Schwarzmann, and K. Sandhoff, 1992, "Biosynthesis of sphingolipids: dihydroceramide and not sphinganine is desaturated by cultured cells", Biochemical and Biophysical Research Communications, Vol. 189, pp. 14-20.

Sheikh, K., J. Forster and L. K Nielsen, 2005, “Modeling Hybridoma Cell Metabolism Using a Generic Genome-Scale Metabolic Model of *Mus musculus*”, Biotechnology Progress, Vol. 21, pp. 112-121.

Slotte, J. P., 1999, “Sphingomyelin-cholesterol Interactions in Biological and Model Membranes”, Chemistry and Physics of Lipids, Vol. 102, pp. 13–27.

Sonda, S., S. Stefanic, and A.B. Hehl, 2008, “A Sphingolipid Inhibitor Induces a Cytokinesis Arrest and Blocks Stage Differentiation in *Giardia lamblia*”, Antimicrobial Agents And Chemotherapy, Vol. 52, pp. 563–569.

Spiegel, S. and A. H. Merrill, 1996, “Sphingolipid metabolism and cell-growth regulation”, FASEB J., Vol. 10, pp. 1388–1397.

Stoffel, W., D. Le Kim and G. Sticht, 1968, “Biosynthesis of dihydrosphingosine in vitro”, Hoppe Seyler's Z. Physiol. Chem, Vol. 349, pp. 1637-1644.

Tanford, C., The Hydrophobic Effect: Formation of Micelles and Biological Membranes, 2nd edn., Wiley, New York, 1980.

Tepper, A. D., P. Ruurs, T. Wiedmer, P.J. Sims, J. Borst and W.J. van Blitterswijk, 2000, “Sphingomyelin hydrolysis to ceramide during the execution phase of apoptosis results from phospholipid scrambling and alters cell-surface morphology”, J Cell Biol., Vol. 150 No.1, pp. 155-64.

Thudichum, J.L.W. 1884, A Treatise on the Chemical Construction of Brain, Bailliere, Tindall and Cox, London.

Toke, D.A., A. S. Fischl, and G. M. Carman, 1998, “Isolation and Characterization of the Saccharomyces cerevisiae DPP1 Gene Encoding Diacylglycerol Pyrophosphate Phosphatase”, J Biol Chem, Vol. 273, Issue 6, pp. 3278-3284.

Ullman, M. D. and N. S, Radin, 1972, “Enzymatic formation of hydroxy ceramides and comparison with enzymes forming nonhydroxy ceramides”, Archives of Biochemistry and Biophysics, Vol. 152, pp. 767-777.

Vance, D. E. and J. E. Vance, 2002, Biochemistry of Lipids, Lipoproteins and Membranes, Elsewier, Amsterdam.

Weiss, B. and W. Stoffel, 1997, “Human and Murine Serine-Palmitoyl-CoA Transferase (SPT): Cloning, Expression and Characterization of the Key Enzyme of Sphingolipid Synthesis”, Eur J Biochem, Vol. 249, pp. 239-247.

Wu, W., Y. Liu, B. Riedel , J.B. Wissing, S.A. Fischl and G.M. Carman, 1996, “Purification and Characterization of Diacylglycerol Pyrophosphate Phosphatase from *Saccharomyces cerevisiae*”, The Journal Of Biologıcal Chemistry, Vol. 271, No. 4, pp. 1868–1876.